Eggshell

Design and fabrication of non-standard, structural concrete columns, using 3D printed thin-shell formwork

Joris Burger
Master thesis

Joris Burger
4152921

Master thesis
23.01.2019

MSc Building Technology
Delft University of Technology

in collaboration with

Gramazio Kohler Research
ETH Zurich

Supervisors
Dr. Ir. Christian Louter
Chair of Structural Design, TU Delft

Dr. Ir. Serdar Asut
Chair of Design Informatics, TU Delft

Dr. Ena Lloret-Fritschi
Gramazio Kohler Research, ETH Zurich

Keywords
Concrete
3D Printing
Digital fabrication
Additive manufacturing
Formwork
Reinforcement

Abstract

Research and development in additive manufacturing with concrete has become more widespread over the last decade. The processes developed range from concrete extrusion, to digital fabrication of formworks and the unification of formwork and reinforcement. Although they enable the production of increasingly material-efficient structures, the individual processes still face various challenges such as implementation of reinforcement, geometrical limitations, scaling and formation of cold joints, in particular because of the layer-based process [1].

This research proposes an alternative method of producing concrete formworks dubbed 'Eggshell'. Combined with a novel casting technique, its aim is to overcome these challenges and make material-efficient concrete production possible. As concrete is the most used construction material in the world [2] its influence on the construction industry is unprecedented. Of the construction costs of concrete, formwork typically makes up 30-80% of the costs [3]. This means formwork considerations are often a key driver in determining the design of concrete structures. Materials used to construct the formwork also have a big impact on the total ecological costs of the concrete building components. As the lifespan of all formwork is finite, this adds to the already considerable amount of waste generated by the building industry [4].

Furthermore, traditional formwork made from steel or wood is ineffective in producing the non-standard, (double) curved geometry that characterizes many contemporary architectural designs. Using innovative means of formwork fabrication, these non-standard building components can potentially be produced in a more cost-, time- and material-efficient way. Moreover, Eggshell opens up possibilities for fabricating structurally optimized geometry, enabling a more efficient use of resources.

The research builds upon previous work done as a part of an interdisciplinary master thesis [5] in a collaboration between Gramazio Kohler Research, the Institute of Robotics and Intelligent Systems and the Physical Chemistry of Building Materials group (ETH Zurich). In the thesis a process was developed in which a thin-shell formwork is 3D printed while a fast-hydrating concrete is simultaneously fed in. By 3D printing the formwork, complex geometries can be fabricated effectively. The printed formwork can potentially also be recycled and reused, making the process fully circular. Furthermore, reinforcement can be integrated into the structures, allowing for the creation of structural building components.

Acknowledgements

This research would have been impossible to conduct successfully without the continuous help and support of many individuals. First of all I cannot thank Dr. Ena Lloret-Fritschi enough, for taking me up as a research intern at Gramazio Kohler Research, first introducing me to the research subject and being essential in making this master thesis possible. I would also like to thank my first and second mentor from TU Delft, Dr. Christian Louter and Dr. Serdar Asut for allowing me to pursue my own direction of research and giving helpful guidance from distance.

Prof. Fabio Gramazio, Prof. Matthias Kohler and Prof. Dr. Robert Flatt are thanked for their faith in me and for bringing this research further in many fruitful discussions. Furthermore, this research would have not been where it is now if not for the enthusiastic involvement of Fabio Scotto and Dr. Thibault Demoulin, assisting me with everything related to concrete and more. Bruno Pinto Aranda and Nizar Taha I would like to thank for their help during and outside of fabrication. Furthermore, Dr. Jaime Mata Falcón is thanked for his involvement and advice in reinforcement of the structures. Lastly my sincere gratitude is expressed to (head) technicians Heinz Richner, Andreas Reusser, Michael Lyrenmann and Philippe Fleischmann. Without their vast technical knowledge the experiments conducted would never have been so successful.

Contents

1 Introduction

In recent decades, architects have gained access to computer-aided design (CAD) software, increasingly allowing them to create geometrically complex designs [6]. As digital design techniques have evolved, so have digital manufacturing processes but perhaps at a slower rate. A discrepancy therefore exists between 'designing' and 'making'. Designers have many cutting edge tools at their disposal to shape and imagine their vision whereas builders are often bound to traditional methods.

Over the years several people around the world have attempted to bridge this gap between designing and making [7]. Although this thesis specifically focuses on digital fabrication of concrete, it also strives towards a more integrated design and fabrication process. By understanding the opportunities and limitations of fabrication, designs can be made that exploit the strengths of concrete construction. Ultimately this should empower the designer, eliminating the need for post-rationalization whilst improving material efficiency.

1.1 Problem statement and objectives

Concrete is the most used construction material in the world [2]. It is often a material of choice for architects and builders because of its low cost, high structural performance and the ability to take any shape when placed into a formwork. In typical concrete construction processes the formwork is removed after the concrete has cured. Essentially this means that two structures are produced: one being the formwork, the other the completed concrete element. In order to reduce waste and high costs caused by disregarded formwork contractors re-use formwork [3]. However, to be able to re-use the steel and wooden moulds, the geometry often needs to be standardized and (post) rationalized. This standardization of concrete formwork is one factor which went on to define the aesthetics of our built environment, as many architectural projects are driven by costs.

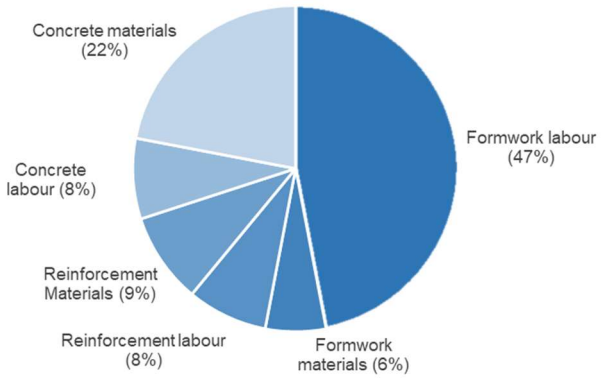

Figure 1-1: Distribution of fabrication costs of a planar concrete element [8].

In Figure 1-1 the distribution of cost for a standard, planar concrete element such as a straight wall can be seen. For these simple geometries, the costs of concrete formwork already make up more than 50% of the total production costs of a concrete element [8]. For more complex,

non-standard, concrete elements with double-curved geometry this number rises up to more than 80% according to [9] (Figure 1-2).

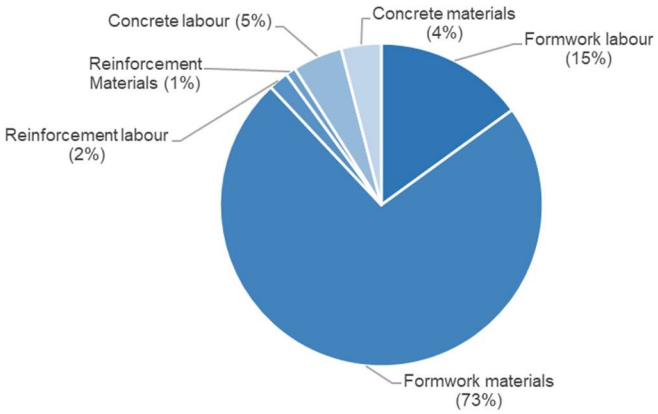

Figure 1-2: Distribution of construction costs of a double curved concrete element [9].

The problem which is thus faced is not only that non-standard concrete elements have a high costs of fabrication, they are also wasteful. As the formwork for non-standard concrete structures is usually discarded after construction, this immediately adds to the already high amount of waste generated by the construction industry. [1] Despite this high waste in formwork, buildings that consist of non-standard concrete geometry can be found.

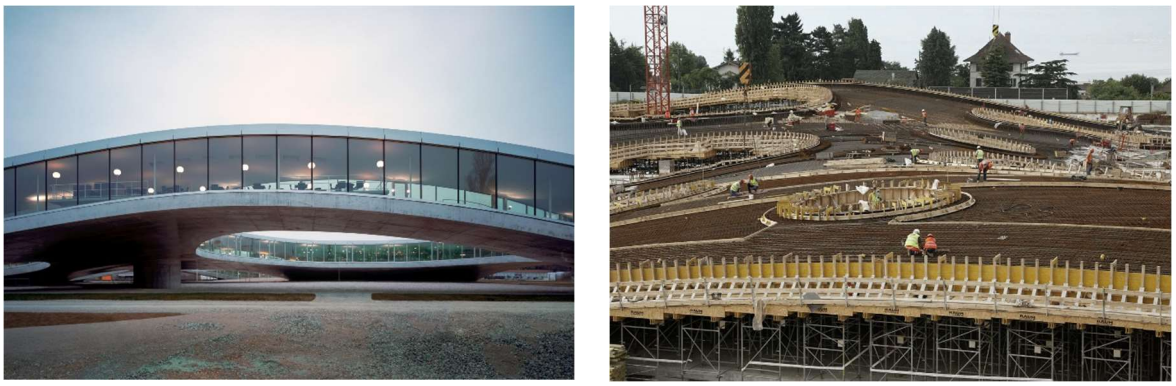

Figure 1-3: The Rolex Learning Centre by SANAA, completed in 2011. a) The completed building and b) Construction showing concrete formwork (Source: https://beautifulrough.wordpress.com/2013/01/24/the-rolex-learning-center/).

For the construction of the Rolex Learning Centre (Figure 1-3), for example, around 1500 sections of formwork, as well as almost 10.000 timber cleats had to be machined, all of which were discarded after construction [10]. Furthermore, the concrete structure as designed by the architect had to be post-rationalized by the fabrication consultancy firm Design to Production to make the construction feasible [11].

Another impressive example of non-standard concrete example can be found in the form of the Meiso no Mori Crematorium by Toyo Ito and Associates (Figure 1-4). However, also in this case the architect's design was post-rationalized by the structural engineer, Mutsuro

[1] According to [4] up to 35% of landfill waste worldwide is generated by the construction industry.

Sasaki [12] and a large amount of formwork waste was generated to realize the concrete roof structure.

Figure 1-4: Meiso no Mori Crematorium by Toyo Ito and Associates, completed in 2006. a) Completed building b) Construction showing complex concrete formwork [12].

The objective of this research is to develop a strategy for the fabrication of non-standard, reinforced concrete elements, whilst generating less waste compared to existing techniques. The potential and feasibility is explored of a fabrication process called Eggshell, also known as Smart Dynamic Casting 2.0. In the Eggshell fabrication process a thin-shell formwork is 3D printed whilst set-on-demand concrete is simultaneously cast. By carefully controlling the early age strength gain of the concrete such as developed in the project Smart Dynamic Casting at the ETH Zurich [13] a thin 3D printed shell can be used as a formwork. The shell material can consist of various materials ranging from thermoplastics to cementitious materials such as clay or concrete. As the shell's thickness is minimized, construction waste due to discarded formwork can potentially be reduced significantly. The research discussed in this thesis limits the shell material to a thermoplastic, as this enables to prove the concept while maintaining a limited scope. Furthermore, as the fabrication process is particularly well suited for the production of vertical elements, it is chosen to focus exclusively on the fabrication of columns.

1.2 Research question and relevance

This research investigates the potential of fabricating full-scale, non-standard, structural performing building elements using thin-shell formwork. The research question which will be investigated in this thesis therefore is:

Can 3D printed, thin-shell formwork be used to construct full-scale, non-standard, structural, concrete columns?

This research addresses the strong societal demand of a more efficient use of building materials. As concrete is such a heavily used construction material and almost all concrete needs formwork, the research project has the potential to reduce material use in concrete construction. Furthermore, Eggshell can enable the fabrication of concrete structures that are

otherwise difficult and expensive to construct. This opens up the design space to architects and engineers, allowing for the creation of architecturally interesting, as well as structurally efficient structures. By taking the fabrication process in consideration during design, a more integrative design and fabrication process can be achieved.

1.3 Research methodology

The research in this thesis uses a physical-empirical methodology. It can be grouped into three main themes: design, material and fabrication. As these themes are all interconnected, constant iterations between the three have to be made. They are then subsequently verified through physical experimentation (Figure 1-5).

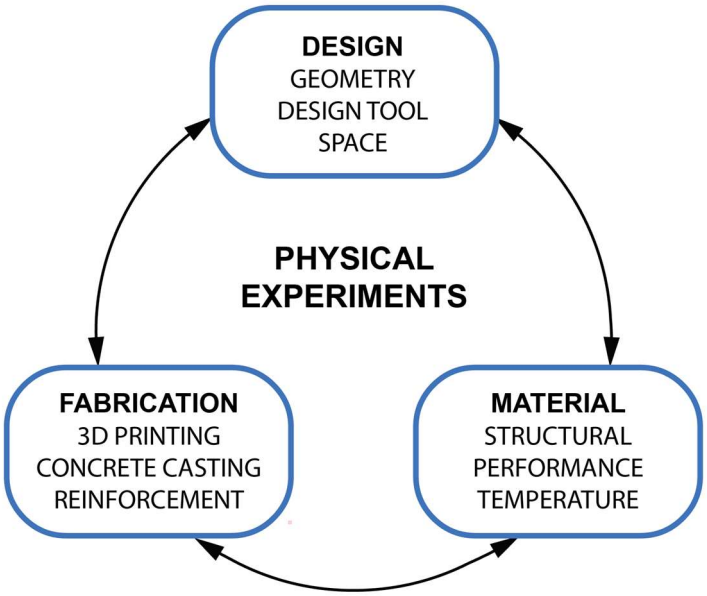

Figure 1-5: Diagram of research methodology used throughout this thesis.

As the goal of this research is a material-aware design- and fabrication process, several aspects must be considered simultaneously. As soon as the geometry changes, structural performance also has to be reconsidered, as well as formwork fabrication and concrete casting. Perhaps changing the design will lead to a higher structural performance; however, it could be impossible to 3D print due to large overhangs. Therefore, to maximize success of the whole process, a material aware design and fabrication strategy has to be adapted, where constant switches between the different domains of the research can readily be made.

1.4 Structure of the thesis

First of all a state of the art is given in Chapter 2. The state of the art covers various topics relevant to this thesis such as conventional concrete formwork, digitally fabricated concrete formwork, digitally fabricated concrete reinforcement and 3D printing.

In Chapter 3 the methods, materials and setup are described for the experiments that are performed. Chapter 4 then consists of a description of these experiments, including

motivation, results and a discussion. The experiments are divided into Phase I: Explorations, Phase II: Scale-up and Phase III: Case-study. Topics that are addressed are (amongst others) the integration of reinforcement into the thin-shell structures, geometrical limitations of the formwork, temperature development during hydration of the concrete and finally the design and fabrication process of the final prototype.

After the case study follows a discussion and conclusion in Chapter 5 in which the research question is answered, as well as the case study results are evaluated. Finally, as there are many more aspects that can still be explored within the subject of this thesis, several pages are dedicated to suggestions for further research in Chapter 6.

1.5 Timeline

The timeline followed during the research can be seen in Figure 1-6. Before starting the research in April, a feasibility study had been done by the author which is described in Phase I: Explorations (Section 4.1). Although Phase I is not officially part of the master thesis, it is important that it is described for completeness and understanding. Phase II started after the P1 presentation and Phase III subsequently started after the P3 presentation.

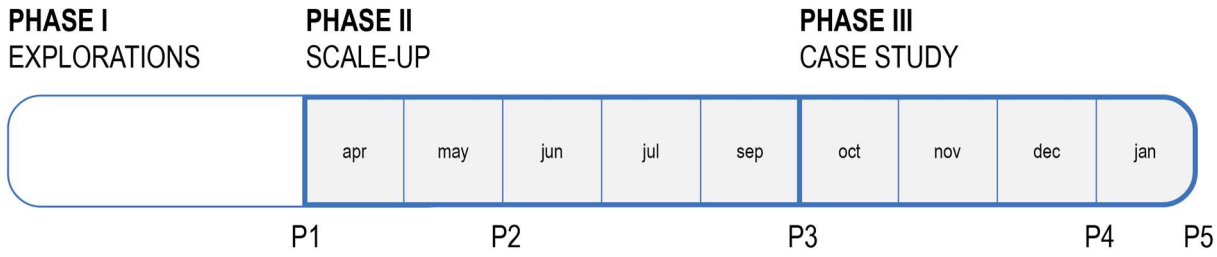

Figure 1-6: Timeline of thesis including P1-P5 presentations.

2 State of the Art

In this chapter developments in the fabrication of formwork, concrete reinforcement and 3D printing are discussed. As the Eggshell fabrication process aims at expanding and improving the possibilities of concrete construction, it is important that the techniques currently in use are studied. In general, a contrast can be identified between the methods currently in use in the construction industry and those under development in research environments. Methods fit for research environments are often experimental and work in controlled environments, whereas methods used in the construction industry are mature, have low risk and robust functionality. As they are both relevant for this research, both standard concrete formwork and digitally fabricated formwork are discussed.

Typically, concrete formwork consists of modular formwork sheets that are placed and assembled together on the construction site [3]. Occasionally alternative fabrication methods are also employed, such as digital fabrication of concrete formwork. Digitally fabricated formwork comes in many different forms, a few themes can however be identified: subtractive fabrication, additive fabrication and adaptive fabrication.

Similarly, the state of the art of digitally fabricated reinforcement is discussed as reinforcement is an essential aspect of concrete construction. Several notable examples of merging concrete formwork with reinforcement also exist. Lastly, as 3D printing is the chosen fabrication method in this research, 3D printing, or more specifically fused deposition modelling (FDM) is discussed.

2.1 Concrete formwork

Various methods to form and shape concrete are employed on contemporary construction sites. Most often, concrete formwork consists of a modular shutter system which is held in place by supporting elements, the falsework. Usually either timber or steel is used as a material of choice, timber having its low weight and versatility as advantages and steel its strength and durability [3]. An example of a wall timber formwork system can be seen in Figure 2-1. Studs supported by braces are clad with sheathing which is held in place by wire ties.

Another formwork technique which has proven to be an effective way of constructing tall (>10m), monolithic concrete structures is slipforming (Figure 2-2). In slipforming a formwork is moved vertically with hydraulic jacks whilst concrete is cast in simultaneously. The formwork moves at the speed with which the concrete is setting, to make sure the concrete is self-supporting once the formwork is slipped out [14].

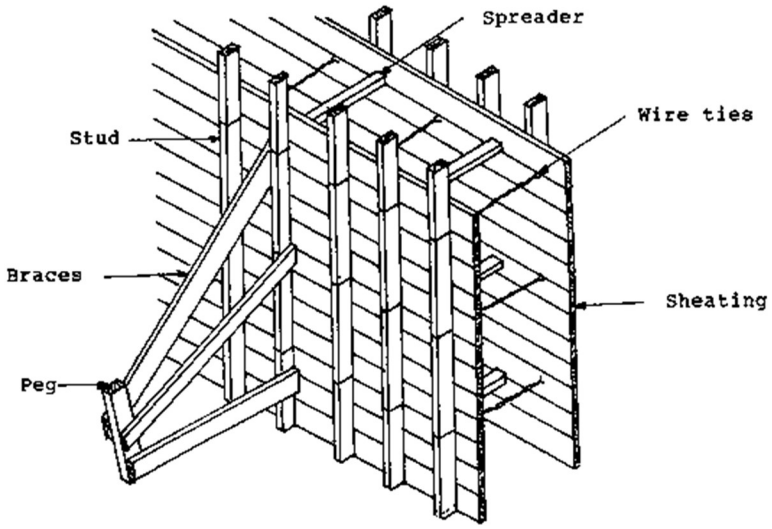

Figure 2-1: A timber wall formwork system (Source: https://theconstructor.org/building/formwork-shuttering-types-walls-columns-footings-slabs/11076/)

Vertical slipforming is most often used to construct large chimneys, cores of high-rise buildings or towers and pillars for oil platforms (Figure 2-2b). In an efficient slipforming process the slipping velocity and thus vertical building speed can range from 40-60 cm/hour. It is also possible to create structures with a variable cross section such as conical towers by changing the cross section of the formwork, usually done by manually adjusting spindles. Slipforming in the construction industry is usually only economically interesting from structures above 10 meters, because of the high initial costs of the formwork [15].

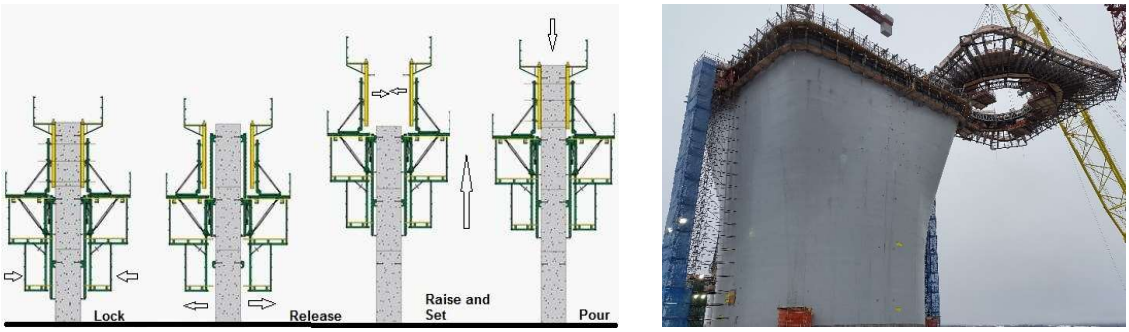

Figure 2-2: a) Diagram of concrete slipforming process (Source: Bruce Paulmac, Wikimedia Commons). b) Slipforming of the Hebron Main Shaft in Newfoundland, Canada [16].

2.2 Digital fabrication of concrete formwork

As described in Section 1.1 it can be very cost- and labour intensive to produce concrete formwork for non-standard shapes. In the last decade methods have been investigated to make non-standard formwork more efficient, by employing digital fabrication methods. These methods range from subtractive, such as milling or wire cutting to additive methods using 3D printing and adaptive fabrication methods such as configurable formworks and

robotic slipforming. This section describes several of these methods and their relevance to the research in this thesis.

All of the methods discussed address either one or more of the following objectives: 1) more material-efficient formwork fabrication process, 2) allowing for geometrical freedom in concrete construction, 3) realizing structurally optimized geometry. As the Eggshell fabrication process aims to provide all three, it is important to note how successful each method is in achieving these objectives.

2.2.1 Subtractive fabrication of formwork

Subtractive fabrication of formwork consist of taking a solid block of a chosen material and subtracting material by means of a computer numerically controlled (CNC) process. Often this process is CNC-milling but it can also be robotic hot blade cutting or robotic hot wire cutting.

Expanded polystyrene (EPS) foam is a popular option for subtractive formwork fabrication, as material can easily be removed, it is available at low-cost and is lightweight. The process of using CNC-milled EPS foam to produce formwork was successfully demonstrated with the construction of the Unikabeton Prototype (Figure 2-3) by researchers from a team which included the Aarhus School of Architecture [17]. The structure's geometry was designed by means of topology optimization, a computational method where within a chosen design space material is added and subtracted to achieve the theoretical optimum of the highest stiffness and lowest material usage [18].

Figure 2-3: The Unikabeton Prototype. a) Assembly of polystyrene moulds at the building site. b) Finished structure [17].

Although by CNC-milling EPS foam blocks a wide range of geometries can produced, it is time-consuming and has a high material waste. In an attempt to reduce material waste, several re-useable materials are being investigated. One approach, currently being researched at the TU Braunschweig uses CNC-milling to remove material from cold blocks of wax which are then used as concrete formwork [19]. The removed wax can be captured and re-melted into blocks of wax. Another method, researched at KTH Institute of Technology, uses ice as the material of choice for CNC-milling [20].

One of the drawbacks of CNC-milling is that it is a slow process. To overcome this, hot wire cutting methods have been developed to shape EPS blocks. The Danish company Odico [21] has successfully demonstrated hot wire cutting as a feasible method for formwork production in a collaboration with TU Delft's Hyperbody group [22]. Hot wire cutting is much faster compared to milling; however, it is only possible to produce ruled surfaces. To expand the geometry to double curved surfaces, hot blade cutting has been developed which uses a hot blade controlled by two robotic arms [23]. A similar method called Spatial Wire Cutting has been researched at the ETH Zurich, using two robots that guide a hot wire through foam [24].

The approaches described are more effective in producing non-standard concrete formwork than traditional methods using timber, which highly depend on the skill of craftsmen and are very labour and material-intensive. These subtractive methods, however, still remain wasteful processes. For the construction of the Kirk Kapital building in Vejle, Denmark, Odico reportedly produced around 4500 m^3 of foam formwork [25], of which all of it had to be discarded after the construction.

2.2.2 Additive fabrication of formwork

Additive manufacturing (AM) is often described as a more material-efficient alternative to methods of subtractive fabrication. Because of its geometric flexibility AM has also been explored as a method of formwork production. As AM has the advantage that material can be only deposited where needed, it does not produce waste from removing material.

Figure 2-4: a) FDM formwork for skelETHon, the Concrete Canoe. b) Resulting concrete canoe after casting [26].

One relevant project to this research is skelETHon, the Concrete Canoe by researchers from the ETH Zurich (Figure 2-4) [26]. A concrete canoe is constructed using formwork produced with Fused Deposition Modelling (FDM). The formwork is 3D printed in parts using desktop 3D printers and then assembled. During casting the formwork is buried in sand to resist the concrete's hydrostatic pressure. It proved successful to construct a complex structure using FDM printed formwork; however, addressing the hydrostatic pressure of the concrete remains a difficult task.

Instead of using FDM, other techniques such as binder jetting with sandstone have also been used to construct concrete formwork [27]. As binder jetting is a fabrication process with a large geometrical freedom, a complex, optimized floor slab could be produced. Recently, researchers at ETH Zurich's Digital Building Technologies group have also showed it is possible to scale up this technology by constructing a 70 m^2 topologically optimized ceiling using sand-stone binder jetting in an experimental building site in Switzerland [28].

One more possibility of additive formwork fabrication is using concrete extrusion to produce formworks for concrete. In this process the speed and geometric freedom of concrete extrusion is combined with traditional concrete casting to produce geometrically complex structures. The formwork can be removed after casting or stay as a stay-in-place formwork. One notable example of a structure made with concrete 3D printed formwork is a column fabricated by French company XtreeE for a school in the south of France [29].

Additive fabrication of formwork has proven itself to be an effective method for producing material-efficient, geometrically complex formworks for concrete. There are however still several disadvantages to the method such as: long fabrication time for full-scale building elements, difficulty of resisting hydrostatic pressure for thermoplastic formworks and challenges of reinforcing the structures.

2.2.3 Adaptive fabrication of formwork

Instead of fabricating a formwork either by subtractive or additive means there are also several research projects that use a reconfigurable or adaptive formwork to produce non-standard structures. Advantages of this method are that they can be essentially waste-less, as the formworks can be reused. These individual processes are usually particularly well suited for a certain type of objects (such as façade panels or columns) and do not attempt to provide a generic solution for all geometries.

One method which has been under investigation for several decades is that of the flexible mould (Figure 2-5a). It consists of a grid of pins which can be adjusted to generate a double-curved surface on top of the pins. On top of this surface concrete can then be casted to create a non-standard panel element. Researchers at TU Delft have explored this method and produced several prototypes using an actuated mould [9].

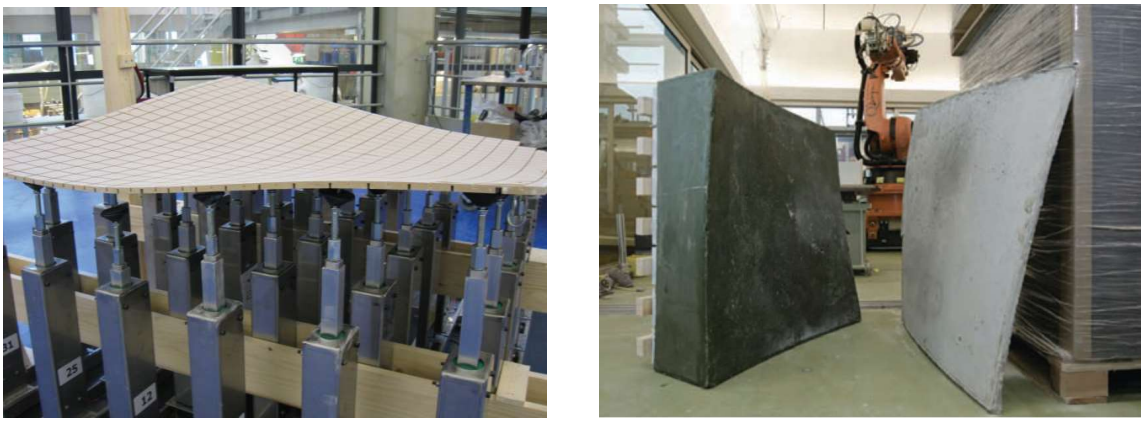

Figure 2-5: a) Flexible mould system from TU Delft [9]. *b) Tailorcrete, ETH Zurich, left: wax formwork, right: concrete element* [30].

In another approach called TailorCrete, by researchers from the ETH Zurich, a flexible mould system is used to create wax-formworks. Concrete is then casted into the wax formworks to create the finished structures. Instead of mechanically actuating the mould, a robotic arm is used to control the geometry pins that shape the final geometry [30].

An advantage of these processes is that no waste formwork is generated as the moulds are either reusable (in the case of the flexible mould) or recyclable (the wax formwork). One disadvantage, however, is that both processes can be time-consuming. This mostly stems from the fact that the finished concrete panel has to stay on the flexible mould for a certain amount of time while curing. During this time the mould cannot be used for the creation of other panels and therefore it can be difficult to scale-up production using a flexible mould system.

Another project which this research uses as a starting point is Smart Dynamic Casting (SDC) developed at the ETH Zurich in a collaboration between Gramazio Kohler Research and Physical Chemistry of Building Materials [13]. SDC is a continuous robotic slipforming process that enables the prefabrication of non-standard, material optimized, structural concrete structures. In this automated process a dynamic formwork significantly smaller than the structures produced is continuously moved vertically and filled with accelerated concrete. This is done with a velocity that enables to shape the concrete in the delicate phase when it changes from a soft to a hard material. Shaping the concrete is done by either rotating a fixed formwork or mechanically actuating a dynamic formwork in various ways.

During the first phase of SDC it was proven that concrete can be shaped in a robotic process, by producing column prototypes of an architectural scale (Figure 2-6a). In the second research phase, a suitable setup for prefabrication was developed for the fabrication of non-standard loadbearing elements. The result of this second phase was a number of reinforced façade elements for the DFAB House at the Empa premises in Dübendorf, Switzerland (Figure 2-6b) [31]

One of the main developments that was made in order to enable the production of the columns is the development of a suitable concrete acceleration strategy. The challenge here is getting

the process window exactly right for successful fabrication. After the concrete exists the moving formwork it has to be hydrated enough to carry its own weight; however, when still in the formwork it has to be soft enough to be shaped. Controlling this particular part of the process lies at the heart of the project. Although fifteen individual mullions were successfully fabricated, it proved difficult to fabricate the mechanically actuated formwork which was used to shape the mullions. As geometry becomes increasingly complex, so does the actuated formwork.

Figure 2-6: a) Column produced using SDC [32] *b) Mullion produced for the DFAB House (Source: http://www.dfab.ch/portfolio/smart-dynamic-casting-sdc/)*

2.3 Digital fabrication of concrete reinforcement

Although concrete performs very well when loaded in compression, it is weak when subjected to tensile forces. The tensile strength of concrete is usually only around 10-15% of its compressive strength [33]. To cope with this deficit in tensile strength, reinforcement is integrated in almost all built concrete structures. Nowadays steel is mostly used to reinforce concrete, although alternatives exist. Since the beginning of the 20th century, reinforcement has become a requirement in almost all concrete structures.

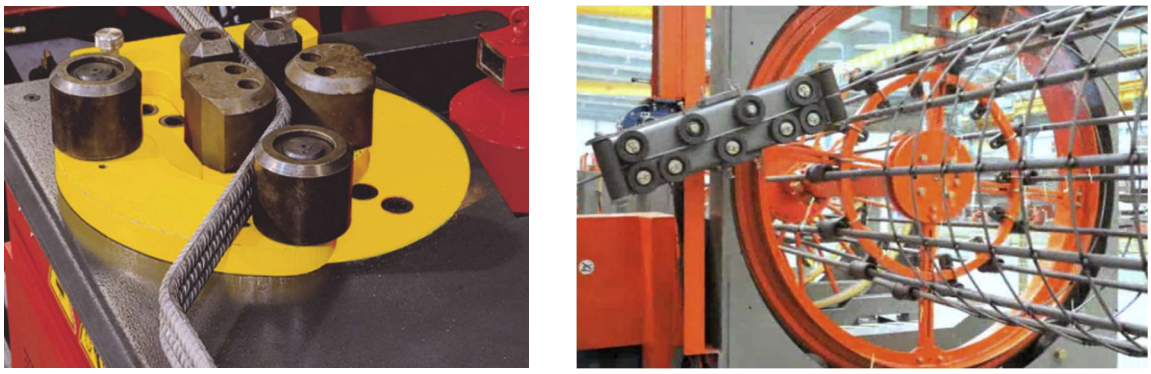

Figure 2-7: a) The "CS 440 Automatic Shaping Center" from the company MEP Group [34]. *b) Rebar cage welding machine from TJK Machinery* [35].

Typically, reinforcement follows the shape of the concrete structures it is imbedded in, as this is usually the most efficient way of transferring forces [33]. When considering non-standard concrete structures, this means reinforcement also has to be non-standard. In order to achieve non-orthogonal shapes, state of the art processes use devises such as "Automatic Link Benders" (Figure 2-7a) [34] or simple manual bending approaches using steel bending equipment.

In an automated process a straight bar is fed onto a turntable, where it is bent around a mandrel. Using this method both 2D and 3D bending of bars is possible. As an advantage, several bars can be bent simultaneously. This is an efficient method for producing curved bars; however, the bars have to be manually assembled after production and this can be laborious. One example of a process where an entire reinforcement cage is fabricated automatically is a "Rebar cage welding machine" (Figure 2-7b) [35]. The longitudinal reinforcement bars are placed manually into revolving discs, after which a coil is wound around, welding every intersection as the disc rotates. Using this approach cages can be made in an automated process with a cross-section ranging from 0.2 to 3 meters.

Further significant research is being conducted in the area of fibre reinforced concrete (FRC). In FRC steel, synthetic, carbon or glass fibres are being added to the concrete mixture. Adding fibres to the concrete has several uses, one of which being the ability to replace large single cracks with a dense structure of microcracks (Figure 2-8a), which may be acceptable from safety and durability standpoints [36].

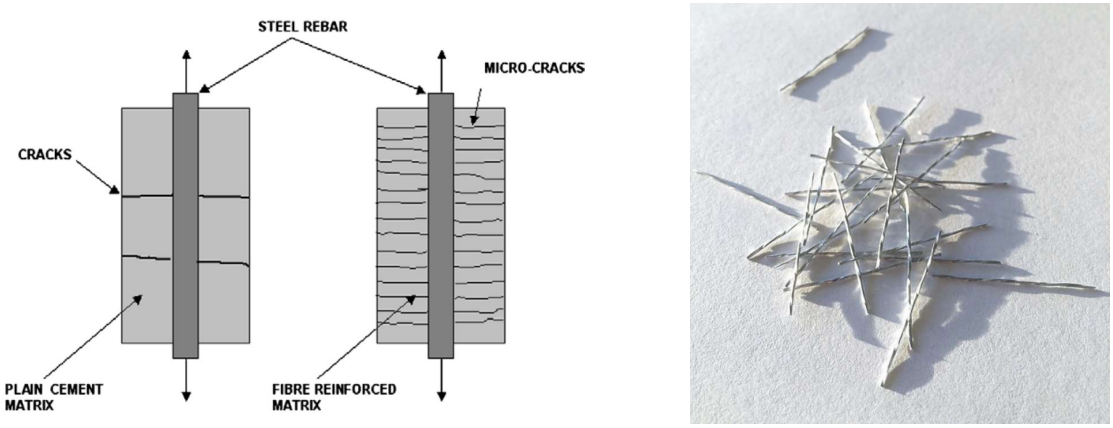

Figure 2-8: a) Crack pattern in reinforced concrete (RC) and fibre reinforced concrete (FRC) elements subjected to tension [36]. *b) Twisted steel fibres by the company Helix Steel* [37].

Although adding fibres to concrete certainly have many advantages it cannot yet replace conventional steel reinforcement in most cases. There are examples, however, of steel fibres replacing conventional reinforcement for applications such as floor slabs. One company called Helix Steel is producing a twisting steel fibre (Figure 2-8b) of which they claim is the only discontinuous concrete reinforcement product with an ISO certified design manual that can

be followed to design vertical applications (such as walls) with Helix Steel as the primary concrete reinforcement [37].

2.3.1 Unification of formwork and reinforcement

Another approach of reinforcing concrete structures is combining reinforcement and formwork into one single system. Several examples of this unification of formwork and reinforcement exist, which potentially could make both formwork and reinforcement more efficient. A disadvantage of this approach is that even though the formwork and reinforcement erection time might be quick, the finishing of the concrete structures is labour-intensive.

One research project which draws inspiration from ferrocement[2] is Mesh Mould, developed by researchers from the ETH Zurich [38]. It consist of a robotic process in which metal meshes are fabricated with a custom developed tool head mounted to an industrial robot. Metal bars are manually fed in and then cut to exact length, placed in position and welded together create a metal cage.

Figure 2-9: a) The Mesh Mould tool head b) Double and single curved metal meshes. c) Filling of a metal mesh with concrete [38].

Mesh Mould therefore aims to unify reinforcement and formwork into a single robotically fabricated material system. A concrete with a large aggregate size and long fibres is fed into the robotically fabricated meshes. The mesh holds the concrete in place, trapping it inside the metal cage. The structure is then finished by applying another layer of concrete to provide the minimum cover required.

A last research project discussed which unifies formwork and reinforcement, called Knitcrete, is conducted at the ETH Zurich [39]. This project uses a custom knitted textile as formwork and reinforcement. A fabric formwork is fabricated using a numerically controlled knitting machine. The knit is then tensioned into place using an external scaffolding. Once stretched into the correct position it is covered with a cement paste, a mortar and finally a layer of

[2] The origins of reinforced concrete can be traced back to the development of ferrocement in 1848 [89]. Ferrocement is a system of mortar, plaster or concrete, which is applied to a metal mesh. Although it proved to be a successful system for the construction of thin shells and hulls it was also labor intensive and not applicable for larger solid structures.

structural concrete. The knitted textile includes spaces for tensile reinforcement such as metal rods.

Figure 2-10: a) Knitted formwork underside. b) Finished concrete bridge [39].

The benefit of Mesh Mould and Knitcrete is the fact that it is material-efficient as one system (either a metal mesh or woven fabric) can be used as both formwork and reinforcement. One of the drawbacks of both systems are that additional steps are necessary to finish the structure. In the case of Mesh Mould, the fabricated structures have to be finished by hand to ensure the proper cover of the reinforcement and in the Knitcrete project multiple layers of concrete finishing are applied.

2.4 3D Printing

3D printing is an umbrella term used to describe various processes in which material is fused together to create a three-dimensional object [40]. The term 3D printing is often used interchangeably with additive manufacturing (AM). Although there are many different 3D printing processes, the research done in this thesis solely focuses on one: fused deposition modelling (FDM). If no other 3D printing technique is specified, it can therefore be assumed that 3D printing is used synonymously for FDM throughout this thesis.

2.4.1 Fused deposition modelling

Fused deposition modelling was invented and patented by Scott Crump, co-founder of the American company Stratasys in 1989 [41]. A diagram of a typical FDM setup can be seen in Figure 2-11. A mobile building platform (1) is used as a base for building the object. A thermoplastic filament (Figure 2-112) is then fed through rollers (3) which pushes the filament through a heated extruder (4). The extruder is usually mounted on a gantry system which allows it to deposit material in a layer by layer basis onto the build plate. Support material (5) can be used to fabricate objects otherwise impossible to build following the layer by layer approach.

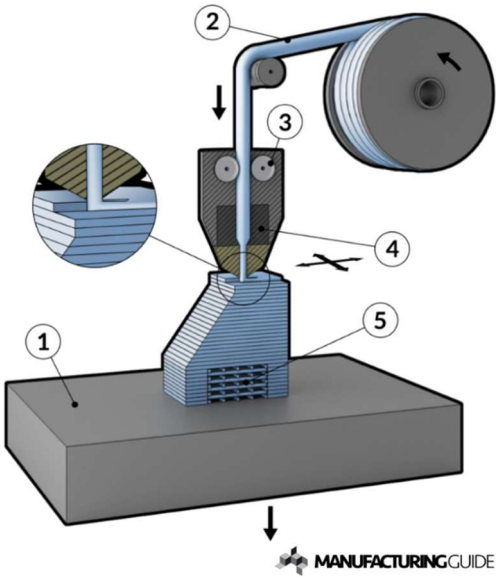

Figure 2-11: FDM process (Source: https://www.manufacturingguide.com/en/fused-deposition-modeling-fdm).

After FDM was commercialized by Stratasys the technology did not immediately become available to consumers, mostly because of the high costs of a 3D printer. An open source project started in 2014 by Adrian Bowyer called RepRap aimed to bring down these costs by openly distributing plans to build a 'self-replicating machine' [42]. The machines were designed so that they could manufacture a large portion of their own parts, bringing the material costs of a 3D printer down to around €350. Following the expiration of the Stratasys patent in 2009, many more manufacturers started offering affordable 3D printers to consumers, making the technology more widespread. Some of the most well-known brands today include: Ultimaker [43], Makerbot [44], Prusa Research [45], and Aleph Objects / LulzBot [46].

2.4.2 Robotic 3D printing

As early as 2010 Dutch designer Dirk van der Kooij designed and fabricated a chair that was robotically 3D printed using recycled plastic. Old refrigerators were disassembled, shred into granulate and extruded using a self-built pellet extruder [47]. An industrial robot was used because of its large reach and heavy payload, allowing the mounting of a heavy pellet-extruder.

Figure 2-12: a) The Endless chair designed by Dirk van der Kooij. b) The robotic setup used for fabrication (Source: https://www.dirkvanderkooij.com)

As robotic arms became more widespread in architectural research, projects started to emerge where a 3D print extruder was mounted onto a robotic arm. One of these projects which has been discussed earlier in an earlier section, Mesh Mould, used robotic extrusion of acrylonitrile butadiene styrene (ABS) to create mesh-like structures in an earlier phase of the research. Similarly to FDM, ABS is extruded from a nozzle but unlike FDM it is not deposited in a layered matter but instead extruded spatially. The ABS is cooled immediately once it exists the nozzle in order to be 'frozen' in space [38].

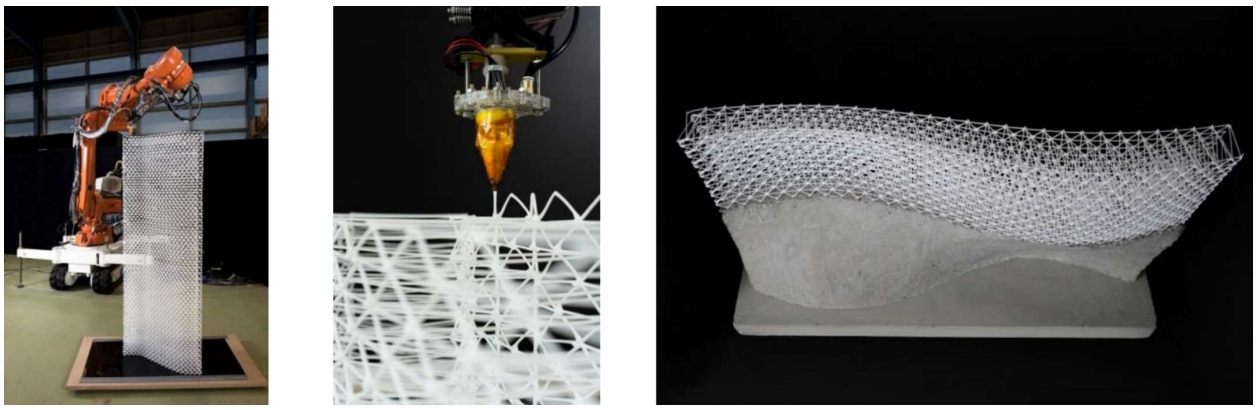

Figure 2-13: Three images showing the spatial extrusion of plastic meshes. a) The robotic arm fabricating a 1:1 scale prototype. b) ABS hardening in mid-air. c) The final mesh structure, half-filled with concrete to create a double curved wall element [38].

Several examples can be found of robotic 3D printing with other materials than thermoplastics, such as ceramics. Researchers at TU Delft's Hyperbody group propose a foam printing method dubbed Design To Robotic Production (D2RP) which includes a custom slicing system and motion path optimization [48]. Students from the Bartlett School of Architecture used a static clay extruder and a building platform mounted to a robotic arm to

produce clay elements of around half a meter in height [49]. Instead of moving the extruder such as is typical in FDM, they are controlling the movements of the building platform (Figure 2-14) At the Institute for Advanced Architecture of Catalonia (IAAC) one project dubbed Pylos [50] uses soil as a material for robotic 3D printing. These natural materials are a sustainable way of construction, however their mechanical properties are most often lower when compared to conventional building materials.

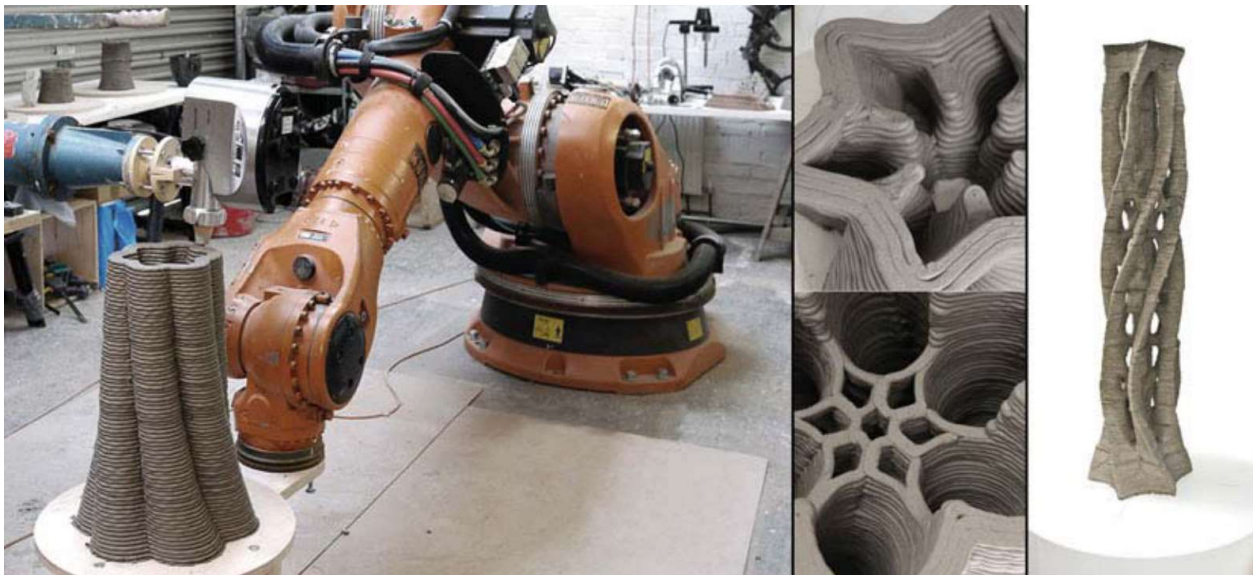

Figure 2-14: Clay extrusion at the Bartlett School of Architecture [49].

3 Methods and Materials

This chapter describes the experimental methods, materials and setup which have been used throughout this research. First, a description is presented of the fabrication process, for which two possibilities exist: simultaneous fabrication and consecutive fabrication. The robotic setup used is described including the filament extruder end-effector. The computational design and control system for the fabrication process are described in the next section. The last section provides a description of the concrete material mixes and processes used. In Figure 3-1 an overview of the setup during fabrication can be seen with the numbered elements matching the sections in which they are described.

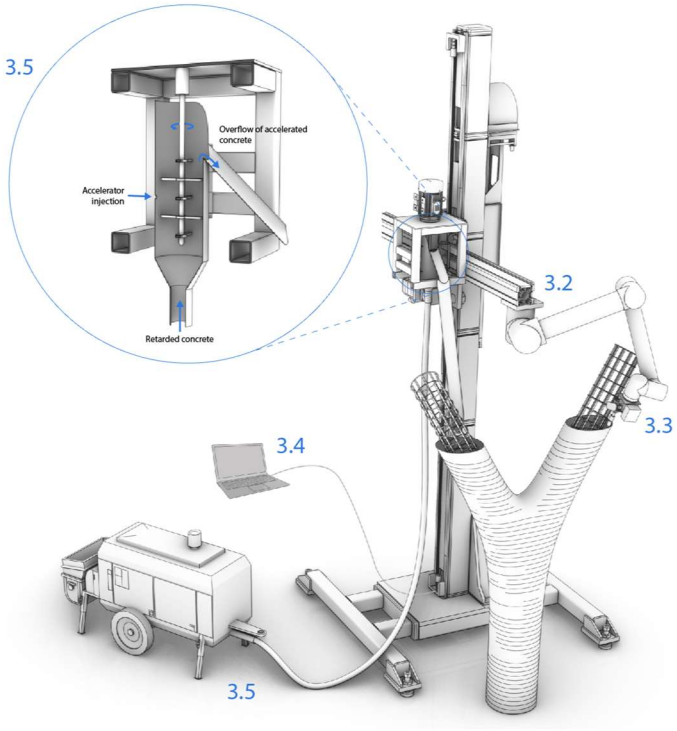

Figure 3-1: The complete Eggshell fabrication process.

The full setup used (Figure 3-1) consists of a six axis robotic arm mounted to an external vertical linear axis (3.2). Mounted to the robotic arm is a thermoplastic filament extruder (3.3) which is used to deposit plastic in a layer-by-layer, fused deposition modelling process. A computer running custom Python, Grasshopper and Arduino scripts (3.4) is used to control the 3D printing, as well as the concrete deposition. While the robotic arm is extruding plastic, concrete is continuously fed in. A concrete pump (3.5) pumps the concrete through a hose into a funnel with a mixer. In the mixer the concrete is mixed with an accelerator, causing the concrete to hydrate quicker. From the mixer the concrete flows into the just printed thin-shell formwork. During or after the process, reinforcement is added.

3.1 Fabrication process

In this thesis two fabrication processes have been considered, simultaneous fabrication and consecutive fabrication.

3.1.1 Simultaneous fabrication

Traditionally, concrete casting relies on a multi-step process: a formwork is erected, reinforcement is added and concrete is casted. In the simultaneous fabrication approach the process of creating a concrete structure is combined into one single step. A formwork is fabricated, whilst simultaneously reinforcement is added and concrete is cast (Figure 3-2). Because the different steps are executed in parallel this has the potential to be a more time-efficient process than a multi-step process. This is also similar to the approach adopted by the construction industry in slip forming of large concrete structures, in which a formwork is moved vertically while concrete is casted and reinforcing bars are inserted [14]. A simplified term for simultaneous fabrication is the *filling while printing* approach.

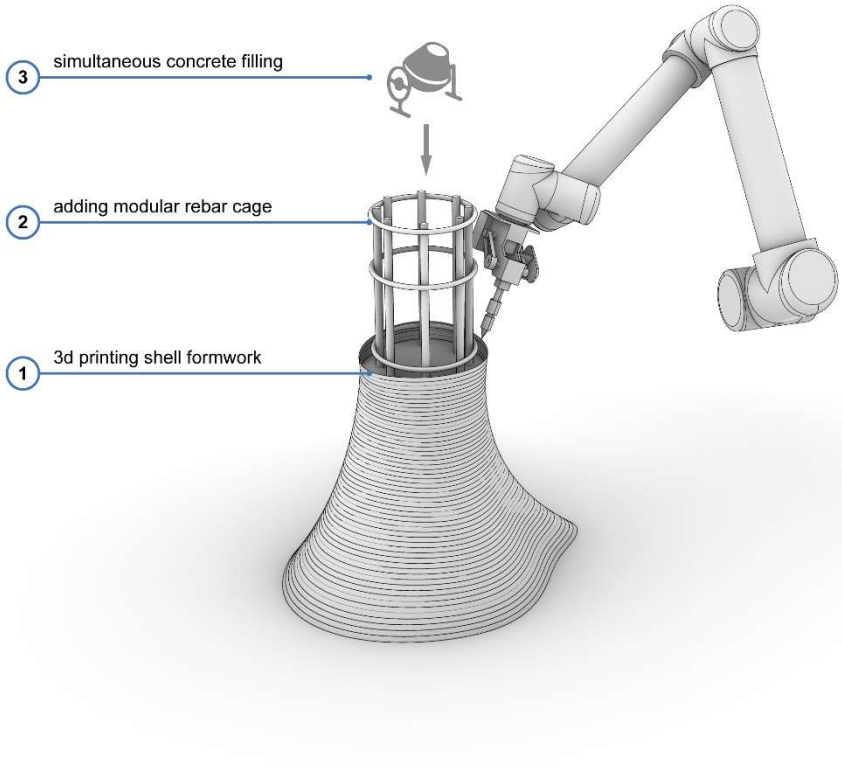

Figure 3-2: Column fabrication process of 3D printing, casting concrete and adding reinforcement simultaneously.

One disadvantage of simultaneous fabrication is that the individual processes can conflict when executed at the same time. When 3D printing and casting concrete simultaneously, the robot movements have to be calibrated appropriately with the concrete casting, so no concrete gets deposited on the moving robot. When adding reinforcement into the process, one more process has to be monitored for collisions, further complicating the fabrication.

3.1.2 Consecutive fabrication

Another option for fabrication the concrete columns is decoupling the processes into a scheme of consecutive fabrication such as depicted in Figure 3-3. By doing so, the process is more closely related to conventional concrete construction. An obvious advantage of consecutive fabrication is that conflicts between the individual processes are avoided. One disadvantage is that more intricate printed geometries might be impossible to fill with concrete due to concrete build-up on the sides of the formwork. Another disadvantage is that it could be impossible to intermix two casted layers in the formwork, as they are enclosed by the formwork. Furthermore, the entire process is more time-consuming than simultaneous fabrication. A simplified term for consecutive fabrication is the *filling after printing* approach

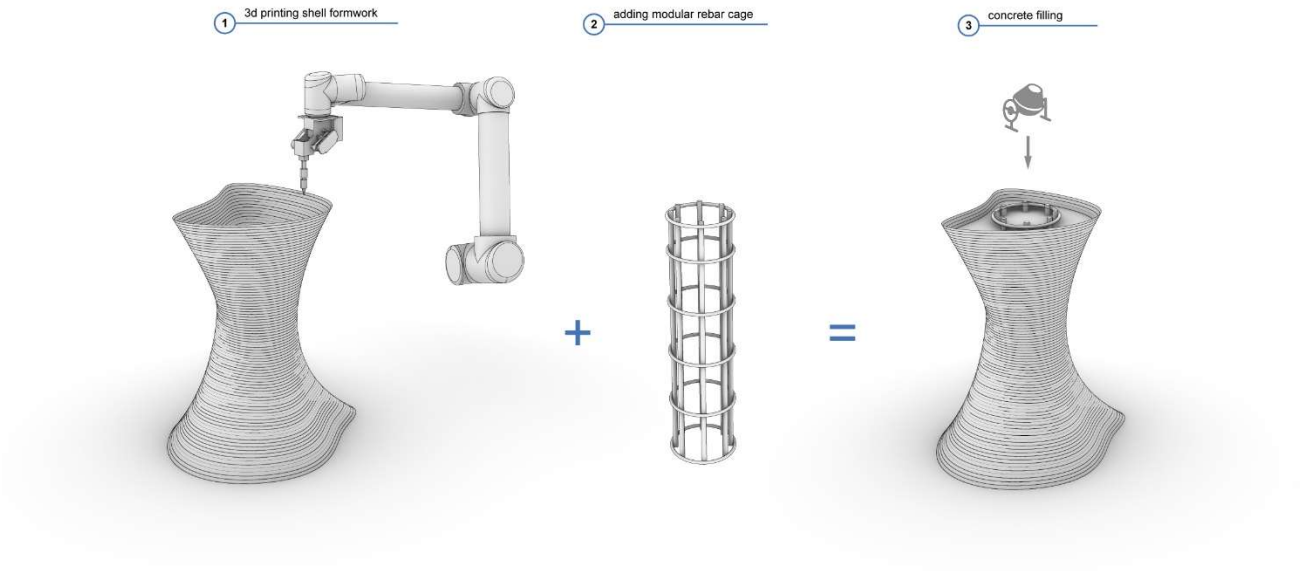

Figure 3-3: Column fabrication by consecutively 3D printing, adding reinforcement and casting concrete.

3.2 Robotic setup

The robotic setup used in this thesis consists of a six axis robotic arm (type Universal Robot UR10 [51]) mounted on a vertical linear axis. The end-effector attached to the robot is a filament extruder which extrudes 2.85mm filament with a nozzle diameter of 1.50mm. Further description of the filament extruder is provided in the following section. The objects are fabricated on a wooden platform which functions as a printing base. As the robot moves in horizontal layers, the vertical axis moves an arm vertically, allowing objects with a greater height to be fabricated.

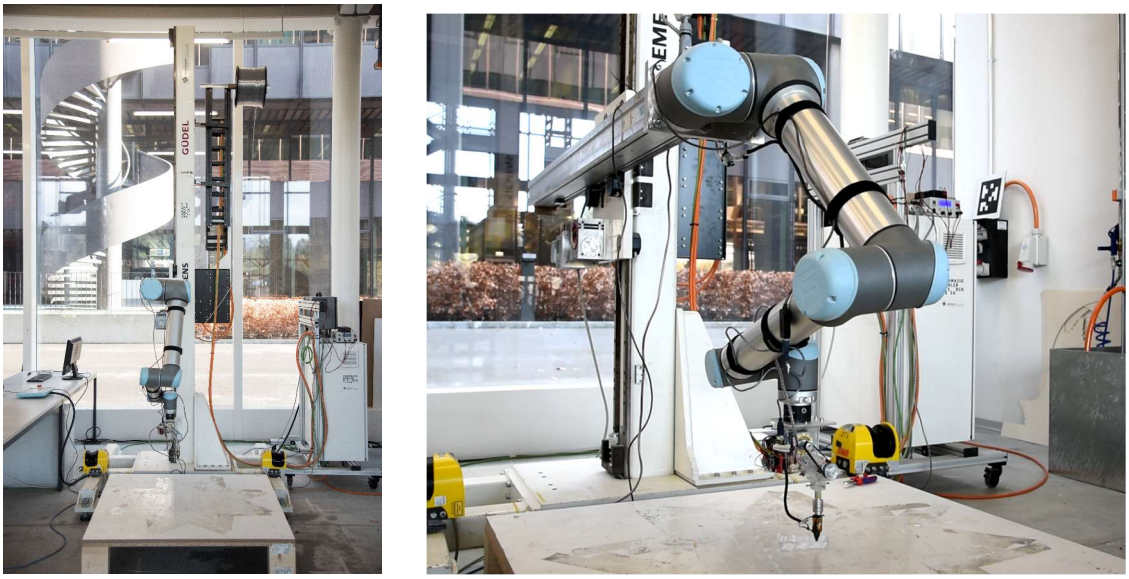

Figure 3-4: Robotic setup used throughout this research. a) Overview. b) Close-up.

3.3 3D Printing

3.3.1 Filament extruder end-effector

The tool used for 3D printing the shell formwork is a filament extruder (Figure 3-5), originally built for the teaching course Spatial Extrusions at Gramazio Kohler Research, ETH Zurich [52]. It consists of a NEMA 23 stepper motor which drives gears that are connected via a belt to two gears used to drive the filament. One important aspect to note is the opposite direction of rotation of the two filament-driving gears. This increases the grip on the filament as it is gripped from two sides.

The filament passes through a hole which orients it exactly above the gears. It then enters an aluminium heatsink where the filament is still in solid state. After the heatsink the filament passes through the heated nozzle where the filament gets heated to a temperature of around 200 °C. This makes the filament viscous enough to be extruded through the nozzle with a diameter of 1.5mm. The entire extruder and motor is housed in laser cut polycarbonate plates, connected with screws.

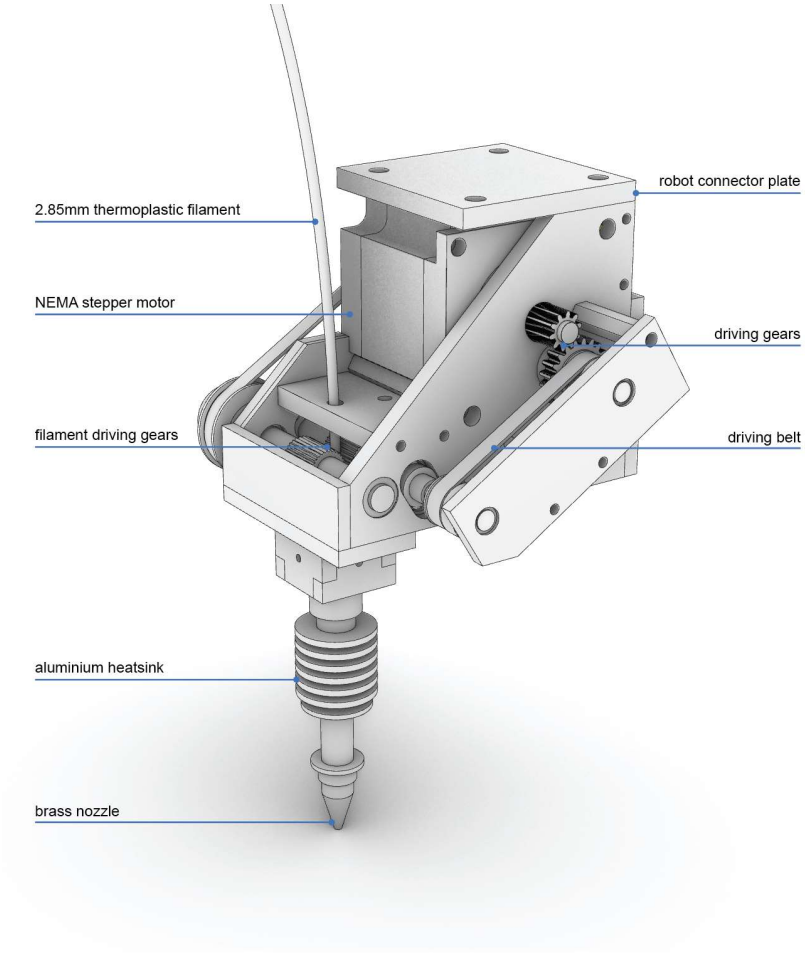

Figure 3-5: Filament extruder end-effector.

3.3.2 Extrusion parameters

In FDM many parameters play a role, of which the most important are described.

Nozzle diameter (mm)

The nozzle diameter determines the diameter at which the heated thermoplastic exists the nozzle. The nozzle diameter used throughout this thesis is kept at 1.5mm.

Layer height (mm)

The layer height describes the height difference between one deposited layer and the next. A lower layer height gives the printed object a higher resolution as the layers are less visible. A higher layer height means a lower resolution but also a faster total print time, as it takes less time to cover a certain height. The maximum layer height is highly dependent on the nozzle diameter and it cannot exceed the nozzle diameter as this would mean subsequent layers are not touching. Usually it is advised to have 75% of the nozzle diameter as a maximum layer height. The layer height for the experiments conducted in this research ranges in between 1.00 – 1.30mm.

Printing speed (mm/s)

The printing speed determines the speed at which the extruder moves while extruding. A higher printing speed means a faster print time. However, the flow rate needs to increase together with the printing speed as more material needs to be deposited in the same amount of time. Maximum printing speed is limited by nozzle diameter, layer height, flow rate as well as the mechanical performance of the 3D printer (stiffness of the frame). The printing speed used throughout this thesis ranges in between 30 – 60 mm/s.

Extrusion temperature (°C)

The extrusion temperature or nozzle temperature determines the temperature to which the material is heated before extrusion. The extrusion temperature is highly dependent on the melting temperature of the thermoplastic used. As the material used throughout this thesis is kept unchanged the extrusion temperature is also kept at a constant 210 °C.

Flow rate (mm^3/s, kg/hr)

The flow rate is the rate at which material is pushed through the nozzle and thus determines the output. The flow rate can be calculated by multiplying the extrusion area with the printing speed: pi * (nozzle diameter / 2)^2 * printing speed. In order to achieve a higher flow rate it is also necessary the heating capacity is increased, because more material has to be heated within the same timeframe. The flow rate during the experiments conducted in this research is dependent on the printing speed and ranges in between 70 – 105 mm^3/s.

Build volume (cm x cm x cm, cm^3)

The build volume describes the maximum volume in which the 3D printer can build an object. A typical desktop printer such as the Prusa i3 has a build volume of 10,500 cm^3 (25 x 21 x 20 cm). A so called 'large scale 3D printer' such as The Box by the Swedish company BLB Industries [53] in comparison has a build volume of 150 x 110 x 150 cm, amounting to a total build volume of 2.475.000 cm^3. This is, however, not typical and one would only find a handful of companies manufacturing 3D printers of this size. The build volume of the robotic setup used is 120cm (length) x 120cm (width) x 300cm (height), so 4.320.000 cm^3.

3.3.3 Materials

Almost any thermoplastic can be used for FDM 3D printing and thus many are available. A few of the most common printing materials are shown in Figure 3-6.

Material	Melting temperature (°C)	Tensile strength (MPa)	Young's modulus (MPa)	Density (g/cm^3)	Comments
ABS	180 – 200	42.5	2150	1.05	
PLA	190 – 200	61	3500	1.22	
PET-G	180 – 200	50	2040	1.30	Good chemical resistance
TPU	180 – 200	42	4000	1.15	Flexible
Nylon	225 – 265	70	1800	1.15	

Figure 3-6: Various materials available for FDM and their properties. Data shown is based on filament from the company extrudr [54] .

The material which is used for this research is a 2.85mm PET-G filament from the company extrudr [54]. More characteristics of the material can be found in Appendix A. The reason the material of choice is PET-G, even though ABS or PLA have superior mechanical properties, is that PET-G overall has a better chemical resistance [55]. As fresh concrete has a highly basic pH value of around 13 [56], the thermoplastic shell should not weaken when brought in contact with concrete.

3.4 Computational design and control

3.4.1 Traditional 3D printers

Traditional 3D printers such as described in Section 2.4.1 are controlled using G-code. G-code consists of a list of textual commands that describe actions or movements. These actions and movements are then executed by the 3D printer to perform the steps needed to complete a 3D print. An example line of G-code sent to a 3D printer might be [57]:

```
11    G1    F900  X197.600    Y29.900     E19.82400
```

Where:

```
11:         Number of line
G1:         Command, in this case 'linear move'
F:          Speed
X/Y/Z:      Coordinates
E:          Feeder movement
```

G-code is not typically generated by users themselves, instead so called 'slicing software' is used. Examples of popular software are: Simplify3D [58], Ultimaker Cura [59] and Slic3r [60]. Within these software programs one can import a 3D model generated in a computer aided design (CAD) software. The 3D model is then analysed and 'sliced' into layers based on a layer height that is defined by the user and the 3D printer model. If the object imported is a

solid, usually the user can select an infill percentage which defines the amount of material that is placed within the object. If the object contains large overhangs, most programs also include the option to add support material that can be removed post-printing. After defining these settings all of the information is converted into g-code which can be transferred to a 3D printer. See Figure 3-7 for a diagram of the process.

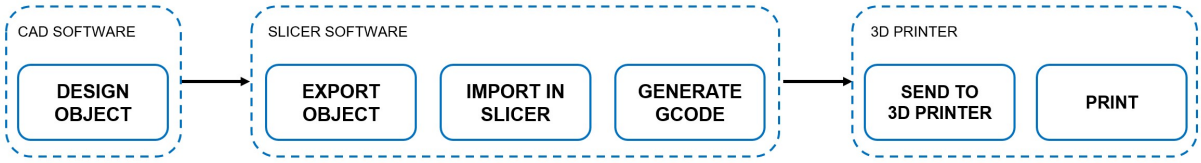

Figure 3-7: Diagram showing traditional 3D printing workflow

3.4.2 Robotic 3D printing

Robotic 3D printing is very similar to 3D printing with a regular 3D printing machine; however, there are some differences. One large difference is that a robotic arm is not controlled using g-code (although converters exist [61]) but most often use a manufacturer-specific programming language. In the case of the UR10 robotic arm used in this thesis this language is UR Script.

Using UR Script the UR10 can be programmed to execute various commands. One of the most important commands is the Linear Move (MoveL) command. This command instructs the robot to move from one plane in space to another plane using a straight line. An example of using the command is:

```
ur.send_command_movel([x, y, z, ax, ay, az], v=speed, r=radius,
a=acceleration)
```

Where:

```
x, y, z:          Coordinates of plane to move to in the robot
                  coordinate system
ax, ay, az        Rotation angle of plane to move to
speed:            Movement speed of robot
radius:           Blend radius between two points
acceleration:     Acceleration of robot
```

By sending multiple coordinates using the MoveL command, the movement part of the 3D printing process is taken care of. What is left is the control of the extruder. The extruder is controlled separately using the open source electronics platform Arduino [62]. Using a custom Arduino script a stepper motor is controlled which drives the gears that feed the filament. The Arduino script also controls a heating wire wound around the hot end of the extruder. A thermistor is used to measure temperature. When the temperature measured is below a set threshold value, the heating wire is turned on and when the temperature reaches the set temperature the heating wire is turned off.

A simplified script for robotically 3D printing a square with two layers (total of nine points) therefore might be:

```
1 UR        Move to home coordinates
2 Arduino   Turn on heating wire
3 Arduino   Wait until set temperature has been reached
4 Arduino   Turn stepper motor on
5 UR        Move to pt[0]
...         ...
13 UR       Move to pt[8]
14 Arduino  Turn stepper motor off
15 Arduino  Turn off heating wire
16 UR       Move to home coordinates
```

The movement data for the robot is thus not generated by an external program such as slicing software, but simply generated directly in the CAD software. The only external input necessary is the control of the extruder which is not directly integrated into the CAD software (See Figure 3-8 for an abstracted diagram of the process and Figure 3-9 for the full flowchart).

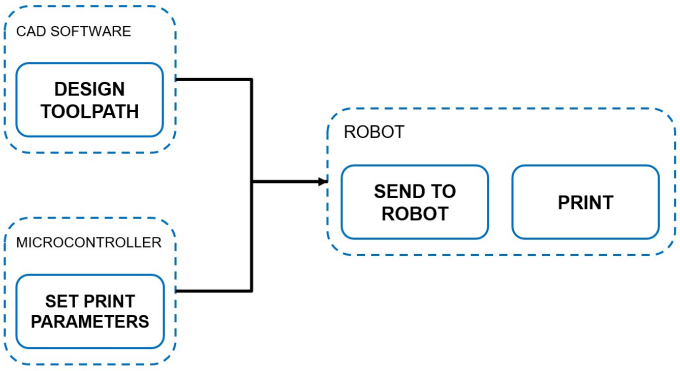

Figure 3-8: Robotic 3D printing workflow.

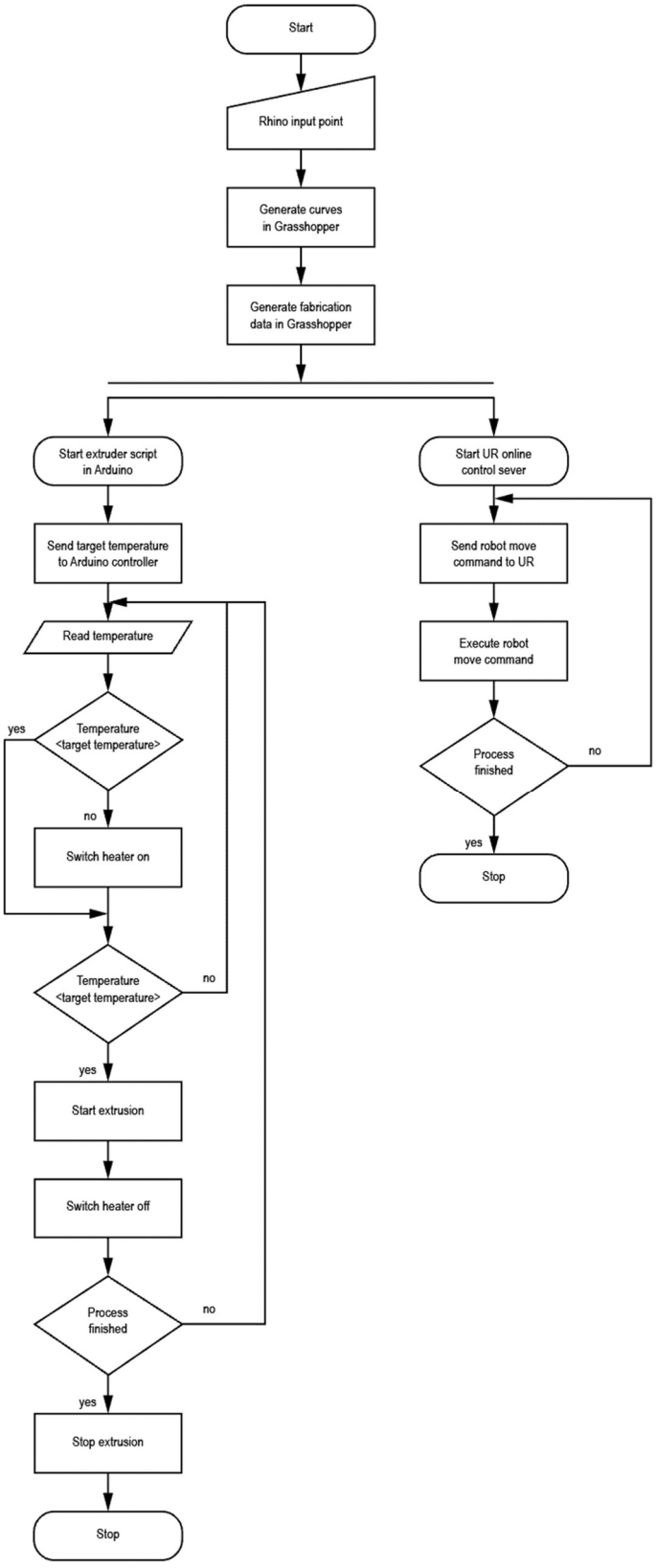

Figure 3-9: Flowchart diagram of entire design and fabrication process of 3D printing.

3.4.3 Printing path generation

As explained in the previous section, the design process of the objects described in this thesis is different from most objects designed for 3D printing. Instead of generating a shape using CAD software and then generating the toolpath using slicing software, the toolpath is directly generated from the CAD program. In Figure 3-10 an example can be seen for the toolpath generation of a simple, extruded, rotated triangle such as fabricated in Section 4.1.1.1.

To design this toolpath the following strategy is followed:

1. Base plane for the geometry is chosen
2. Three planes are generated around the base plane with a certain distance `[radius]`
3. The three planes are copied in the z direction a certain amount of times `[number_of_layers]` with a certain distance `[layer_height]`.
4. The resulting planes are rotated around the base plane with a certain rotation angle `[rotation_angle]`

The parameters that influence the design are therefore: `radius`, `number_of_layers`, `layer_height and rotation_angle`.

An advantage of this design strategy is that one has direct control over the complete toolpath and thus the robot movements. The designer is able to directly send the desired geometry to the robot without any interference from other software. One can also easily implement certain fabrication constraints into the design, such as maximum angle between layers or maximum length of straight paths. A disadvantage is that one can only design using the manipulation of points and other techniques such as mesh editing or the lofting of curves are not directly available.

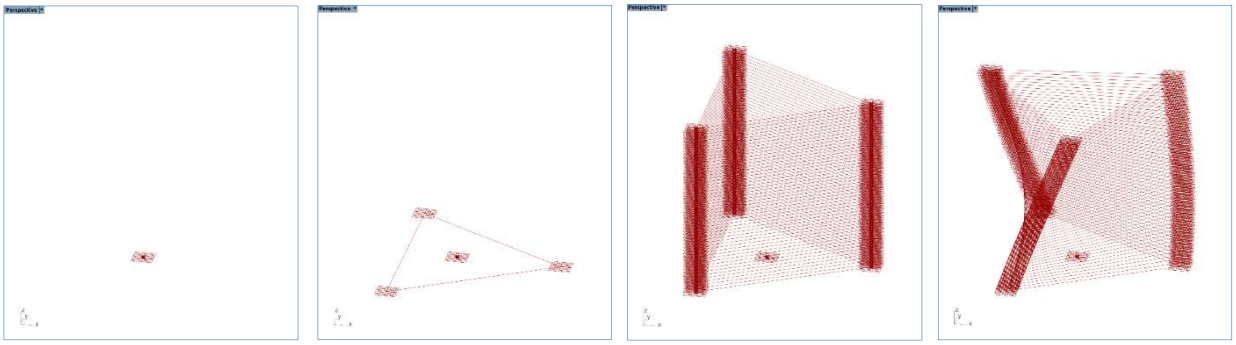

Figure 3-10: Example of the toolpath generation of an extruded, rotated triangle. a) Starting with a single plane. b) Generating three planes around the base plane. c) Copying these planes up according to the layer height. d) Rotating these planes around the base plane to generate the final shape.

3.5 Concrete setup

3.5.1 Acceleration and casting process

The key technology for allowing concrete to be placed in a thin formwork without causing the formwork to break due to the hydrostatic pressure of the concrete, is the controlled addition of an accelerator. This accelerator causes the concrete to rapidly hydrate, enabling the concrete to sustain its own weight. The process of using an accelerated concrete to create columns was developed in the interdisciplinary research project Smart Dynamic Casting [32].

For a fabrication process where one has control over the exact time of hydration of the concrete, it is most important when and how the accelerator is added. Two ways of acceleration and casting are used throughout this thesis and are described below.

3.5.1.1 Manual acceleration and casting

In the process of manual acceleration a person is manually controlling the time after which the accelerating admixture is added. The process consists of the following steps:

1. Mixing a large batch of retarded concrete.
2. Dividing the large batch into multiple smaller batches.
3. Adding the accelerator to a small batch of retarded concrete and mixing.
4. Dividing the small, accelerated batch into multiple layers.
5. Casting the layers into the formwork with a certain interval between layers.

3.5.1.2 Automated acceleration and casting

In the process of automated acceleration and casting the process described in the previous section is automated. This is done with a computer-controlled concrete pump and mixing funnel [63]. The process can be described as follows (Figure 3-11):

1. Mixing a large batch of retarded concrete.
2. Placing the large batch into a pump which is connected to a mixing funnel.
3. The concrete pump pumps retarded concrete into the mixing funnel at certain intervals (3).
4. In the mixing funnel an accelerator is added to the retarded concrete and mixed for a certain amount of time (4).
5. The mixing funnel overflows with accelerated material due to new material pumped by the concrete pump, the accelerated material flows into the formwork (5).

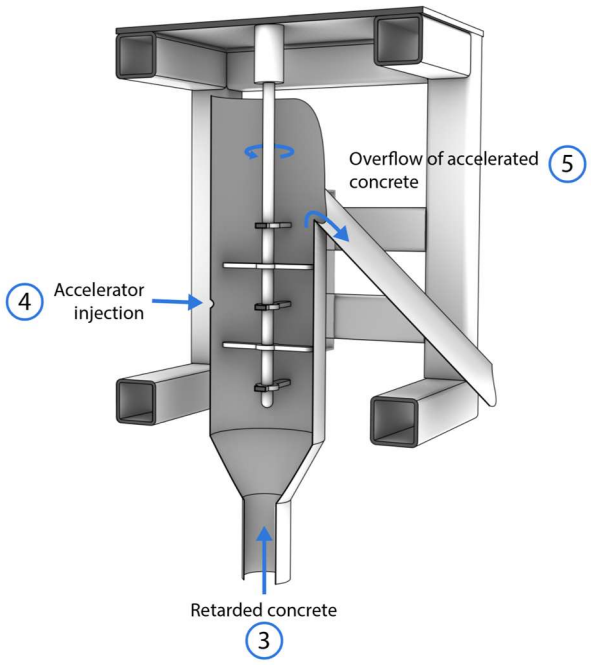

Figure 3-11: Diagram of mixing funnel.

3.5.2 Concrete mixes

Two concrete mixes have been used for the experiments conducted in this thesis. The materials of the mixes can be found in Figure 3-12.

Mix 1 – SDC

The first mix is a mix which was modified from the mix used during the project Smart Dynamic Casting [32]. As binders it contains a CEM I 52.5R Portland cement, Normo 5R from Holcim AG, a Class F pozzolanic coal fly ash, also from Holcim AG and a Elkem Micro silica 971-U from BASF. The aggregates consist of fine sand with a maximum diameter of 4mm, which classifies it as a mortar rather than a concrete [64]. To enable the concrete to be workable with a low water to binder (w/b) ratio of around 0.25, a Glenium ACE 30 superplasticizer from BASF is used. To delay the hydration of the mix, sucrose from Sigma-Aldrich is used as a retarder. Finally, to cancel the effect of the retardation from the admixtures a SikaRapid C-100 accelerator is added.

Mix 2 – SACAC

The second mix is a mix under development by the Physical Chemistry of Building Materials group at ETH Zurich. It consists of the same cement, fly ash and micro silica base; however, it has larger aggregates up to 8mm in diameter which classifies it as a concrete. As admixtures it makes use of the same superplasticizer, but also stabilizer is added, Stabilizer-4R by Sika. The SACAC mix also contains polypropylene (PP) fibres with a diameter of 18 μm.

	Mix 1 - SDC	**Mix 2 - SACAC**
Binders	Cement	Cement
	Fly ash	Fly ash
	Micro silica	Micro silica
Aggregates	Fine 0-4mm	Fine 0-4mm
		Coarse 4-8mm
Admixtures	Superplasticizer	Superplasticizer
	Retarder	Stabilizer
	Accelerator	Retarder
		Accelerator
Additional		Fibres
Water	Water	Water

Figure 3-12: Materials in the concrete mixes used throughout this thesis.

4 Experiments and Results

This chapter describes a number of experiments that have been done to gain knowledge on the possibilities of fabricating large-scale, structural columns, as described in the objectives in Section 1.1. Every section in this chapter contains an experiment which is described by stating the motivation, method and results and a discussion and conclusion.

4.1 Phase I: Explorations

The experiments conducted in this phase have been done by the author prior to starting the official thesis period. They are, however, important to describe as the work done in Phase II and Phase III is based around knowledge gained during Phase I. The concept of the experiments conducted was developed by during an interdisciplinary master thesis project [5] in a collaboration between Gramazio Kohler Research, the Institute of Robotics and Intelligent Systems and the Physical Chemistry of Building Materials group (ETH Zurich).

This section describes the work that has been done in the "Exploratory phase". Several prototypes were made as a 'proof of concept' that the process of using thin-shell formworks can be used for constructing objects above 1m of height.

For all of the prototypes described the method of 'simultaneous fabrication' (Section 3.1.1) was used. This means concrete was filled in to the formwork while the 3D printed formwork was being 3D printed. The acceleration of the concrete was done using automated acceleration such as described in Section 3.5.1.2.

4.1.1.1 Prototype 1: Twisting triangle

The geometry that was printed was a twisting extruded triangle with a height of 300mm and a length of 150mm per side. It was printed and simultaneously filled with accelerated concrete over a time of 2 hours. The layer height varied between 0.25 – 0.40mm over three tests and the robot was moving at a speed of 50 mm/s. This amounted to a vertical build rate of 150 mm/hr or 2.5 mm/min.

In Figure 4-3 the result of this test can be seen. What can be clearly distinguished are the cold joints in between layers of concrete. When the time in between layers is too long, a layer is already hydrating before the next layer is cast on top. Because of this there is no proper layer intermixing, creating so called cold joints which can affect the mechanical performance and surface quality [65].

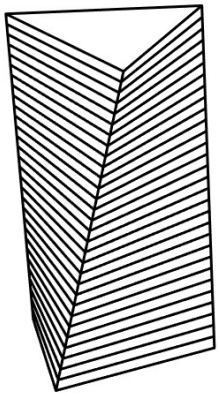

Height	300mm
Printing speed	50 mm/s
Layer height	0.25 – 0.40mm
Vertical build rate	2.50 mm/min
	150 mm/hr
Total time	2 hours

Figure 4-1: Geometry and parameters of first prototype

Figure 4-2: a) Final result first prototype. b) Close-up of surface with dotted lines indicating the different casting layers visible in the surface.

4.1.1.2 Prototype 2: Twisting hexagon

After the tests described in the previous section, it was clear that the issue of cold joints had to be resolved in order to create a structurally viable column. The cold joints stem from the fact that the time in between layers was too long. However, the filling time (and thus time in between layers) came from the vertical build rate which in turn is a product of printing speed and layer height. Printing speed and layer height therefore had to be improved in order to achieve a better result.

As the extruder used had already reached the maximum possible layer height and printing speed, it was decided to switch to another extruder (described in detail in Section 3.3.1). Using the new extruder a layer height of 1.20mm could be achieved, a factor three improvement of the previous extruder. This meant that when using the same geometry, vertical build rate would improve by a factor three as well. As it was also possible to build higher within the same timeframe another column geometry was designed in the shape of an extruded, twisting hexagon.

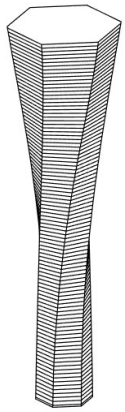

Height	900mm
Printing speed	50 mm/s
Layer height	1.00mm
Vertical build rate	5.90 mm/min
	350 mm/hr
Total time	3 hours

Figure 4-3: Geometry and parameters of second prototype

Because of the increased vertical build rate, the time in between layers had also been shortened. This would hypothetically cause fewer cold joints occurring. As can be seen in Figure 4-4 this the surface seems to show no signs of cold joints and looks satisfying. This shows the forming of cold joints and consequent influence on the surface texture can indeed be avoided by filling at a faster rate.

Figure 4-4: a) Final result second prototype. b) Close-up of surface.

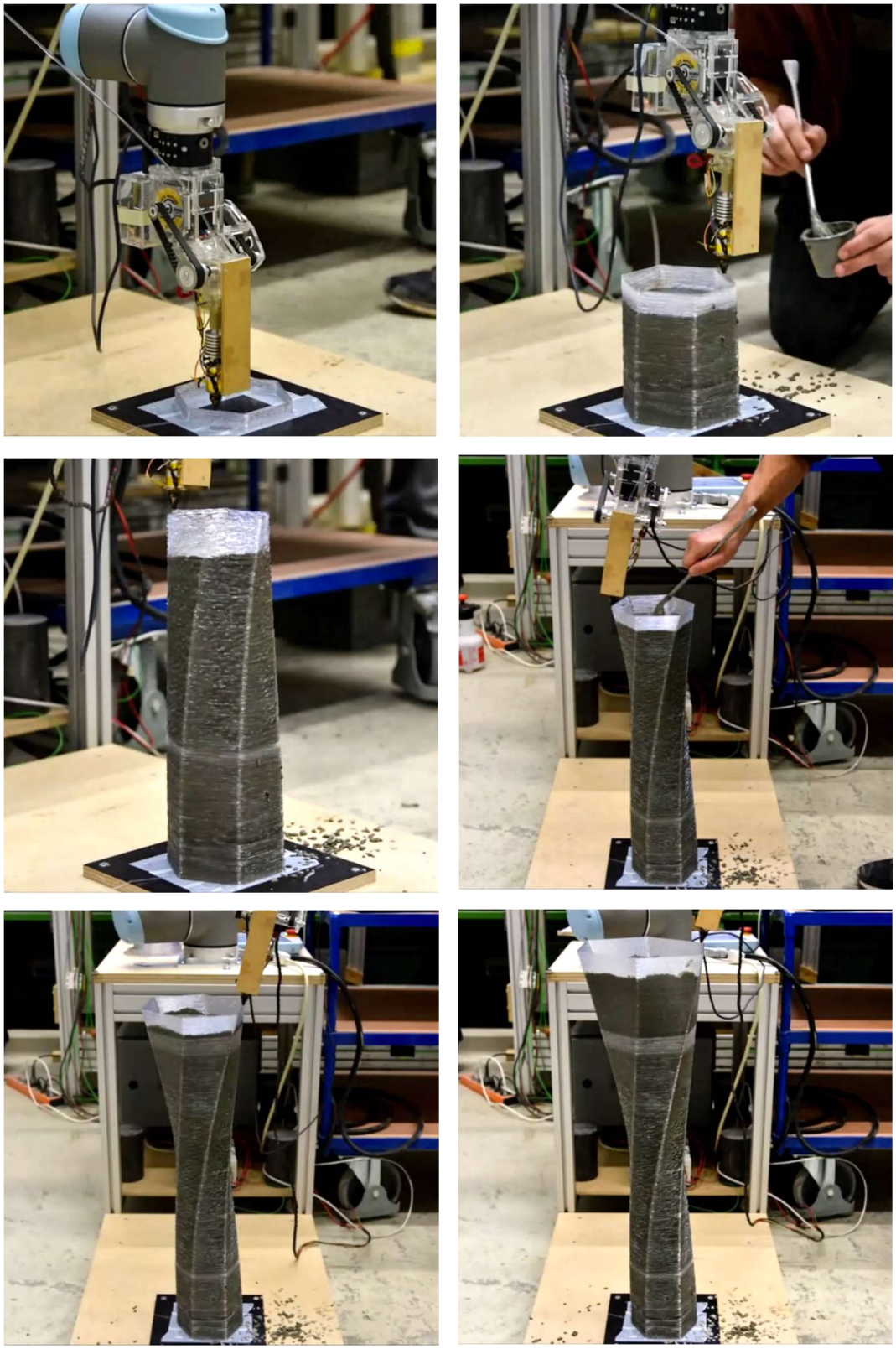

Figure 4-5: Fabrication process of second prototype

4.1.1.3 Prototype 3: Freeform branching structure

With a solution found for the occurrence of cold joints in the columns, more geometrical freedom could be explored. One area of interest where this fabrication technique could prove advantageous is the fabrication of branched columns. Branching columns offer the possibility of efficiently distributing loads but are typically difficult to fabricate, especially in concrete [66]. The third prototype should therefore aims to display these possibilities in a full-scale prototype.

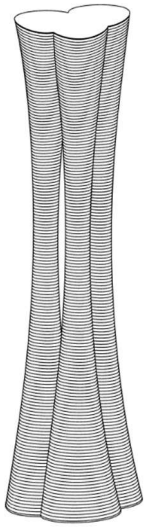

Height	1600mm
Printing speed	50 mm/s
Layer height	1.20mm
Vertical build rate	3.80 mm/min
	230 mm/hr
Total time	8 hours

Figure 4-6: Geometry and parameters of third prototype

As can be seen from the parameters in Figure 4-6 this column prototype has a lower average vertical build rate than the second prototype. This is, however, due to the larger volume and thus longer printing path, the printing parameters have been kept the same. The third prototype shows it is possible to realize branched structures in an efficient way. Producing this geometry would have been difficult to using, for example, CNC-milled formwork due to the small gaps in between column sections.

Figure 4-7: Finished third prototype

4.1.2 Discussion

From these three initial prototypes can be concluded that using thin-shelled formwork for concrete columns has a potential to be used in a structural, architectural context. However, these initial structures have all been unreinforced concrete, while in construction reinforcement is almost always a necessity.

Furthermore, filling of the prototypes while the robot was 3D printing proved to be a difficult exercise. As filling was done manually, the robot had to be evaded during the entire fabrication process. Although no collisions with the robot were made, if this would have happened the process would have stopped and it would have been difficult to restart. Also material processing proved to be of key importance to the filling. Working with a material that did not have the right fluidity or strength gain could cause major problems during fabrication and an insufficient surface and structural result.

4.2 Phase II: Scale-up

Phase I had shown that it was possible to fabricate columns above 1m in height. Although much had been learned about the process, all of the experiments were aimed at producing prototypes as a proof of concept. After the results from Phase I it was decided to apply the Eggshell technology on a real construction site, with the fabrication of this non-standard, structural concrete column.

The case study taken up in this thesis is a small pavilion outside the office of the Swiss engineering company Basler & Hofmann [77]. Basler & Hofmann are one of the leading Swiss engineering, planning and consulting firms. Their projects range from buildings, bridges and dams to tunnels and stations. For the redevelopment of their office in Esslingen, a small city around 15km outside Zurich, they are interested in exploring the possibilities of employing digital fabrication in architecture.

The pavilion consist of a robotically fabricated timber reciprocal frame structure, landing on a non-standard concrete column (Figure 4-8). The timber roof structure is designed and built using experience gained during several research projects at Gramazio Kohler Research concerning robotic timber fabrication [78], [79].

The shape of the column stems from the reciprocal frame roof structure. It follows the lines coming down from the roof by extending eight concrete ribs outwards to meet the timber beams. The column is hollow as there is a drainage pipe placed in the centre of the column.

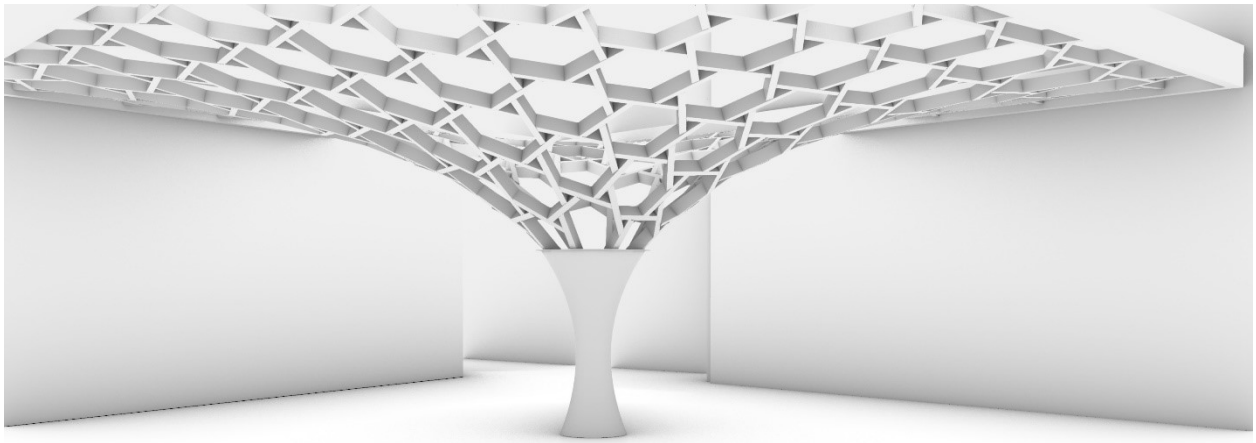

Figure 4-8: Sketch visualization of pavilion.

To be able to fabricate the column several questions had to be investigated and answered. This section describes a series of experiments which are conducted in order to make the fabrication of this case study possible. The experiments address integration of reinforcement, large scale 3D printing, formwork hydrostatic pressure resistance and the temperature development of concrete during hydration.

4.2.1 Integration of reinforcement

4.2.1.1 Motivation

All of the columns fabricated in the Exploratory Phase I (Section 4.1) had been unreinforced concrete structures. As reinforcement is an essential part of concrete construction and required by building regulations, this section will address the integration of reinforcement into the columns. Several experiments are conducted which aim to determine the most effective method (in terms of fabrication) of adding reinforcement to the columns.

4.2.1.2 Method and results

Several approaches can be considered for reinforcing the thin-shell formworks studied in this thesis. An overview of the approaches that were considered can be seen in Figure 4-9.

1	**3D Printing formwork around a prefabricated reinforcement cage** Use a conventional reinforcement cage and print around the cage with a six axis robot.
2	**3D Printing formwork around a prefabricated, modular reinforcement cage** Use a conventional reinforcement cage split up in parts and print around the cage with a six axis robot, whilst adding parts.
3	**Adding prefabricated reinforcement cage after formwork 3D printing** Producing the formwork and reinforcement separately and combining before casting.
4	**3D printing of reinforcement** 3D Printing of steel reinforcement during simultaneous fabrication.
5	**Cast in place reinforcement in thermoplastic formwork channels** 3D print hollow channels into the column before casting concrete. These channels are then filled with cast-in-place steel after the concrete has cured, acting as reinforcement.
6	**Post-tensioning** 3D print hollow channels into column which are used for post-tensioning.

Figure 4-9: Reinforcement approaches considered to be tested.

From the approaches described in Figure 4-9, the three most feasible methods were selected. The reasons for selecting these methods are that they make use of conventional reinforcement, making the technique directly applicable into construction. More experimental approaches, such as steel 3D printing or casting steel into hollow channels could be interesting to explore but are beyond the scope of this thesis. Furthermore, post-tensioning is quite common in construction of concrete slabs but when applied as a reinforcement for columns it is usually only to mitigate damage for earthquakes [67]. As the case-study is not located in an earthquake prone area this approach has been discarded. The three approaches that will be tested experimentally are therefore:

A) 3D printing around prefabricated reinforcement cage
B) 3D printing around prefabricated, modular reinforcement cage
C) Adding prefabricated reinforcement cage after formwork 3D printing

A) 3D printing around a prefabricated reinforcement cage

To test the feasibility of this approach, a simple setup was made with six threaded rods which simulate vertical reinforcement bars. The main aim of the experiment was to see if it is feasible to 3D print a formwork when the filament is extruded at an angle. For simple geometries such as straight columns it is not necessary to rotate the extruder but for more intricate structures with non-standard reinforcement this could be required. An object with a height of 500mm was fabricated using a printing speed of 40 mm/s, a layer height of 1.20mm and a printing angle of 30° (Figure 4-10).

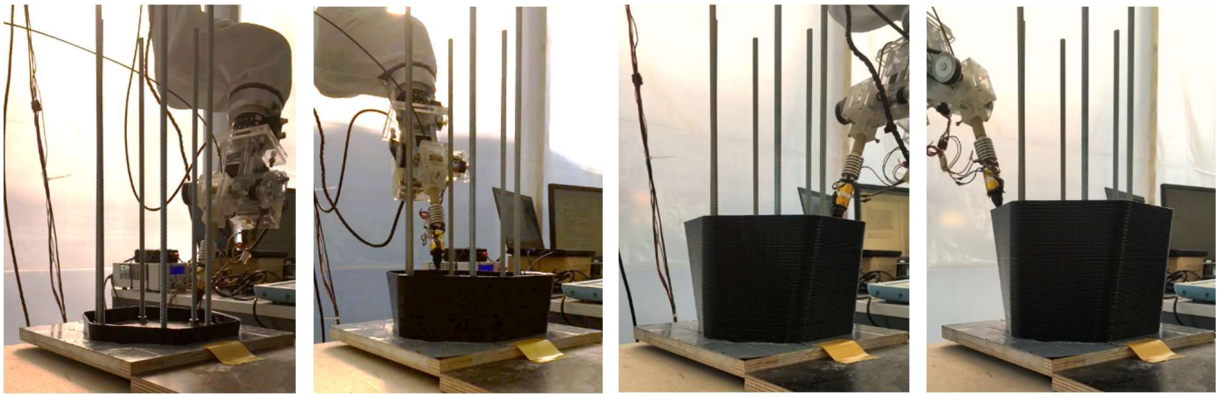

Figure 4-10: Process of printing around a prefabricated rebar cage, simulated by threaded rods.

B) 3D printing around a prefabricated, modular reinforcement cage

In this approach the robotic arm is printing around a prefabricated reinforcement cage, similar to the previous method; however, the cage is split up into parts. These parts are then manually added during the printing and casting process. They are connected using mechanical couplers such as shown in Figure 4-11. The advantage of this approach is that a robotic arm does not have to fully evade an entire prefabricated reinforcement cage, but can instead navigate around parts of the cage. Similarly to Approach A) the robot is 3D printing at an angle in a back and forth motion (Figure 4-12).

Figure 4-11: Mechanical rebar coupler (Source: Dextragroup, https://www.dextragroup.com/activities/technical-solutions-for-construction/solutions/24-concrete-construction/rebar-splicing/51-rolltec)

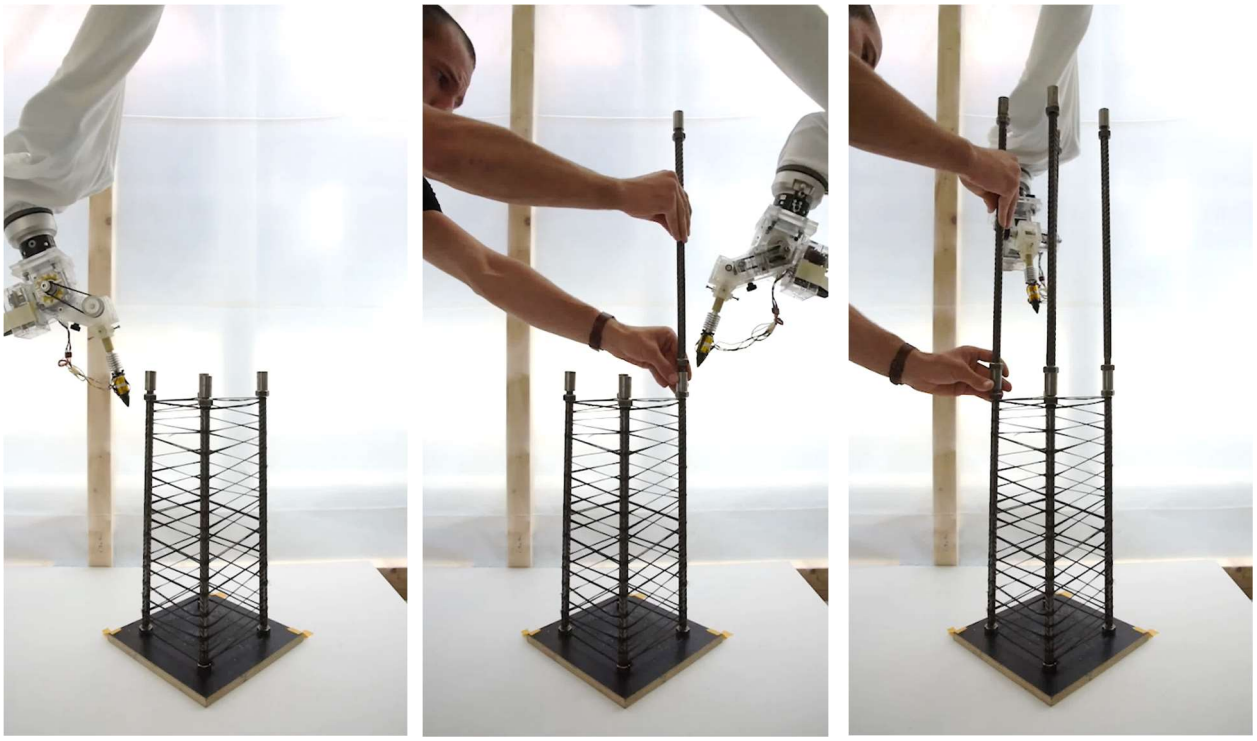

Figure 4-12: Process of printing around a prefabricated cage with manual intervention of adding additional cage sections.

C) Adding prefabricated reinforcement cage after formwork 3D printing

This approach has to most similarity to conventional construction, where a formwork is erected and reinforcement is subsequently added. This has as an advantage that the fabrication of the formwork and reinforcement are separate processes which do not conflict with each other.

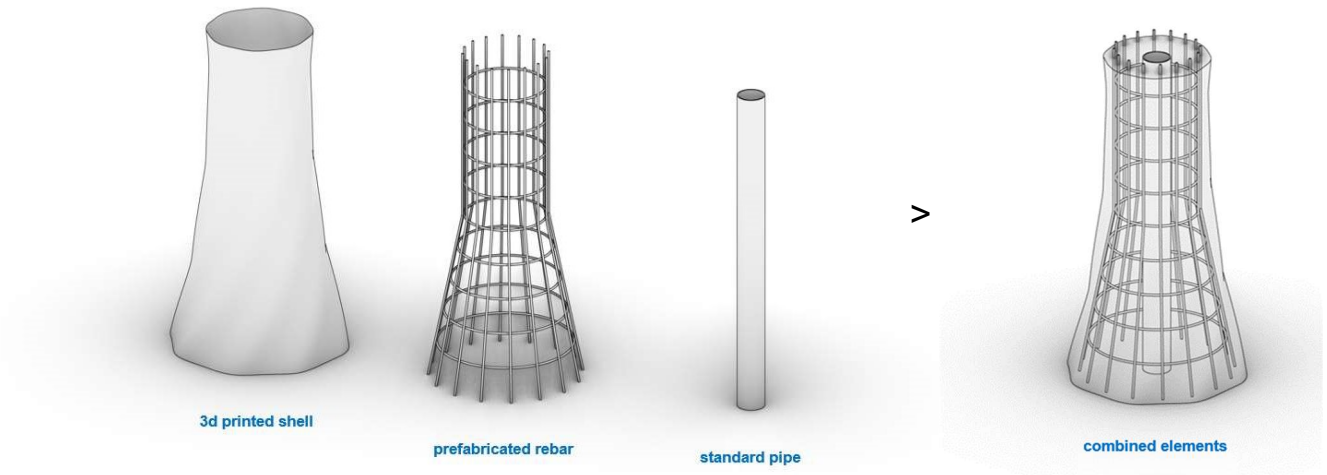

Figure 4-13: The printed formwork, rebar cage and pipe are combined to form one object that is ready to be filled with concrete.

To test this approach a thin-shell formwork was 3D printed and a reinforcement cage fabricated (Figure 4-14). The combined formwork and reinforcement was then filled using the

set-on-demand principle. In contrast to the Exploratory Phase described in Section 4.1 where an automatic filling system (mixing funnel) was used (Section 3.5.1.2), in this test the concrete would be manually mixed with accelerator (Section 3.5.1.1).

Figure 4-14: Objects used for the experiment, a) Reinforcement cage. b) 3D printed formwork combined with reinforcement cage.

A 1m threaded rod was used to stir down into the concrete as much as possible to intermix layers. It proved difficult to reach down to stir all the way into the formwork. After around half of the column was casted it became easier to access and stir the layers due to the smaller height. After the entire column has been filled it was put to rest for three days, after which the formwork was removed with a heat gun. The results can be seen in Figure 4-15.

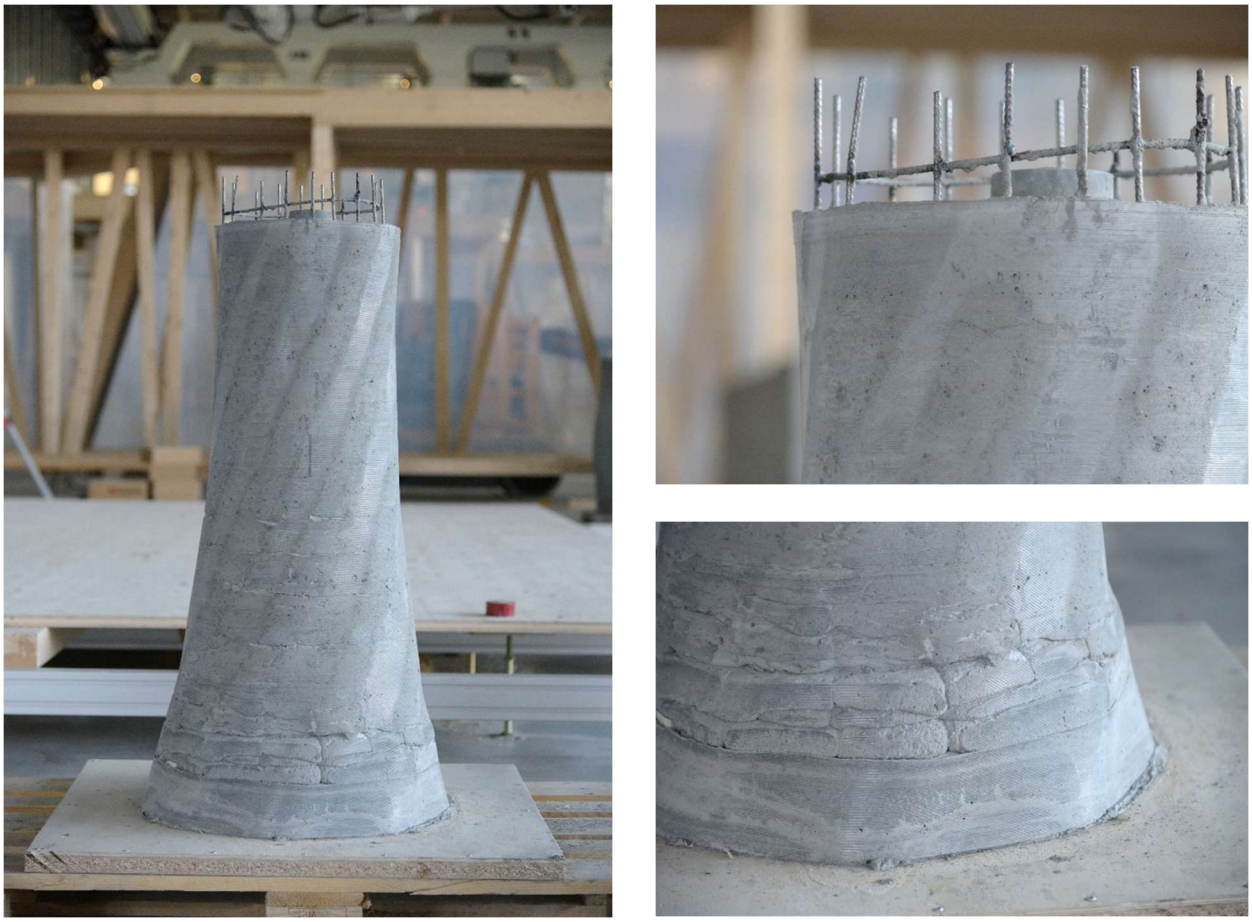

Figure 4-15: a) Resulting concreted column. b) Close-up of top part. c) Close-up of bottom part.

4.2.1.3 Discussion

The three reinforcement approaches tested attempt to answer which method would be most effective for reinforcing the structures. The answer to this question is not straightforward; however, as every approach has its advantages and drawbacks.

3D printing around a prefabricated reinforcement cage has as an advantage that a cage can be fabricated separately from the formwork, allowing full freedom in the production of the reinforcement. The biggest implication of using a fully prefabricated cage is that the robotic arm has to print around the reinforcement. This means that the size of an object is very much limited by the reach of the robot arm. As the aim of this research is to produce large scale objects for buildings, it would then require very large machines to fabricate these objects. This potentially limits the application as these large setups are not widely available. For these practical reasons it was chosen to discard the approach; however, theoretically it could be possible.

The second approach tested, 3D printing around a prefabricated, modular reinforcement cage, addresses this challenge by gradually building up the reinforcement cage out of modular parts

simultaneously with the formwork. As a result, a robotic arm does not have to move around the entire cage but only around a section of controllable height. One challenge in employing this approach is the fact that manual interventions (placing the next section of reinforcement) are necessary in an otherwise automated process. When the 3D printing process is assumed to be continuous, the reinforcement sections have to be placed while the robot is moving. This provided some difficult to overcome logistical challenges. If the 3D printing process can be paused and resumed, adding the next section is much simpler, making the approach feasible.

In the last approach, all three steps of formwork 3D printing, reinforcement fabrication and concrete casting are completely separated. One limitation here is geometry, it can be physically impossible to combine a formwork with a reinforcement cage of a certain shape (Figure 4-16)

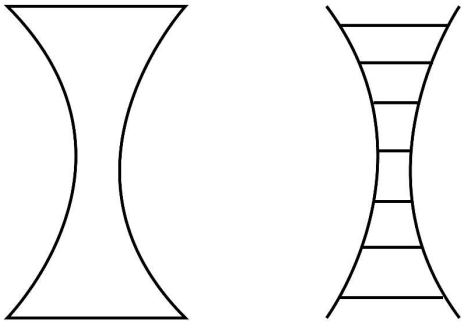

Figure 4-16: A formwork and its reinforcement that are physically impossible to combine unless either is split up.

A solution is to either split up the formwork or the reinforcement in separate parts. This does require a joining strategy needs to be formulated for either the reinforcement or formwork. As an advantage one has full freedom when fabricating the formwork and reinforcement. When the concrete is cast; however, one is actually hindered by both formwork and reinforcement. In conclusion, although this method of consecutive fabrication is not ideal, it is the most feasible in terms of fabrication and direct application.

4.2.2 Challenges of large scale 3D printing

4.2.2.1 Motivation

The first step of fabricating any object using the Eggshell fabrication method meant 3D printing the formwork. As the column investigated in the case-study had larger dimensions than any object printed before, it was unknown if a formwork of such a scale could actually be fabricated using a single layer extruded shell. The question that will be addressed through the experiments described in this section therefore is whether it is feasible to fabricate a large scale, single layer FDM formwork.

As 'large scale' can be interpreted in many different ways, it is defined in this thesis as any object with dimensions larger than a conventional, desktop 3D printer. As a reference a

commercially available 3D printer with fairly large dimensions is taken, the Raise3D N2 Plus FFF 3D Printer [68] with maximum printing dimensions of 30.5x30.5x61cm or 56.745cm^3.

4.2.2.2 Method and results

To test the feasibility of 3D printing the formwork, tests were conducted in which a formwork of a dimension similar to the case-study design was 3D printed. The geometry of the print was varied in between tests and the resulting surface quality was studied. Printing parameters were kept the same in between tests, a constant printing speed of 50 mm/s was used, a nozzle temperature of 200 °C and PET-G filament from the brand extrudr. An overview of the tests conducted is presented in and Figure 4-18.

Test	Shape	Diameter (mm)	Micro pattern	Edge length (mm)	Division points (#)	Point offset (mm)	Fillet (mm)	Layer height (mm)	Quality (1-5)	Comments
1	Polygon filleted	1000	-	-	20	50	450	1	1	Layer delamination and stringing
2	Polygon	1000	-	-	10	100	0	1	1	Layer delamination and stringing
3	Polygon	1000	-	-	10	0	0	1	1	Layer delamination and stringing
4	B&H Top	1000	-	-	100	0	0	1	3	Slight layer delamination
5	Polygon filleted	1000	-	-	10	100	450	1	3	Slight stringing
6	Circle	1000	-	-	100	0	0	0.60 - 1.20	2	Layer delamination in bottom layers
8	Circle	1000	Undulated polygon	20	80	15	0	1	5	Perfect quality
8	Circle	1000	Undulated polygon	25	60	15	0	1	4	Good, slight stringing
9	Circle	1000	Undulated polygon	40	40	15	0	1	4	Good, small delamination at corners

Figure 4-17: Test parameters for large scale 3D printing tests conducted.

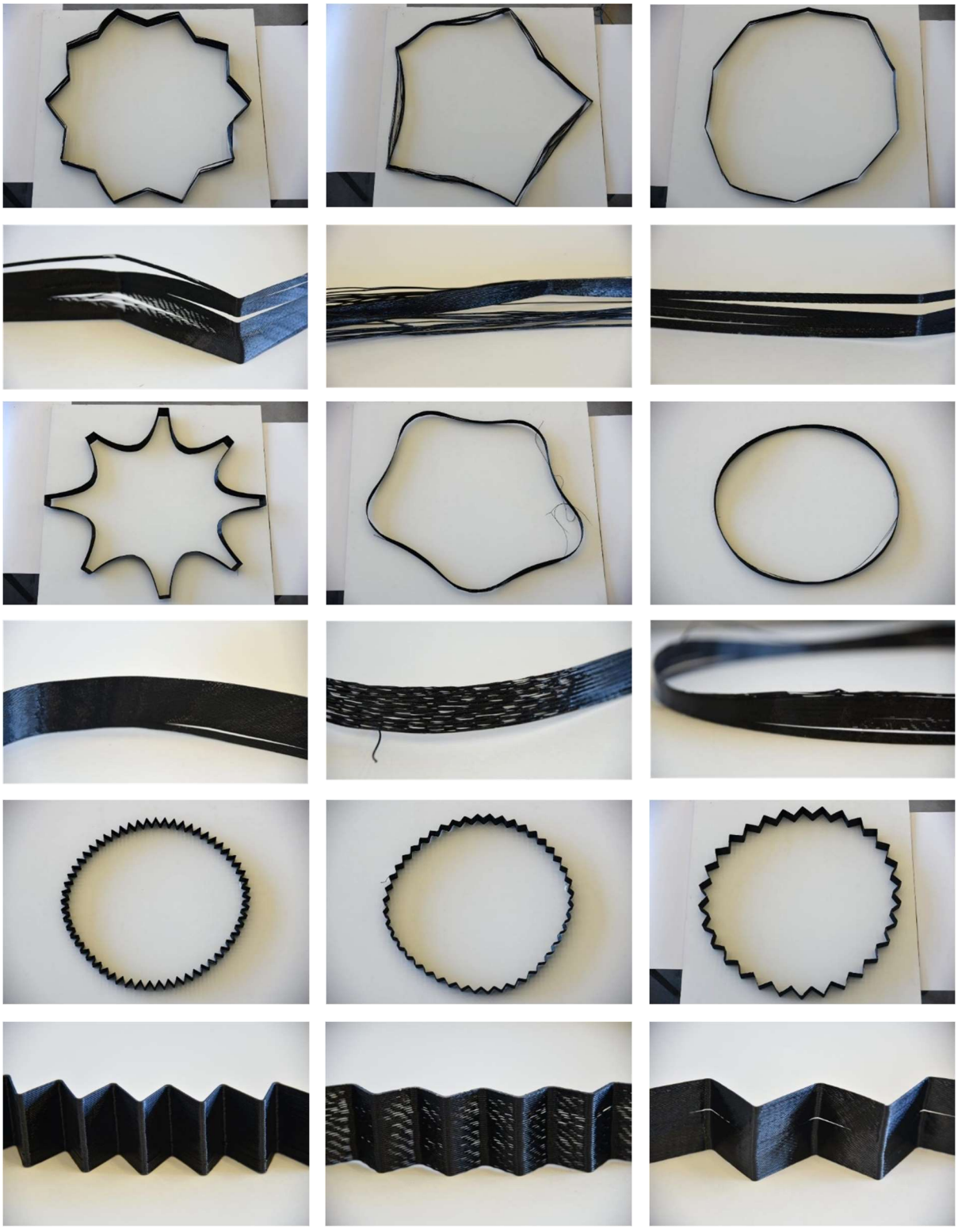

Figure 4-18: Overview and close-up of test 1-9.

4.2.2.3 Discussion

What can be seen from the 3D printed results is that problems of layer delamination are the most prevalent in tests 1-3 (Figure 4-17). The models printed in test 1-3 are not structurally viable and would not be able to function as formwork due to many gaps in between layers. These effects then become less evident in tests 4-6 but are still present. Tests 7-9 then show a much better surface and structural quality.

The underlying problem that causes the layer delamination to occur is best explained as the effects of shrinkage. Deformation or warping due to shrinkage are a common problem in FDM 3D printing [69]. All thermoplastic materials expand when heated up and shrink when they cool down. The percentage of shrinkage depends on the material and more specifically on the glass transition temperature (T_g). The glass transition temperature can be explained as the temperature at which a material changes from a hard, brittle, glass-like state into a soft, rubbery state. The glass transition temperature is usually not a fixed temperature but instead a range in between which the material changes state. For simplification, however, it will be assumed that in this case the glass transition temperature is a single value and not a range.

A diagram of the process can be seen in Figure 4-19, the values are taken as an example. A nozzle is heated to a temperature of 210 °C. A thermoplastic material is then extruded from the nozzle and the temperature of the just printed layer (T_{hot_layer}) is equal to the glass transition temperature (T_g) of the material, in this example 70 °C. The printed layer material then cools to the temperature of the air (T_{air}, T_{cool_layer}). The resulting difference in temperature (ΔT) can then be found with the following formula: $T_g - T_{air} = \Delta T$, filled in to this example: 70 °C - 20 °C = 50 °C. This means the printed layer will be affected by shrinkage for the entire time it takes to cool down 50 °C. During this time the layers which are cooling are pulling on the top layers, as illustrated by the arrows. This pulling effect is what causes the layer delamination due to shrinkage.

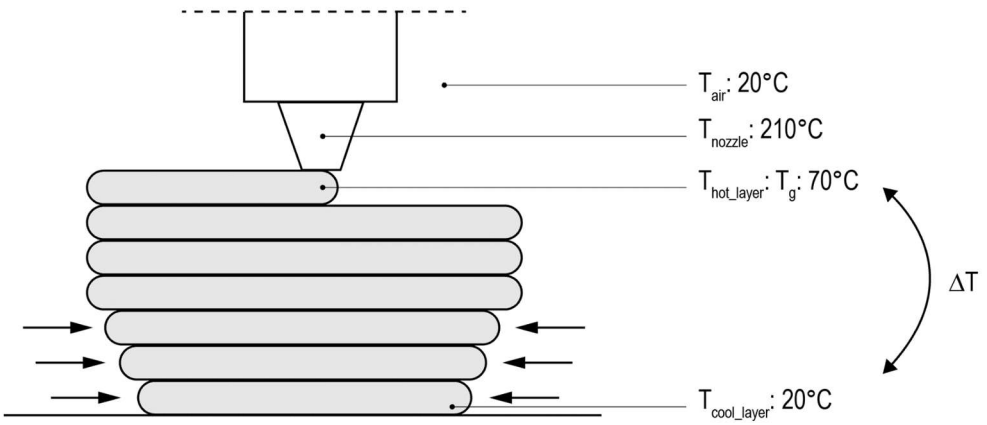

Figure 4-19: Diagram showing effect of shrinkage on printed layers.

To explain the superior print quality of test 7-9 we can look to the micropattern applied. Test 1-6 did not have any micropattern applied to the surfaces whereas in test 7-9 an undulated zigzag pattern was used. As shrinkage always occurs in the longitudinal direction of the filament (the printing direction) the shrinking force concentrates in the corners (Figure 4-20). A shrinking force (s) acts from both corners of a filament thread in opposite direction. Once the filament thread changes direction, the direction of the shrinking force also changes direction. Therefore, in a corner of 90°, the net force can be calculated using Pythagoras theorem and results in a higher net force of s√2. This shows the forces and therefore the stresses concentrate in the corners, causing the corner delamination of Figure 4-21a.

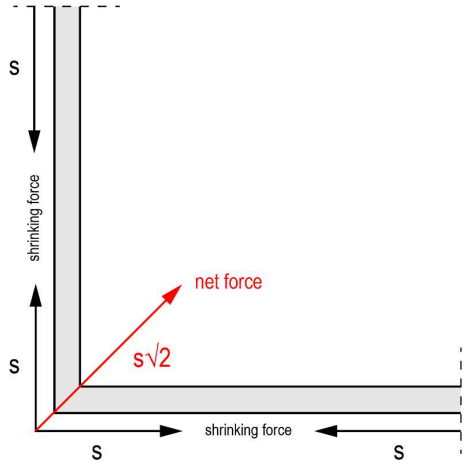

Figure 4-20: Diagram illustrating concentration of shrinking force in corners.

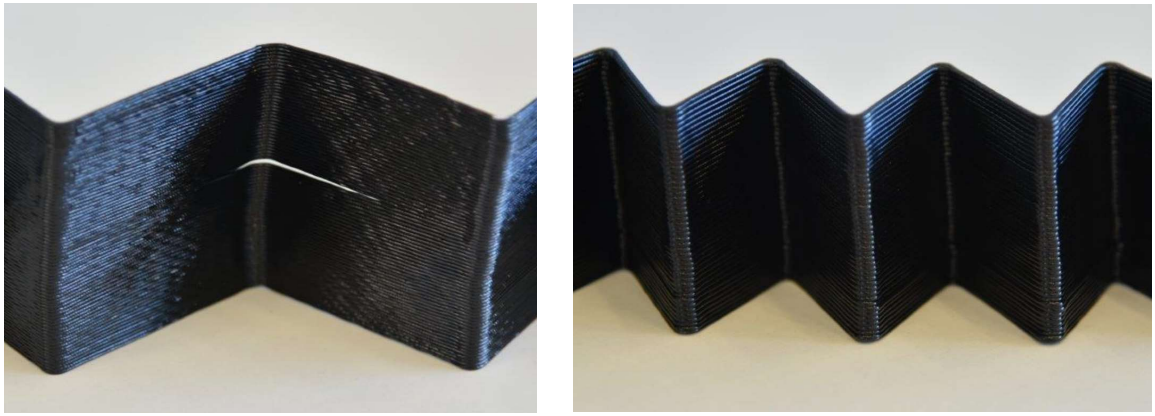

Figure 4-21: a) Close-up of test 9 with large undulations. b) Close-up of test 7 with smaller undulations.

If we compare the results of test 9 with test 7 we can clearly see the effect of stress concentrations in the corners. Test 9 has an edge length of 40mm whereas test 7 has an edge length of 20mm (Figure 4-17). This means the forces acting on the corners will be twice as high in test 9 as in test 7 (Figure 4-22). The force acting on the corner in test 9 is enough to cause layer delamination, whereas the force in test 7 is low enough to avoid layer delamination. It can therefore be concluded that if the edge length is kept under a certain maximum (around 20mm), layer delamination can be avoided. However, to provide a decisive answer on the

lower- and upper-limits of the edge length and the corresponding force, more tests are needed.

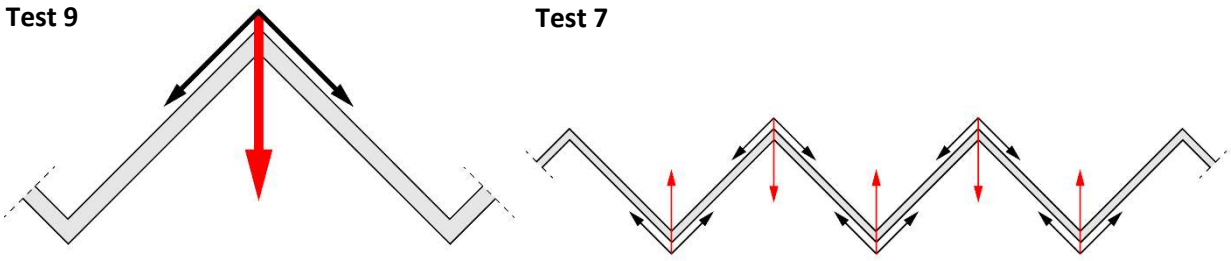

Figure 4-22: a) Diagram illustrating shrinking forces with larger undulations. b) Diagram illustrating shrinking forces with smaller undulations.

4.2.3 Structural performance of formwork subjected to hydrostatic pressure

4.2.3.1 Motivation

Although during the Exploratory Phase several prototypes have been successfully fabricated without the formwork breaking, thus showing that the thin shell can resist a certain hydrostatic pressure. It is, however, still unknown what the maximum hydrostatic pressure is that the shell formwork can resist without deforming and breaking. This section therefore aims to make a first estimate on the structural behaviour of the shell when subjected to the hydrostatic pressure exerted by the concrete during casting.

4.2.3.2 Method and results

To test the formwork's resistance to hydrostatic pressure several tests were conducted where a formwork was filled with concrete and the moment of failure was recorded. Concrete was cast either using the set-on-demand filling process (Section 3.5.1.1, filling accelerated concrete in a layer-by-layer approach stretched over time) or by filling the formwork in one batch of concrete. The physical experiments were also modelled using finite element modelling (FEM) software.

Two main series of experiments were conducted during which the following aspects were tested: A) Overhang tests. B) Formwork undulations.

A) Overhang tests

For the first series of tests, the maximum angle of overhang (α) that can be successfully fabricated is tested. Four models were 3D printed that featured an overhang of 15°, 25°, 35° and 45° (Figure 4-23). Each base consisted of a square measuring 150x150mm and a wider top, depending on the angle of overhang. All objects measured 300cm in height.

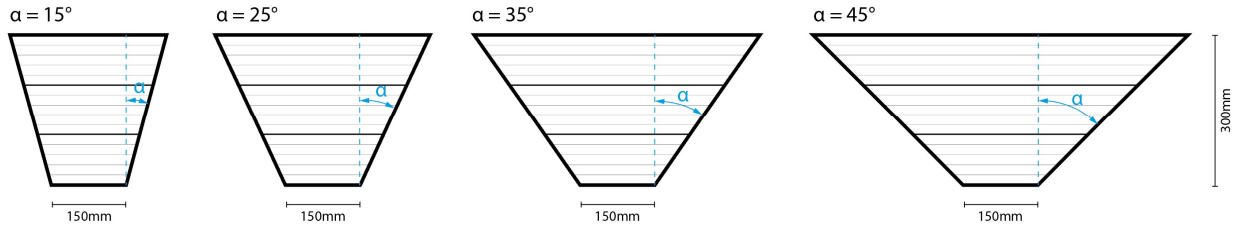

Figure 4-23: Diagram showing geometries which were tested.

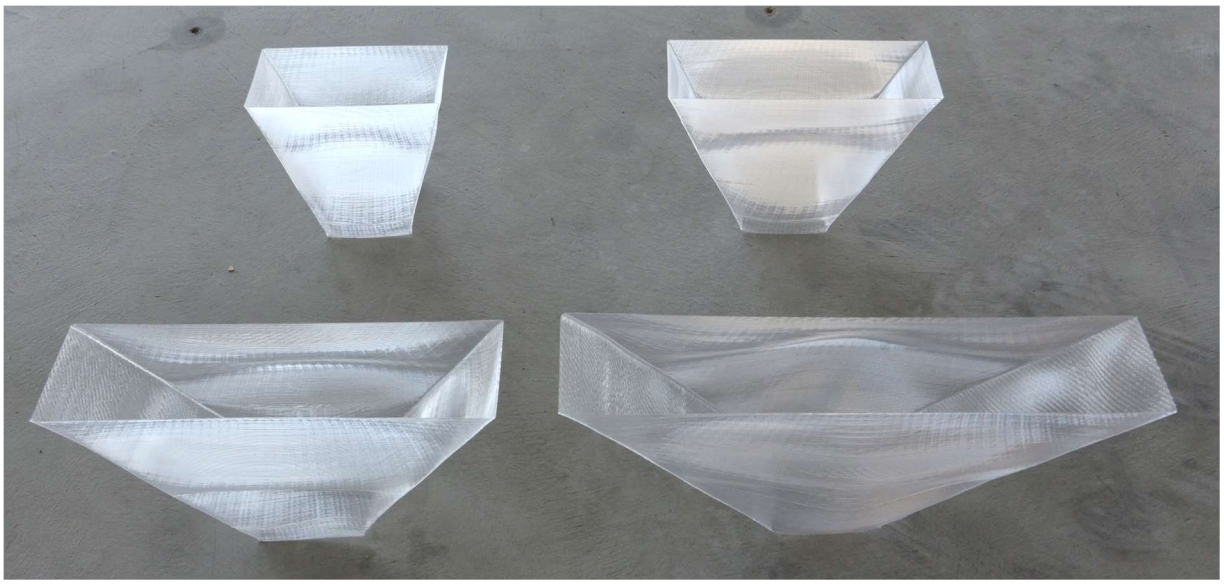

Figure 4-24: 3D printed models to be tested. a) Overhang of 15°. b) Overhang of 25°. c) Overhang of 35°. d) Overhang of 45°.

After 3D printing the objects were filled with concrete using the set-on-demand layer based method. They were filled with a filling speed of 2mm/min, amounting to a total of 150min or 2,5hr to fill the formworks. The hydration time of the concrete was 50 minutes, this meant 100mm of liquid concrete was exerting pressure onto the formworks. This pressure is equal to $P = 2300\ kg/m^3 * 9.81\ m/s^2 * 0.1m = 2.26kN/m^2$. The results can be seen in Figure 4-25.

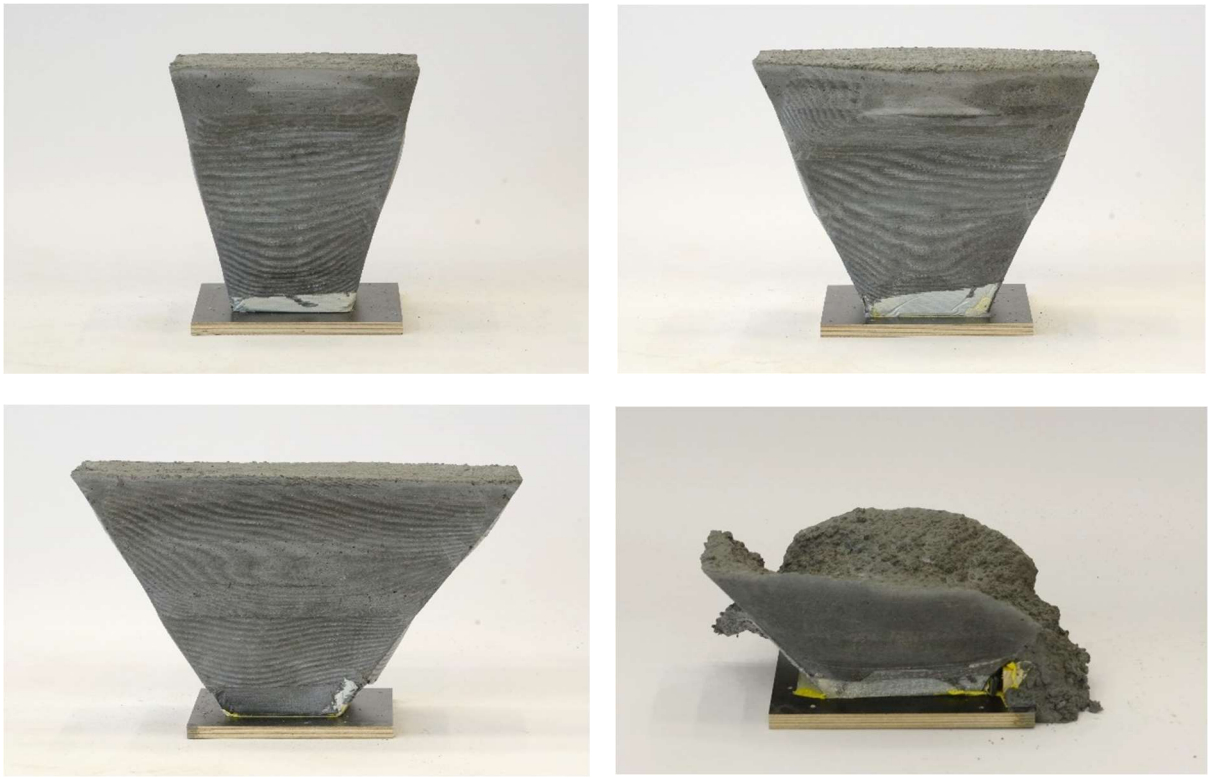

Figure 4-25: a, b, c) Resulting successful concrete models of 15°, 25°, 35 overhang°. d) Failed concrete model of 45° overhang.

As can be seen, the models with an overhang of 15°, 25° and 35° were successfully fabricated. The model with an overhang of 45°; however, failed during fabrication after 50 minutes. At this point there was the maximum amount of liquid concrete in the formwork, 100mm. The point of failure was, as expected, on the short side with the overhang (Figure 4-26).

Figure 4-26: Failure of model with 45° overhang.

In order to compare the physical results obtained with simulation, the experiments were modeled in FEM software. This could potentially be used to predict failure without the need of physical experimentation. The geometry was exported to Abaqus Unified FEA [70] and the four geometries were modeled and the corresponding hydrostatic pressure of 2.26kN/m^2 was applied to the first 100mm. The parameters used can be seen in Figure 4-27 and the results are shown in Figure 4-28.

Parameter	Value
Density of shell	1.3 x 10^{-9} mm^3
Poisson ratio	0.4
Shell thickness	1.5 mm
Hydrostatic pressure applied	0.002254 MPa

Figure 4-27: Parameters used for simulation in Abaqus.

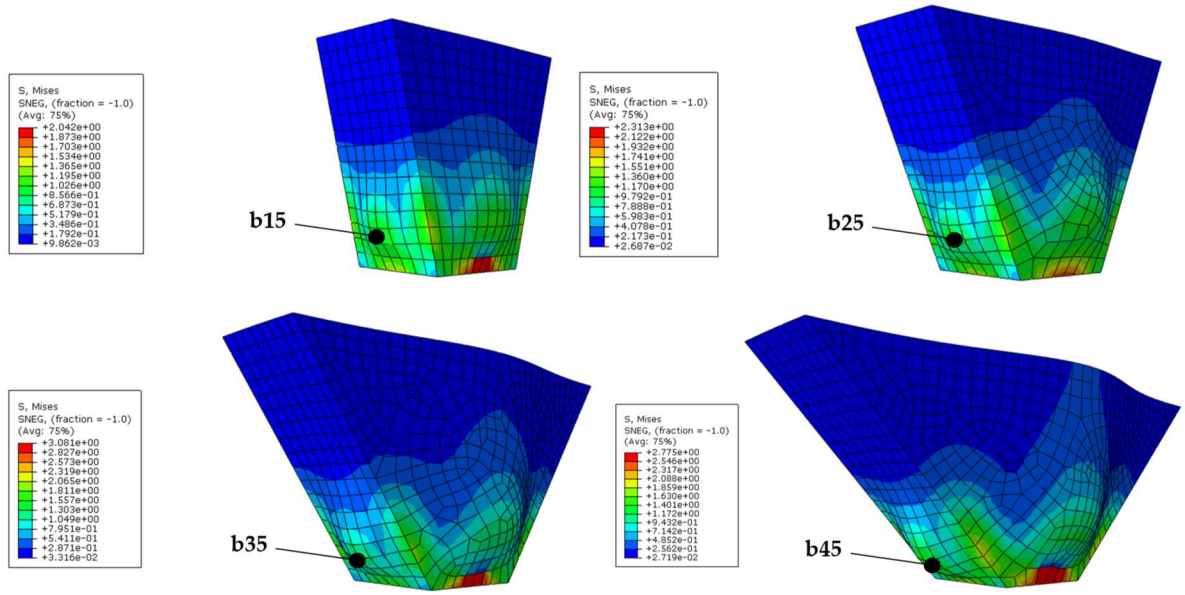

Figure 4-28: Visualization of Von Mises stresses in the models.

The maximum stresses in all of the models are occurring in the bottom, since the hydrostatic pressure scales with height. However, in the physical experiments this was not the point of failure, most likely because this point was constrained by a wooden piece which held the formwork in place. Instead, the point of failure was at the point where a bulge can be seen in the 3D models, indicated by b15, b25, b35 and b45. The stresses at these points can be seen in Figure 4-29. Although the stresses are slightly higher in point b45 (which was the only point where failure occurred during physical experimentation) it is only a marginal difference.

Overhang of model (°)	Point name	Von Mises stresses (MPa)
15°	b15	1.11
25°	b25	1.25
35°	b35	1.40
45°	b45	1.50

Figure 4-29: Stresses in points b15, b25, b35 and b45.

B) Formwork undulations

In Section 4.2.2 it has been described how it is necessary for successful 3D printing of the shell formworks that the printing path features undulations. To check the structural performance of geometries with these undulations some experiments were conducted. Four models were 3D-printed, two standard extruded squares and two with the undulated zigzag pattern applied to the surface (Figure 4-30). These models were then filled with concrete in a conventional manner, not applying the set-on-demand filling principle. This was done because the aim of the experiment was to compare the performance of the undulated formworks with the non-undulated formworks and they were expected to break.

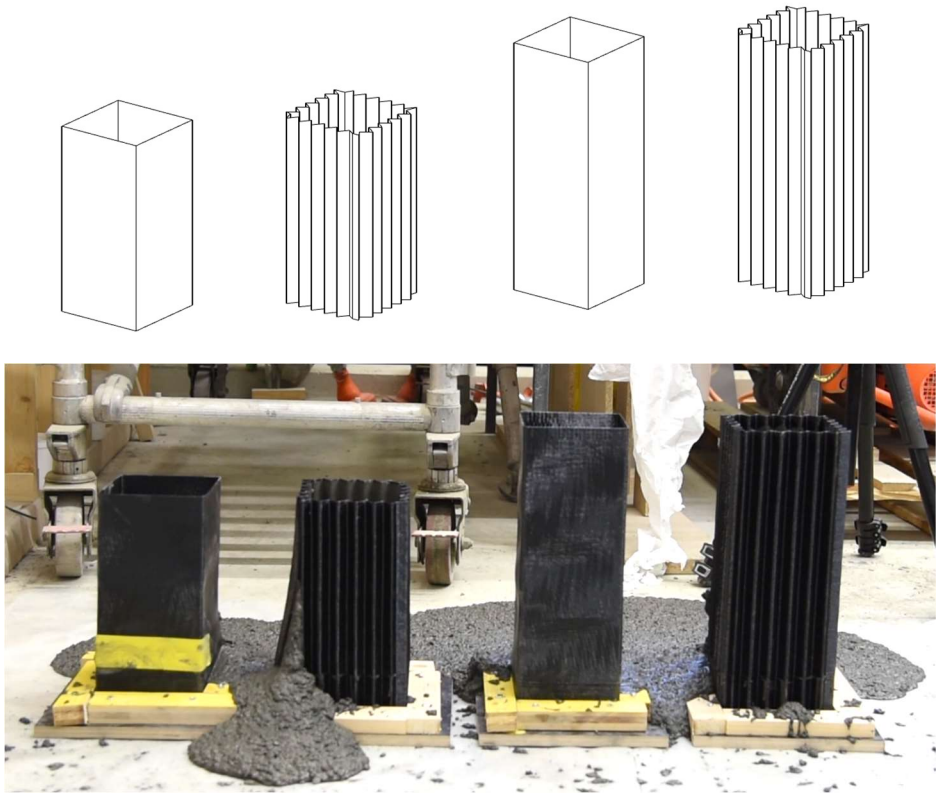

Figure 4-30: a) Diagram of models to be tested. b) Image taken during experiment showing failure of all the models.

Name	Pattern	Height (mm)	Moment of failure (min after starting)	Liquid concrete height at moment of failure (mm)
s1	No pattern	300	23	200
u1	Undulated zigzag pattern	300	29	300
s2	No pattern	400	25	250
u2	Undulated zigzag pattern	400	27	370

Figure 4-31: Data obtained during experiment.

The moment of failure (in minutes after starting) was recorded, as well as the height of liquid concrete at the moment of failure (Figure 4-31). From the data obtained can be seen that the first model to fail, 23 minutes after starting was s1, the 300mm tall model without pattern. Hereafter s2 failed and finally u1 and u2. What is evident is that both of the models without a pattern failed before the models with a pattern applied. The models without a pattern also failed at a lower concrete height compared to the models with a pattern, at 200mm and 250mm as opposed to 300mm and 370mm.

This points towards a superior structural performance for the models with an undulated pattern applied, something that could also be explained due to the undulations providing a structural depth.

In order to verify these findings the geometries were also simulated using Abaqus FEA. The parameters shown in Figure 4-27 were used for modelling the geometries, except the hydrostatic pressure was increased to 0.00676 MPa, corresponding with 300mm of height.

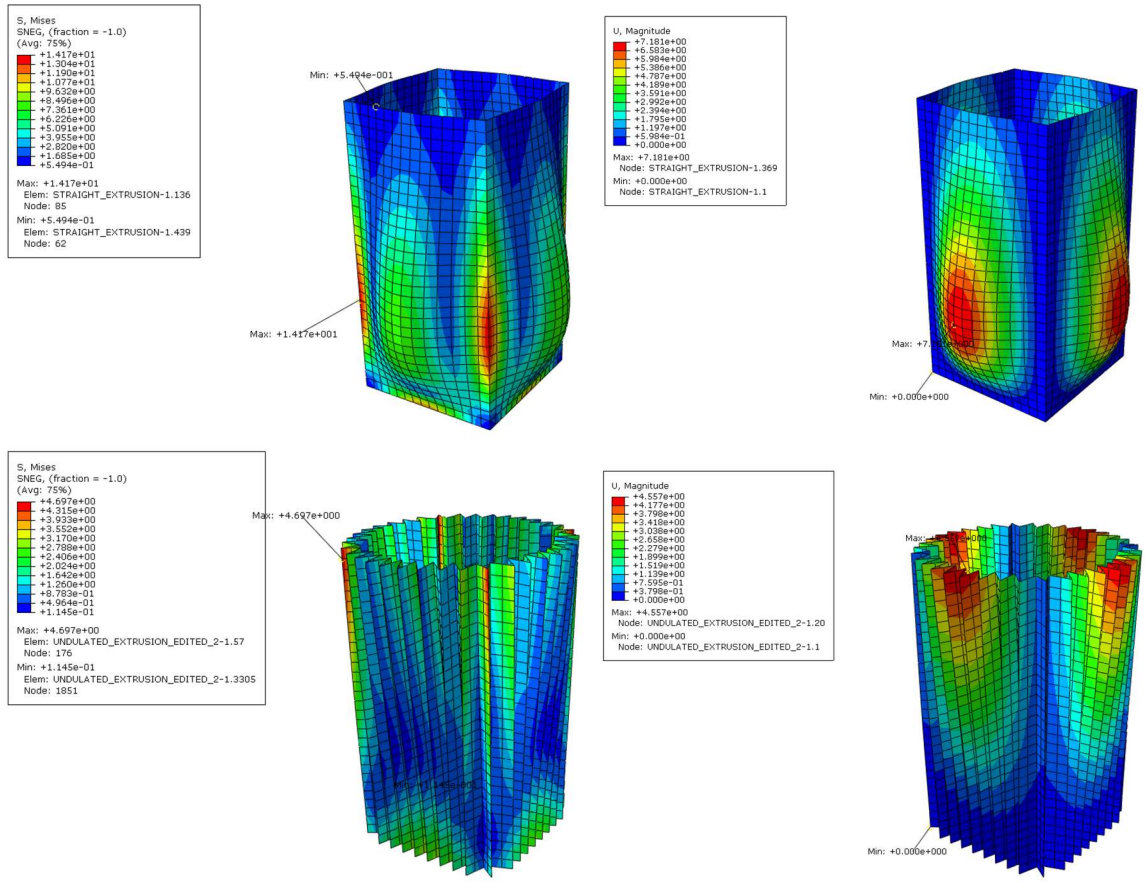

Figure 4-32: Visualizations obtained from FEM analysis. a) Von Mises stresses. b) Maximum displacement. c) Von Mises stresses. d) Maximum displacement

	Maximum stresses (MPa)	**Maximum displacement (mm)**
No pattern	14.2	7.2
Undulated zigzag pattern	4.7	4.6

Figure 4-33: Maximum stresses and displacement obtained from the FEM model.

It can be seen that the maximum stresses are around a factor three higher in the formwork without a pattern applied (Figure 4-33). The maximum displacement is around one and a half time higher in the formwork without pattern. This corresponds with the findings obtained from the physical experimentation (Figure 4-31), with the formwork without pattern failing before the formwork with undulated pattern.

What is interesting to note is the difference in deformation between the two models (Figure 4-32b,d). In the case of no pattern the four sides bulge out at a height of around one third of the formwork. As hydrostatic pressure scales with height, the highest deformation and stresses occur in the bottom area. They, however, do not occur at the absolute bottom since the formwork is completely fixed at this point.

In the formwork with undulations the maximum stresses and displacement occur at the highest point of the formwork. This is perhaps counterintuitive, as hydrostatic pressure is the

lowest at the top and highest at the bottom. In terms of displacement this can be explained; however, as the stresses are much lower (by a factor three) than at the formwork without pattern. This means the bulge that occurs due to hydrostatic pressure in the first example does not form because of the structural depth of the undulations. The deformation of the formwork does work all the way through to the top of the formwork where the shape starts to resemble a circle because of the hinging flexibility in the undulations.

4.2.3.3 Discussion

In the experiments described in this section it was attempted to relate physical experiments with numerical modelling. This has proven to be only partly successful. In the case of formwork overhang it was shown that although the numerical simulation indeed provided higher stresses in a formwork with a larger overhang, the differences were only marginal (0.1 MPa difference between failure and success). It would therefore most likely be difficult to actually predict failure because of an overhang with these models.

An important aspect that is not taken into account in the modelling of the formworks is the fact that they are not a homogenous shell but in fact built up out of layers. In a vertically extruded formwork this might not be as important, as the same error is taken into account for every case; however, with an overhang this can make a large difference. This is because when printing layers that are not stacked vertically, only part of a layer is actually in contact with another layer. When printing an object with an overhang of 45°, only 50% of a layer is in contact with another layer (Figure 4-34). The reduced contact surface makes the object weaker and this is not taken into account by the numerical simulation. In order to successfully simulate objects with an overhang this should be implemented in the model.

In the case of testing overhang it is therefore better to follow the results gained from physical experimentation. As the model with an overhang of 45° had failed, but the 35° model was successful, it can be concluded that in order to stay within safe design limits, a maximum overhang of 35° should be kept into account.

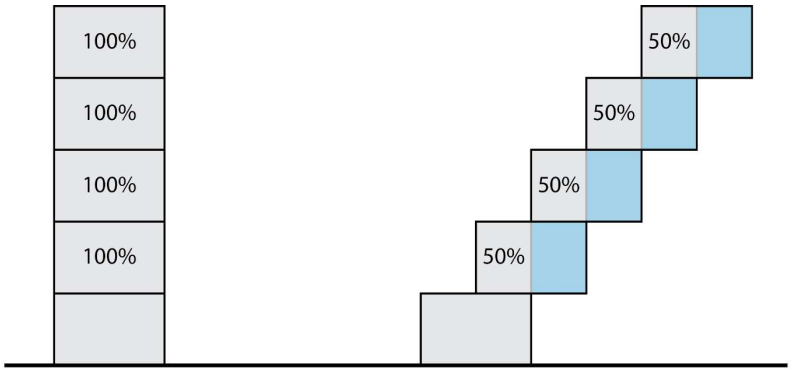

Figure 4-34: Difference in contact surface for a vertically stacked 3D printed and one with an overhang. The blocks represent 3D printed layers and the numbers describe the amount of contact surface with the previous layer.

As for formwork undulations, a structurally better performing result was obtained by the formwork with a pattern, in both the physical experiments as in the simulation. This means it is theoretically possible to see the effects various patterns have on the structural performance of a formwork. However, this needs to be verified with additional tests of different patterns.

In general it can be concluded that numerical simulation using FEM is a promising approach for the prediction of deformation, stress and ultimately failure. As physical experimentation is labour-intensive, it would be undesirable to have to conduct physical experiments for every new geometry fabricated and therefore numerical simulation could provide an effective solution. Before it can directly be applied, however, more tests are needed that study the relation between the physical and digital behaviour.

4.2.4 Temperature development of hydrating concrete

4.2.4.1 Motivation

When concrete hydrates an exothermic reaction occurs between water and cement. The amount of heat generated is highly dependent (amongst other aspects) on the amount and type of cement used. For a concrete structure with a large solid mass the heat gain during hydration is usually higher as there is no possibility for the concrete to release heat to its surroundings. A high temperature during hydration is not an issue in concrete structures by itself, but a steep temperature gradient (fast temperature increase) can cause two main problems: cracks in the concrete due to high thermal stresses and a lower later compressive strength [71].

As the column studied in the case-study contains a large volume of concrete compared to earlier tests (300L as opposed to 100L), there were concerns that the temperature of the hydrating concrete might reach very high levels. No previous temperature measurement tests had been done on the particular concrete mix used throughout this thesis and therefore it was necessary to gather data on the temperature development.

4.2.4.2 Method and results

To test the temperature reached by the concrete an experiment was conducted in which a section of the column was fabricated and the temperature was measured during hydration. As a high temperature is likely to occur in an object with a large mass, the top part (largest part) was fabricated. The top 300mm of the column was 3D printed and fixed to a wooden base using hot glue. Eight reinforcement bars were added, as well as a pipe in the middle to simulate reinforcement and a drainage pipe as in the design of the column (Figure 4-35a). Attached to the reinforcement bars are ten thermocouples, placed at various positions inside the formwork. The thermocouples are spread around the formwork, but all placed in the vertical middle of the formwork, at a height of 150mm. Their positions can be seen in Figure 4-19b. All of the thermocouples are connected to a computer which records the data.

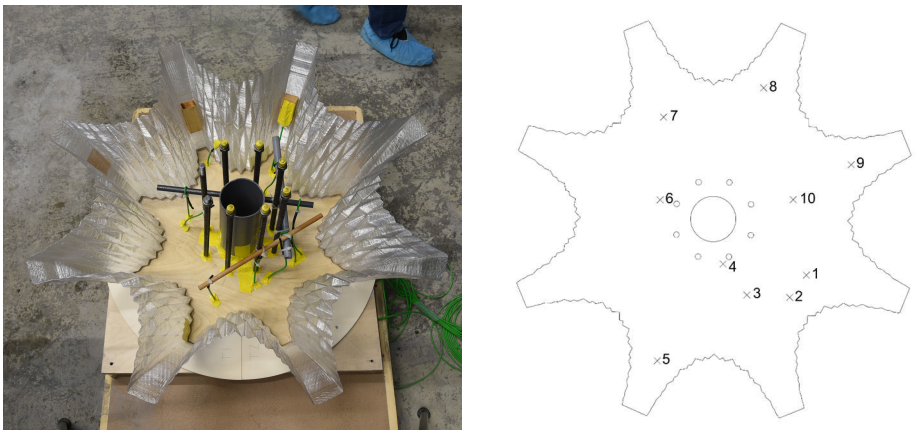

Figure 4-35: a) Experimental setup. b) Position of thermocouples inside the formwork.

The formwork was filled with the SACAC material mix using manual acceleration and casting such as described in Section 3.5.1.1. The filling rate of the formwork was 2 mm/min, casting a 10mm layer every 5 minutes. This amounted to a total casting time of 150 minutes and with a concrete hydration time of 50 minutes this meant a theoretical maximum of 100mm of liquid concrete.

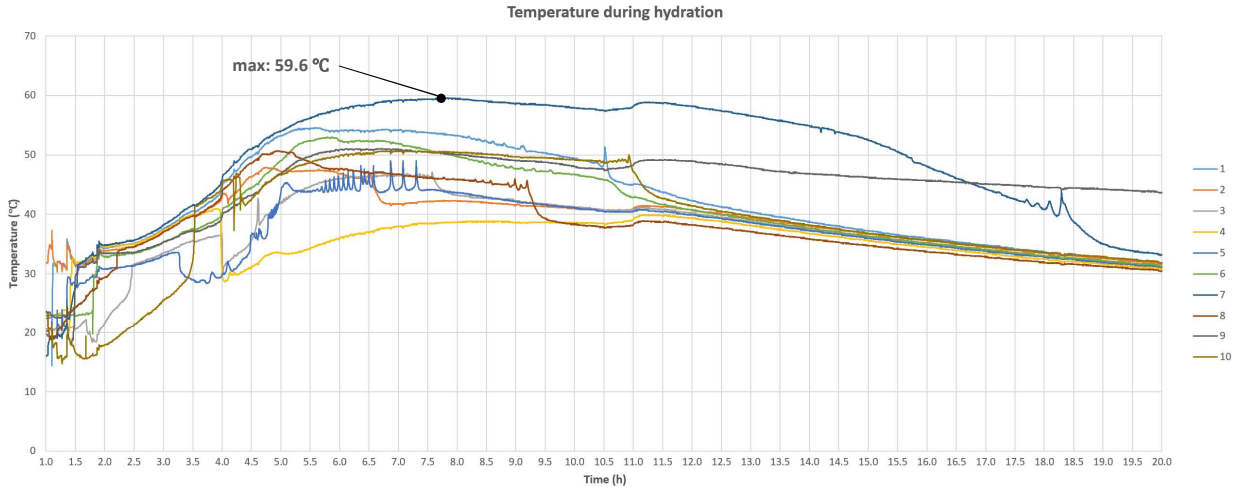

Figure 4-36: Graph showing the temperature over time as measured by the thermocouples placed inside the formwork.

The measurements were started as soon as the first layer of concrete was cast into the formwork and stopped 20 hours later. The peak temperature of 59.6 °C was reached at 7 hours and 46 minutes in sensor 7 (Figure 4-36).

4.2.4.3 Discussion

What can be concluded from the measurements taken is that the temperature of almost 60 °C reached by the concrete is relatively high. Maximum advised temperature values for concrete range in between sources, from 57 °C [72] to 70 °C [73]. One aspect that has to be mentioned is that these maximum values are applicable for mass structures. Mass structures are defined by

ACI 116R [74], an American document on cement and concrete terminology as "any volume of concrete with dimensions large enough to require that measures be taken to cope with generation of heat from hydration of the cement and attendant volume change, to minimize cracking". As this is a broad definition, usually objects with a thickness above one meter are assumed as mass structures. The column studied in this thesis has an upper diameter of one meter; however, it gets narrower towards the bottom and therefore it is questionable if the column classifies as a mass structure.

Regardless of whether the column classifies as a mass structure, in order to stay within safe limits the maximum temperature during hydration should stay below 50 °C. In order to achieve this reduction several measures can be taken such as:

- Reducing cement content of the material.
- Reducing mass of the object.
- Adding active cooling during hydration

Reducing the mass of the column (for instance by scaling the column) will have implications on many aspects such as reinforcement, external connection details and structural performance and is therefore not preferred. One solution that can be undertaken without changing the geometry of the column is changing the mix design to have a reduce cement content. Part of the cement can be replaced by limestone, which is a commonly used filling material [75]. In order to verify the effectiveness of this solution in terms of heat reduction, as well as make sure the compressive strength is not significantly lower, more experiments need to be conducted with the modified material.

Another interesting solution is employing active cooling by creating an air or water flow through the drainage pipe which is already present in the middle of the column (Figure 4-37). This solution is deemed the most effective method of reducing temperature during hydration by one study [76] and could be directly applied with relative ease.

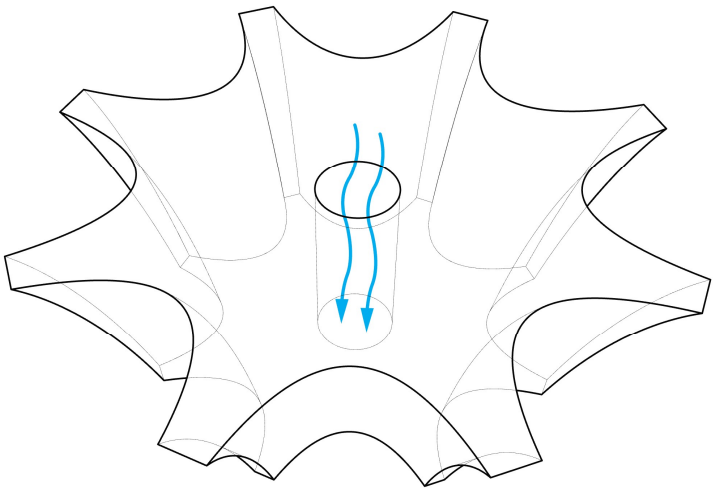

Figure 4-37: Active cooling using cold air circulation through drainage pipe.

4.3 Phase III: Case study

After the open questions from Phase II had been addressed the results could be fed into the design and fabrication of the case study. Using the knowledge gained on the reinforcement, maximum overhang and micro pattern a design was made. The design was then 3D printed in four parts, reinforcement fabricated and finally the reinforcement and shell were combined and filled with concrete. This section describes several reference projects and the design, as well as the fabrication process and lessons learned from the design and fabrication.

4.3.1 Reference projects

Many reference projects in terms of fabrication have already been described in Chapter 2. As for references of form and material one can look back to Pier Luigi Nervi who constructed many great buildings. One example is the restaurant of Karsaal which he built in Ostia Lido, Italy (Figure 4-38). The building features a central concrete column supporting his signature ribbed floor slab [80]. As Nervi did not have access to digital fabrication methods the formwork for the concrete column was built entirely out of wood scaffolding. Although cost- and labour intensive, it resulted in a spectacular space.

Figure 4-38: Karsaal Restaurant, Pier Luigi Nervi (Ostia Lido, 1950). Source: Maxxi, Museo Nazionale Delle Arti Del XXI Secolo, URL: http://www.maxxi.art/en/events/cibo-paesaggio-architettura-archivi/)

Another more contemporary reference is the station Arnhem Centraal designed by UN Studio. The station features a large column in the main hall of the station, supporting the roof structure. The column was originally envisioned to be built in concrete but was later changed to steel due to the difficulty and costs envisioned of the concrete construction [81]. The Eggshell fabrication approach described in this thesis could perhaps be used in the future to construct structures such as this one.

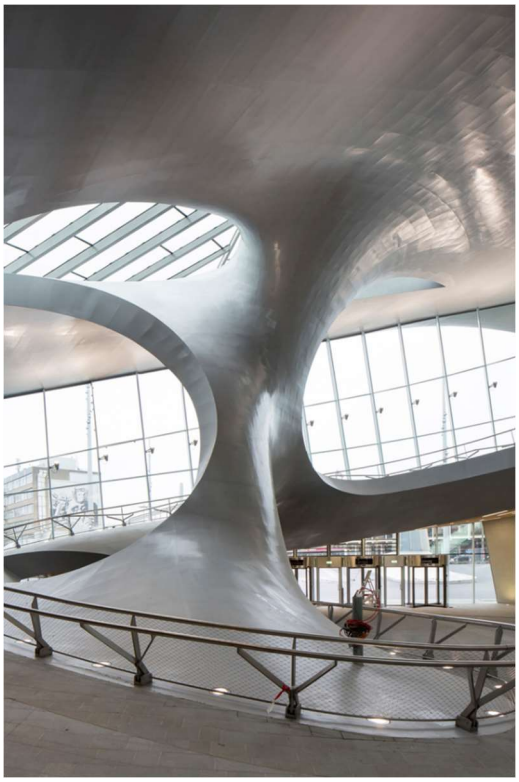

Figure 4-39: Station Arnhem Centraal, UN Studio (Arnhem, the Netherlands, 2015). Source: Frank Haswijk

4.3.2 Design

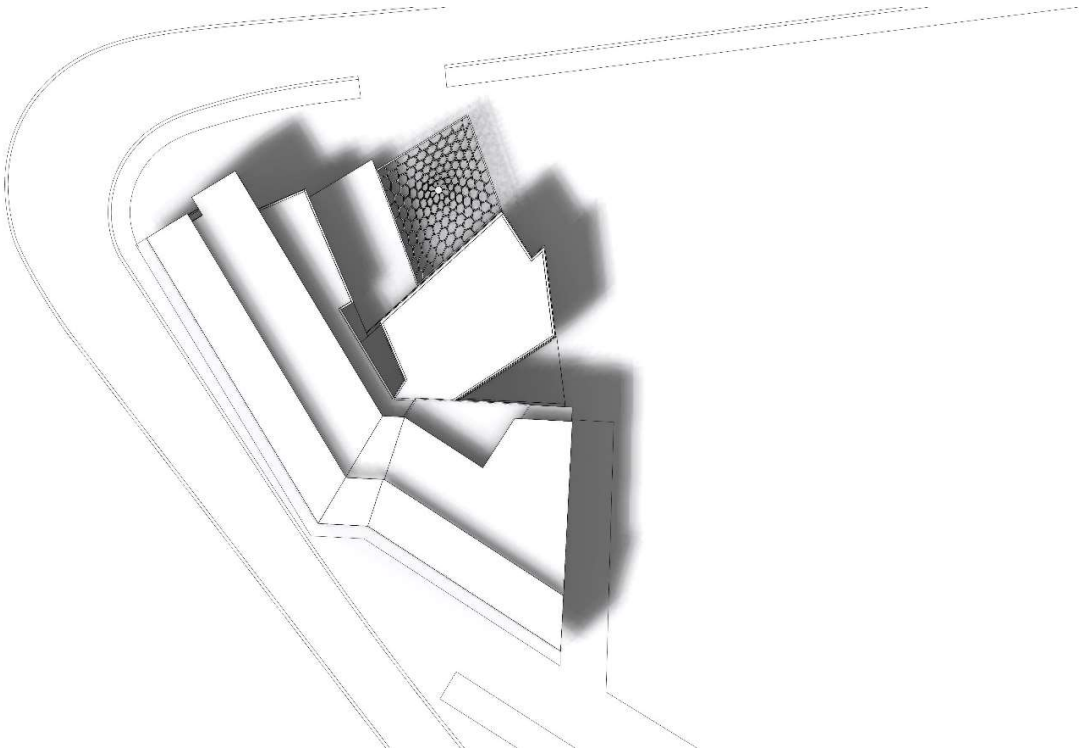

Figure 4-40: Plan view showing existing building, new building and planned pavilion.

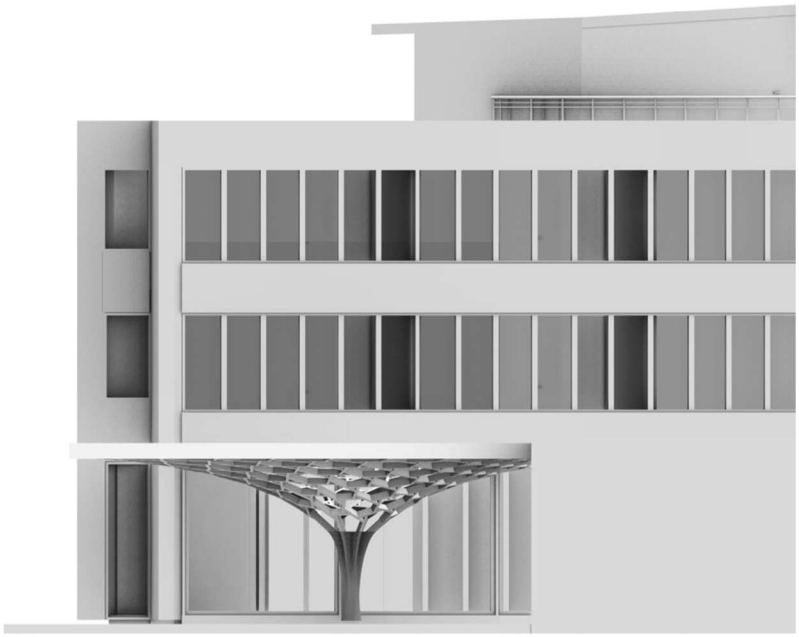

Figure 4-41: North-West elevation of pavilion including building.

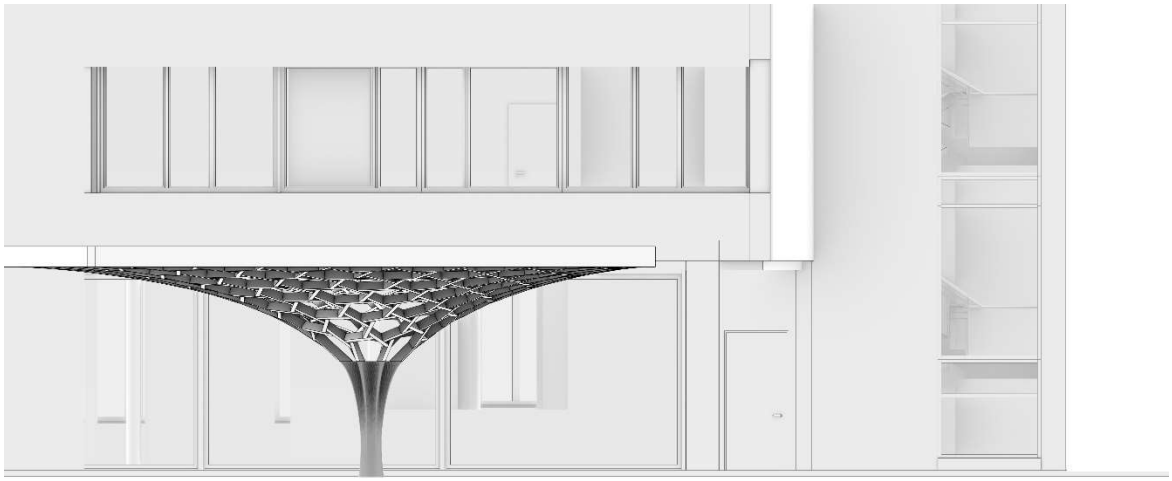

Figure 4-42: North-East elevation

Figure 4-43:North-West elevation

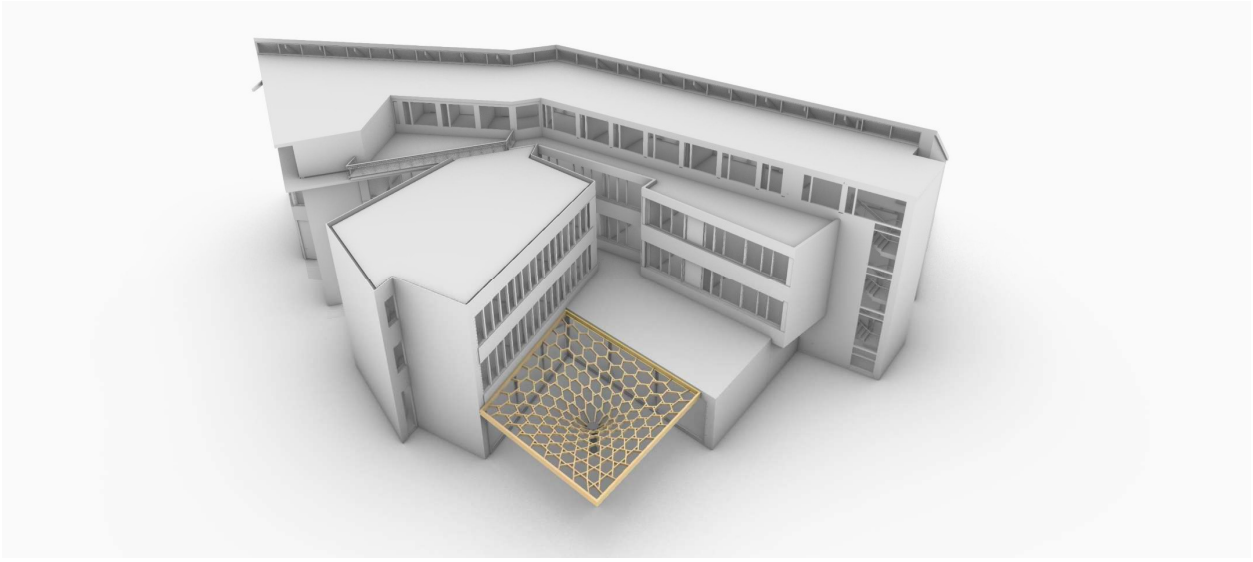

Figure 4-44: Birds-eye view of pavilion and building.

Figure 4-45: Eye-height visualization of pavilion.

4.3.3 Fabrication

After the preliminary design had been fixed, a full scale prototype could be fabricated. Fabrication consisted out of three steps: 3D printing the shell formwork, assembling the reinforcement cage and concrete filling.

4.3.3.1 3D Printing

The full column was 3D printed in four individual parts, as it was impossible to leave the robotic setup running overnight due to safety. Total fabrication time for the four parts amounted to 25 hours, with a toolpath length of over 4000m. The total weight of the parts was 7.5kg. After the parts had been 3D printed (Figure 4-46) they were assembled using hot glue.

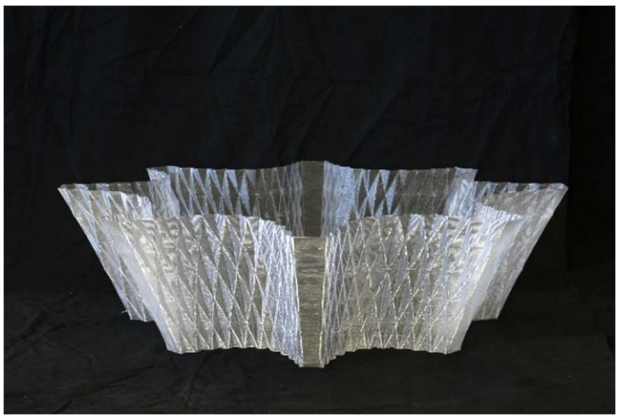

PART 4/4

Toolpath length	1292 m
Print time	8 hr
Print speed	45 mm/s
Weight	2.39 kg
Height	300mm
Number of layers	300

PART 3/4

Toolpath length	1179 m
Print time	7.3 hr
Print speed	45 mm/s
Weight	2.18 kg
Height	400mm
Number of layers	400

PART 2/4

Toolpath length	834 m
Print time	5.1 hr
Print speed	45 mm/s
Weight	1.54 kg
Height	500mm
Number of layers	500

PART 1/4

Toolpath length	745 m
Print time	4.6 hr
Print speed	45 mm/s
Weight	1.38 kg
Height	600mm
Number of layers	600

Figure 4-46: The four 3D printed parts of the column and the corresponding printing parameters.

4.3.3.2 Reinforcement

As had been determined in Section 4.2.1, the most feasible method of reinforcing the column was by adding the reinforcement to the shell formwork post-printing. The reinforcement cage was designed in collaboration with Jaime Mata Falcón from the Concrete Structures & Bridge Design group (Prof. Walter Kaufmann) at the ETH Zurich. Starting point for the reinforcement design was attempting to follow the shape of the concrete column as much as possible, while keeping the geometry relatively simple to fabricate. See Appendix B for the reinforcement drawings.

The reinforcement bars were cut and bent by Swiss reinforcement firm Debrunner Acifer Bewehrungen [82], after which they were shipped to ETH and manually assembled using standard rebar ties (Figure 4-47).

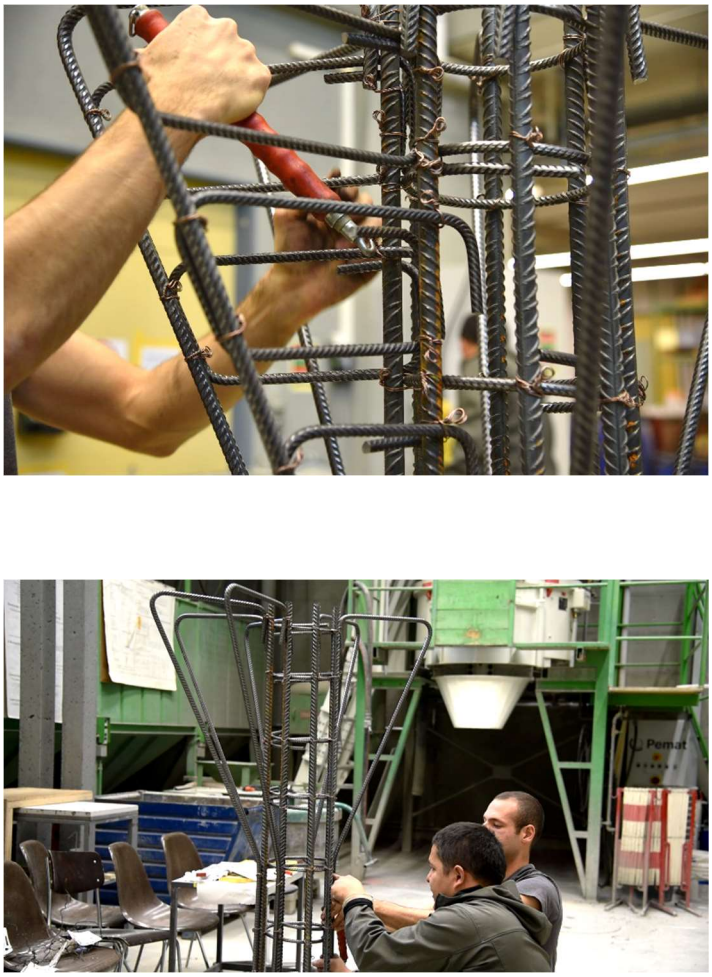

Figure 4-47: Assembly of reinforcement cage.

4.3.3.3 Filling

After prefabrication of both the reinforcement cage and the thin-shell formwork had been completed (Figure 4-48), they could be combined. The reinforcement was lifted into the formwork by crane and placed into position. Foam distance holders were placed in between the reinforcement and formwork to keep the correct distance without damaging the formwork. The combined shell and reinforcement were then placed next to a table and stack of pallets to allow for easy access (Figure 4-49).

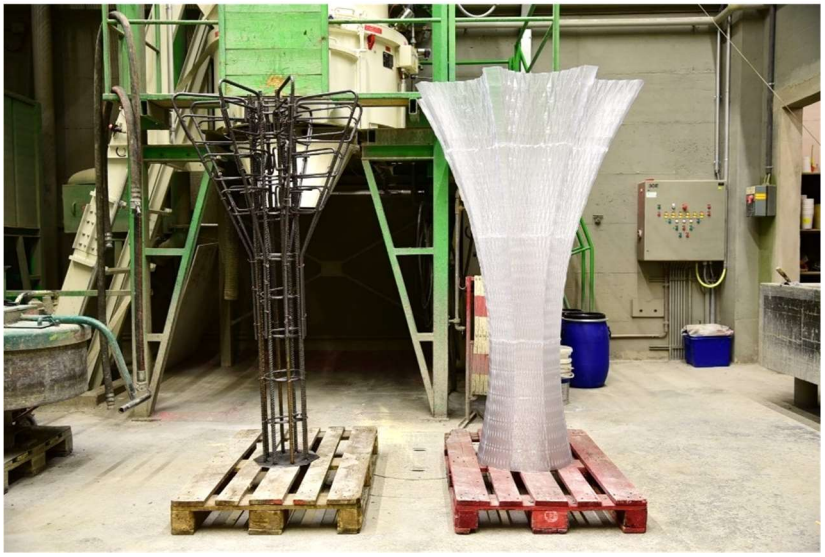

Figure 4-48: Completed prefabrication of reinforcement (left) and 3D printed formwork (right).

Figure 4-49: Combined formwork and reinforcement.

The formwork was filled with concrete (SACAC mix) using the manual acceleration approach (Section 3.5.1.1). This meant 50L retarded batches of concrete were mixed approximately every hour. These retarded batches were then split up into smaller batches of which the size depended on the column geometry (Figure 4-50). These batches were then accelerated at a predefined time, which was calculated from the filling rate. For the bottom, middle and top part different filling rates were taken, respectively 5 mm/min, 3 mm/min and 2 mm/min.

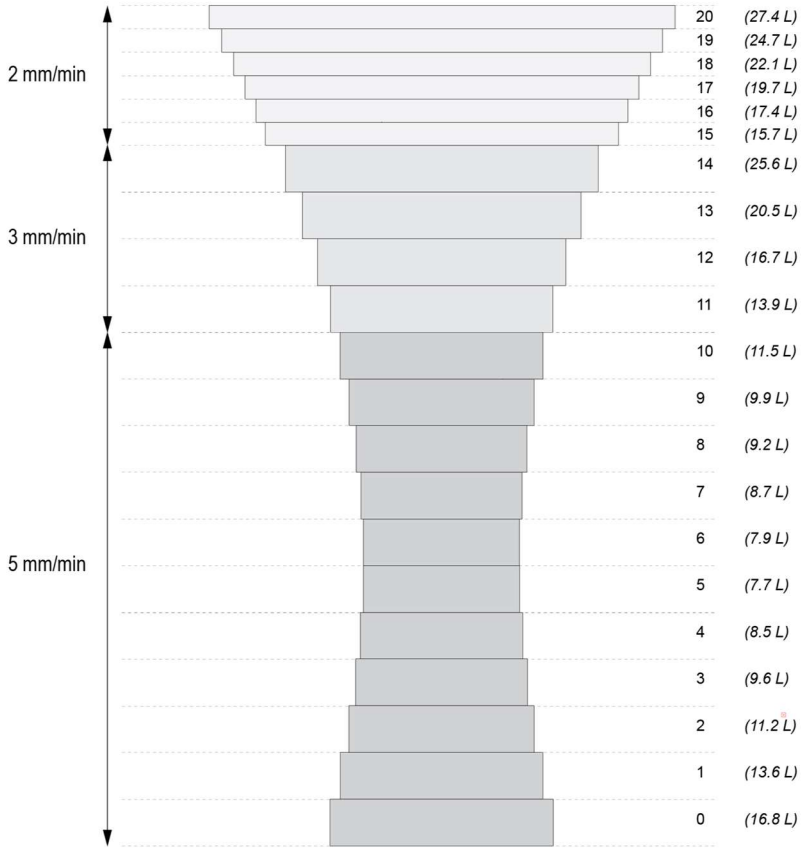

Figure 4-50: Batching strategy for column filling.

After acceleration of a batch, it was divided into four layers. These layers were then filled into the formwork, approximately every five minutes (depending on the filling rate). The total filling time of the column amounted to around nine hours. During filling, the concrete layers were manually intermixed using a long metal rod. After filling had been completed the column was covered with plastic to avoid cracks due to dehydration, and left to cure for several weeks.

4.3.4 Result

Figure 4-51: Finished full scale prototype.

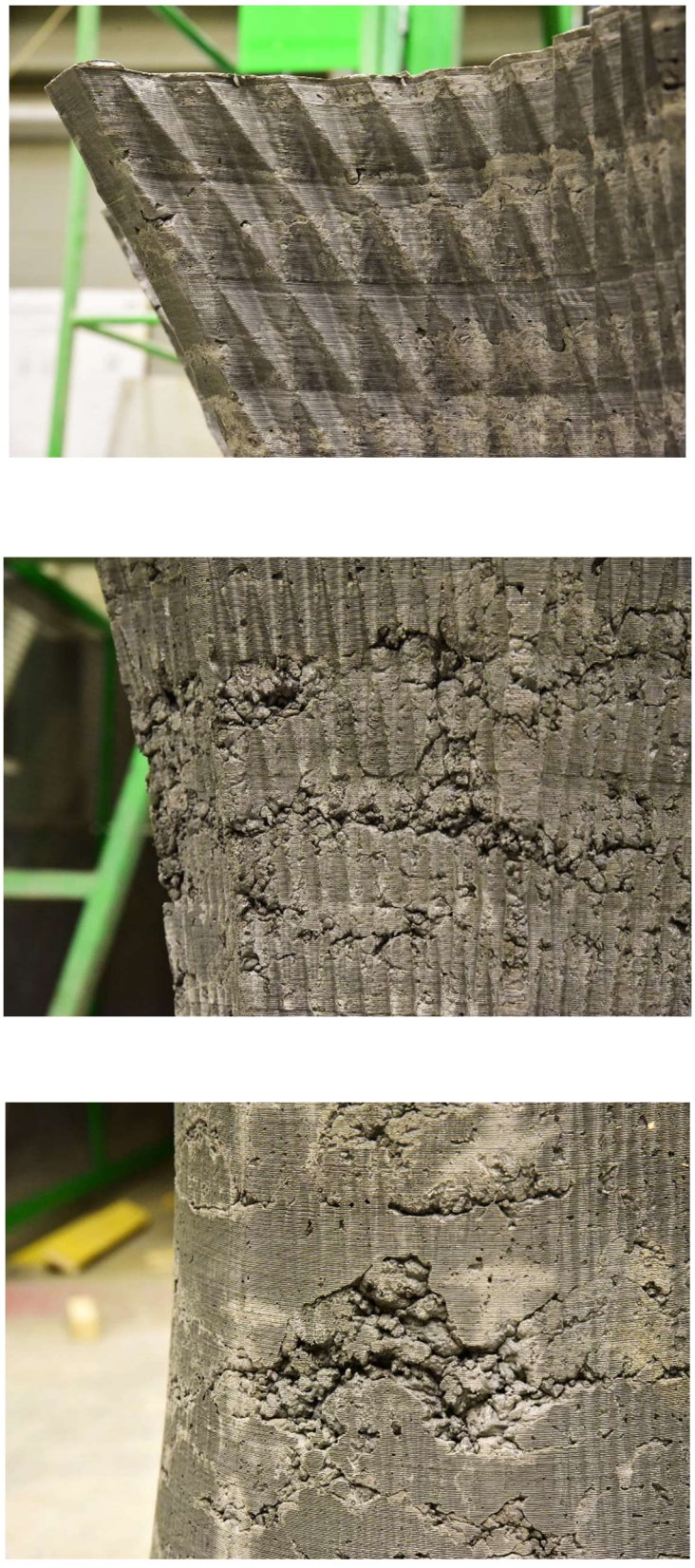

Figure 4-52: Close-up of column. a) Top. b) Middle. c) Bottom.

4.3.5 Discussion

It has been proven successful to fabricate the full scale prototype according to plan. No leakages or formwork breakages have been observed and although slight deformation of the formwork occurred at the top this did not affect the final result. There were, however, some problems encountered during fabrication. For the filling of the column, a certain hydration time of the concrete (which was obtained through previous measurements) was assumed. Based on this hydration time a filling schedule was made which determined at what time each concrete batch would be accelerated and thus at what time each concrete batch would start to hydrate.

The hydration time of the concrete can be determined by measuring the strength of the concrete with a penetrometer. The full procedure is described in the PhD "Smart Dynamic Casting" [32]. In short it consists of taking measurements at a certain interval and plotting the curve of the penetrometer resistance. An exponential graph should form and from the point where the resistance starts to go up exponentially, the hydration time can be determined.

The hydration time which the filling planning was based on was 90 minutes, however as we can see from Figure 4-53, the strength of the concrete already starts to increase exponentially after around 60-70 minutes. This means a 20-30 minute difference from what was expected and thus the concrete already had a much higher strength and therefore much lower fluidity when cast into the formwork.

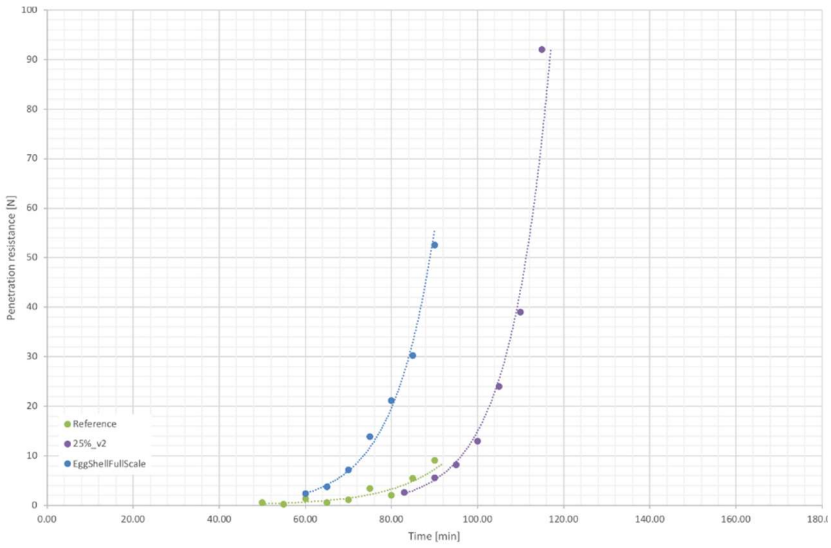

Figure 4-53: Penetrometer resistance over time from three concrete mixes. The blue curve (EggShellFullScale) represents the mix used during fabrication of the column prototype, the green and purple curves are reference mixes of the same material which were done before.

This loss in fluidity therefore is the cause of the lower surface quality, especially in the middle and bottom parts of the column (Figure 4-52). When the column filling started, no measurements were taken and the first batches of concrete were filled in. Although it was visible the concrete was thicker and less fluid than usual it was chosen to continue the experiment. As no measurements had been take, the flow loss could not be verified. Because

the full nine hours of concrete casting had been carefully planned and this planning was not easily altered, filling continued according to plan. After around five hours penetrometer measurements were taken and it was found out that the material was indeed behaving differently. The planning was then altered and concrete filling continued at a faster face. Because of this adjustment in planning, the top part of the column has a much better surface quality in comparison with the middle and bottom parts.

The unexpected early strength gain of the concrete (and therefore flow loss) could potentially be caused by small changes in room temperature and humidity. Although the temperature in the concrete laboratory is always around 22 degrees, it can fluctuate by several degrees. The same holds true for humidity as changing weather conditions affect the humidity in the laboratory. Both of these values were not measured during the experiment, which makes it difficult to be conclusive about the behaviour of the concrete. It has been shown in other research however, that temperature and humidity can have large effects on the strength and behaviour of the concrete mixture [83].

In order to account for the changing conditions it is therefore vital that more measurements are taken before and during fabrication. Instead of determining a fixed filling schedule, an adaptive filling schedule could be used which can be adjusted based on measurements taken during fabrication. As concrete will always have a certain degree of uncertainty, this should be accounted for. If this uncertainty can be addressed, future fabrication tests will most likely yield a better result, matching the standard set by the construction industry.

5 Summary and conclusions

In this thesis a novel fabrication method for non-standard concrete elements has been developed to a point where it is feasible to produce elements of a relatively large scale. Starting from small (20cm), unreinforced prototypes, the research has evolved to enable the production of a 180cm tall reinforced concrete column.

The main motivation for developing the fabrication process has been the high material waste in the fabrication of non-standard concrete elements. Eggshell makes use of a thin, 1.5mm shell formwork and thus starkly lowers the amount of material necessary to fabricate the formwork. Using the Eggshell fabrication process it was possible to fabricate a column of around 750kg with just 7.5kg of formwork material.

In this chapter a summary of the achieved results will be provided, as well as the overall conclusions of this thesis.

5.1 Summary of results

Phase I: Explorations

The starting point of the research was an interdisciplinary master thesis [5] done in a collaboration between Gramazio Kohler Research, the Institute of Robotics and Intelligent Systems and the Physical Chemistry of Building Materials group (ETH Zurich). In this thesis, concrete structures had been produced using a simultaneous 3D printing and casting system. This had proven the concept to work in a small scale, but it was unknown whether the same principle could be used to construct objects of an architectural scale. After this initial feasibility study three more prototypes were made by the author, measuring 30cm, 90cm and 160cm. This work has been done prior to starting the thesis work (Section 4.1). Upon completing these three prototypes, the main body of work described in this thesis was started.

Phase II: Scale-up

The opportunity had arisen to apply the Eggshell fabrication technology into an architectural project. A non-standard concrete column, carrying a timber roof structure of around 100m^2 presented itself as a case study. In order to directly apply the technology onto a real building site several questions had to be addressed.

Integration of reinforcement

The first challenge was the integration of reinforcement into the concrete column. For the column to perform structurally they had to include steel reinforcement. Several reinforcement approaches were chosen and tested for feasibility. From the experiments conducted, a method of prefabricating reinforcement and formwork presented itself as the most successful. In this method a reinforcement cage was fabricated separately from a 3D printed formwork. The

reinforcement and formwork were then combined and filled with concrete, resulting in the final structure. It proved successful to fabricate a 1m high prototype; however, the resulting surface quality was not very good due to the concrete not being fluid enough (Section 4.2.1).

Challenges of large scale 3D Printing

As the column studied in the case study had larger dimensions (a top diameter of 1m) than any formwork previously fabricated using this technology it proved challenging to 3D print the formwork because of issues of layer delamination of the filament. The layer delamination was found out to be caused by high stresses due to the shrinkage. After generating several designs with an alternative geometry, it was discovered that by applying a pattern of undulations to the formwork these high stresses could be avoided and a large formwork could successfully be printed (Section 4.2.2).

Structural performance of formwork subjected to hydrostatic pressure

Another challenge resulting from the large dimensions and overhang of the studied column was a high pressure from the concrete on the formwork. The resistance of the formwork against hydrostatic pressure was then studied with several physical experiments. An attempt was also made to make models of the structural performance using numerical simulation. It was found, however, that in order to apply simulation results in a physical environment more research is required. The experiments conducted did show that formwork with an undulated pattern has a superior structural performance over formwork without any pattern. The overhang tests conducted also provided some design constraints (Section 4.2.3).

Temperature development of hydrating concrete

A last study focused on the temperature development of the hydrating concrete. Due to the high mass of concrete in the column, high temperature peaks were expected during hydration. This was studied by inserting temperature sensors into a formwork during fabrication and from these a relatively high temperature peak of around 60 °C was found. Several measures can be undertaken to lower the peak, such as reducing cement content or applying active cooling (Section 4.2.4).

Phase III: Case-study

Finally, all of the findings were brought together into a full scale column prototype. Four formworks were 3D printed and assembled using hot glue. A reinforcement cage was then assembled and lifted into the shell formwork. The combined formwork and reinforcement were filled with concrete over a period of around nine hours. After casting the concrete was left to cure for approximately three weeks. When curing had finished the shell formwork could be removed using a heat gun. What remained is a full scale, reinforced, non-standard concrete column fabricated using a thin-shell 3D printed formwork.

5.2 Conclusions

The objective of this research has been to develop a strategy for fabricating full scale, non-standard, structural concrete columns in a less wasteful manner compared to existing methods. This was approached by means of fabricating the concrete elements using a thin-shell, 3D printed formwork method dubbed Eggshell. With the production of a full scale prototype the feasibility of this method for architectural structures was successfully demonstrated.

If it is assumed that a formwork for a non-standard concrete element is completely discarded after its use (meaning no re-use or recycling is possible), Eggshell provides a material-efficient alternative to existing methods. In this case material-efficiency is defined as being the percentage of costs spent on the formwork. This is because in the case of a one-off element, all resources spent on creating the formwork are essentially wasted because they will not become part of final product, nor can they be re-used.

For fabrication of a non-standard concrete element through milling of timber formwork, as high as 88% of the costs are taken up by formwork labour and materials [9]. For the final prototype fabricated using the Eggshell formwork; however, formwork only makes up for 14% of the costs (Figure 5-1). A lower cost for the lost formwork therefore means either a higher percentage of the cost could go towards the materials that will actually be placed on the building site (the concrete and reinforcement), or the total cost of a non-standard structure could go down. As the cost of non-standard architectural elements is brought down, this could give architects and builders freedom in realizing their designs.

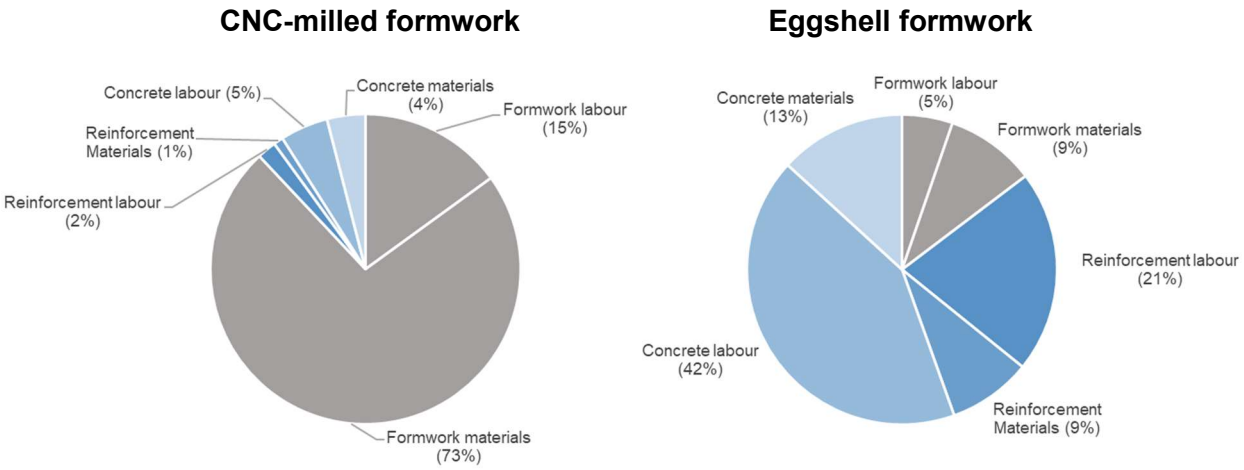

Figure 5-1: Cost comparison between existing ways of formwork fabrication [9] *(milling of timber elements) and the Eggshell formwork fabrication process for a non-standard concrete element. Formwork costs are highlighted in grey.*

What is remarkable is the high increase in percentage of costs for concrete labour (Figure 5-1), in normal formwork this only accounts for 5% while in the Eggshell formwork this is more than 40%. This is however, due to the fact that filling of the prototype was still done manually. This means several people had to be employed for the entire duration of the filling, which caused the increase in costs. Research is currently ongoing to realize an automatic filling strategy, if this were to be adopted the high concrete labour costs would decrease significantly.

Another aspect which has been applied throughout this thesis and for the final prototype, is the reunification of designer and maker into a single entity. In a traditional building process, the architect is in charge of the design of a building, after which the design gets handed off to a contractor, who is in charge of executing the design [84]. When striving for a material-aware fabrication process; however, it is important that no discrepancy exists between the possibilities of fabrication and design.

An example of material-aware design and fabrication can be found in the pattern which was applied to the formwork surface. The necessity of creating undulations in the toolpath to redistribute stresses arose from insights gained during fabrication, which then went on to influence the design language of the column. This meant several iterations were made in between design, fabrication and material to arrive at a final prototype. An iterative process such as this would have been difficult, if not impossible to achieve, had the designer and maker not been the same entity.

Although the thesis overall objective was achieved, there are certainly many aspects which can either be improved or need future research. Several of these such as using alternative materials, recycling of formwork or alternative methods of reinforcement are discussed in Chapter 6. What can be said for the final prototype produced during this thesis is that the necessity of integrating reinforcement has been the main limitation in design and fabrication. Although the formwork has been created with state-of-the-art 3D printing methods, the reinforcement cage is similar to what can be found on many a construction site and has been assembled manually.

Moreover, because it was chosen to add reinforcement after the shell formwork had been 3D printed, the method of simultaneous fabrication (concrete filling while 3D printing) had to be abandoned for this prototype. The alternative filling method of consecutive fabrication (concrete filling after 3D printing), then was partly responsible for the lower surface quality of the final prototype. Lastly, reinforcement considerations lead to a more constrained design space for the column. As the reinforcement and shell had to fit together post-production, the column design could not include elements such as gaps or branching geometry.

From this can be seen that in order for the Eggshell fabrication technology to become more mature, it is vital developments are made in the integration of reinforcement, as well as in 3D printing and material processing. As these three domains come together in the process, they cannot be addressed individually. Nevertheless, the results obtained during this

research make a valuable addition to the field of additive manufacturing with concrete. As the Eggshell process is able to overcome many limitations currently present in other digital fabrication processes, it has the potential to enable future design and fabrication with concrete to be material-efficient, sustainable and beautiful.

6 Outlook

Although this thesis has shown the potential thin-shell formwork has for fabricating non-standard concrete structures, there are still many aspects which can be explored in further research. An overview is therefore presented of suggestions for future research.

Alternative materials

The research conducted in this thesis has exclusively been making use of thermoplastic materials for the fabrication of the thin-shell formwork. In concept, it is however, not limited to thermoplastic materials and many alternative materials could be considered. One interesting option to provide a fully recyclable material is clay. In recent years clay has established itself as a material well-fit for 3D printing large objects and its potential is being researched around the world [50]. Other sustainable options for formwork materials that could potentially be of interest are recyclable wax [85], algae [86] or other natural materials.

Another possibility is using concrete not only as a filling material but also as a material for the shell. Instead of removing the formwork after casting, the shell could serve as a stay-in-place formwork. Using concrete as a shell material would be advantageous because of the high printing speed, strength and many developments made in concrete extrusion [87].

Recycling of shell material

The 3D printing material used throughout this thesis has been PET-G. PET-G can be recycled by shredding the 3D print and extruding the resulting granulate into filament with a pellet extruder. In the case of recycling the lost thin-shell formwork, the question remains whether the formwork can be cleaned well enough of any remaining concrete particles. The shell already comes of relatively clean after being removed from the concrete; however, remaining concrete residue could cause problems with recycling.

Feedback during fabrication

One aspect which has not yet been explored for this fabrication process is the active monitoring of relevant parameters during fabrication. An active monitoring system with feedback loop could enable the process to be dynamically adjusted. One possibility would be to measure the deformation of the formwork during fabrication and adjust the concrete filling rate and shell printing speed accordingly. Another possibility would be to measure the hydration time of the concrete on the day of fabrication, so any changes in the mix due to temperature or humidity can be accounted for.

Digital concrete casting

During this thesis most of the experiments conducted have been making use of the manual acceleration and casting process, where concrete casting and the addition of acceleration admixtures were done by hand. If this were to be replaced with a fully automated process it could be possible to dose concrete layers more carefully and thus create a more robust process. Furthermore, if a feedback system (such as described in the previous paragraph) is paired with a digital concrete casting system one could easily adapt the process on the fly.

Improved design and simulation tool

Although a digital design and fabrication tool has already been used for this thesis, it can still be improved. The tool already provides the user with some information regarding the feasibility of the 3D print (such as angle between layers) but it does not give information on the performance of the formwork when subjected to the hydrostatic pressure of the concrete. During the design phase the designer therefore does not always know whether the design is actually able to be fabricated. Having this information would be valuable for narrowing down options in the early design phase.

On-site construction

This thesis has been focused on creating prefabricated structures which could then be transported to site. By opting for prefabrication in a controlled environment unexpected results due to changing environmental conditions could be ruled out. If, however, the entire process would become more robust it could be feasible to 3D print and cast on-site. This could provide advantages such as lower transport and crane costs.

Alternative reinforcement methods

As stated in Section 5.2, the integration of reinforcement proved to be one of the most challenging aspects of fabrication. Alternative methods of reinforcement, such as adding steel fibres to the concrete mix could possibly provide an effective reinforcement solution, without having to compromise in geometrical limitations.

Other building components

Although the research in this thesis has specifically focused on fabricating columns, it is not limited to column geometry. Other possibilities could include the fabrication of wall elements, façade panels, beams or floor slabs. The Eggshell fabrication technology; however, is especially well suited for the production of vertical elements, due to its inherent vertical layer-based casting method and the self-levelling properties of concrete.

[88]

Bibliography

[1] T. Wangler *et al.*, "Digital Concrete: Opportunities and Challenges," *RILEM Tech. Lett.*, vol. 1, p. 67, 2016.

[2] J. M. Crow, "The concrete conundrum," *Chem. World*, no. March, pp. 62–66, 2008.

[3] D. W. Johnston, "Design and construction of concrete formwork," in *Nawry, Edward G. editor. Concrete construction engineering handbook*, New Jersey, USA: CRC Press, 2008, p. 7.1-7.49.

[4] S. O. Ajayi *et al.*, "Waste effectiveness of the construction industry: Understanding the impediments and requisites for improvements," *Resour. Conserv. Recycl.*, vol. 102, pp. 101–112, 2015.

[5] T. Ulrich, "Enabling and Expanding Geometries for Smart Dynamic Casting," ETH Zurich, 2017.

[6] K. Oosterhuis, *Towards a New Kind of Building. A Designers Guide for Nonstandard Architecture*. Rotterdam: NAi Uitgevers, 2011.

[7] M. Kohler, F. Gramazio, and J. Willmann, *The Robotic Touch: How Robots Change Architecture*. Park Books, 2014.

[8] R. H. Lab, "Think Formwork – Reduce Costs," *Struct. Mag.*, no. April, pp. 14–16, 2007.

[9] H. R. Schipper and S. Grünewald, "Efficient Material Use Through Smart Flexible Formwork Method," no. 1, pp. 1–8.

[10] A. Weilandt, M. Grohmann, K. Bollinger, and M. Wagner, "Rolex Learning Center in Lausanne: From conceptual design to execution," in *Proceedings of the International Association for Shell and Spatial Structures (IASS) Symposium 2009, Valencia*, 2009, pp. 640–653.

[11] N. Williams, H. Stehling, F. Scheurer, S. Oesterle, M. Kohler, and F. Gramazio, "A Case Study of a Collaborative Digital Workflow in the Design and Production of Formwork for 'Non-Standard' Concrete Structures," *Int. J. Archit. Comput.*, vol. 9, no. 3, pp. 223–240, 2011.

[12] Toyo Ito & Associates, "Meiso no Mori Crematorium Gifu," *C+A*, no. 10.

[13] E. Lloret *et al.*, "Complex concrete structures: Merging existing techniques with digital fabrication," *Computer-Aided Design*, vol. 60. pp. 40–49, 2015.

[14] J. F. Camellerie, "Vertical slipforming as a construction tool," *Concr. Constr.*, pp. 262–273, 1978.

[15] R. G. Batterham, *Slipform Concrete*. New York: The Construction Press, 1980.

[16] Slipform.us, "Hebron Main Shaft Completed," 2016.

[17] A. Søndergaard and P. Dombernowsky, "Unikabeton Prototype," in *Fabricate*, B. Sheil and R. Glynn, Eds. UCL Press, 2011.

[18] O. Sigmund and K. Maute, "Topology optimization approaches: A comparative review," *Struct. Multidiscip. Optim.*, vol. 48, no. 6, pp. 1031–1055, 2013.

[19] E. Herrmann, J. L. C. Mainka, H. Lindemann, F. Wirth, and H. Kloft, "Digitally fabricated innovative concrete structures," *ISARC 2018 - 35th Int. Symp. Autom. Robot. Constr. Int. AEC/FM Hackathon Futur. Build. Things*, no. Isarc, 2018.

[20] V. Sitnikov, "Ice Formwork for Ultra-High Performance Concrete: Simulation of Ice Melting Deformations," in *Humanizing Digital Reality*, 2018.

[21] "Odico Formwork Robotics." [Online]. Available: https://www.odico.dk/en. [Accessed: 01-Dec-2018].

[22] J. Feringa and A. Søndergaard, "Fabricating architectural volume: Stereotomic investigations in robotic craft," in *Fabricate 2014*, F. Gramazio, M. Kohler, and S. Langenberg, Eds. 2014, pp. 76–83.

[23] A. Søndergaard *et al.*, "Robotic Hot-Blade Cutting," in *Robotic Fabrication in Architecture, Art and Design 2016*, 2016, pp. 151–164.

[24] R. Rust, "Spatial Wire Cutting," ETH Zurich, 2017.

[25] "Kirk Kapital, Odico." [Online]. Available: https://www.odico.dk/en/references/kirk-kapital-3. [Accessed: 01-Dec-2018].

[26] A. Jipa, B. Dillenburger, and M. Bernhard, "skelETHon Formwork 3D Printed Plastic Formwork for Load-Bearing Concrete Structures," *XXI Congr. Int. la Soc. Iberoam. Gráfica Digit.*, vol. 3, no. 12, pp. 345–352, 2017.

[27] M. Aghaei Meibodi, M. Bernhard, A. Jipa, and B. Dillenburger, "The smart takes from the strong: 3D printing stay-in-place formwork for concrete slab construction," *Fabr. 2017*, no. May 2017, pp. 210–215, 2017.

[28] "Smart Slab," 2018. [Online]. Available: http://dbt.arch.ethz.ch/project/smart-slab/. [Accessed: 12-Nov-2018].

[29] "Post in Aix-en-provence." [Online]. Available: http://www.xtreee.eu/post-in-aix-en-provence/. [Accessed: 09-Jan-2019].

[30] S. Oesterle, A. Vansteenkiste, and A. Mirjan, "Zero Waste Free-Form Formwork," *Icff 2012 - Second Int. Conf. Flex. Formwork*, no. Figure 1, pp. 258–267, 2012.

[31] F. Scotto, E. Lloret Fritschi, F. Gramazio, M. Kohler, and R. Flatt, "Adaptive Control System for Smart Dynamic Casting," *Learn. Adapt. Prototyp. - Proc. 23rd CAADRIA Conf.*, vol. 1, pp. 255–264, 2018.

[32] E. Lloret Fritschi, "Smart Dynamic Casting - A digital fabrication method for non-standard concrete structures," ETH Zurich, 2016.

[33] J. C. McCormac and R. H. Brown, *Design of Reinforced Concrete*, 10th editi. Hoboken, New Jersey: John Wiley & Sons, Inc., 2016.

[34] "CS 440 Automatic Shaping Center." [Online]. Available: http://www.mepgroup.com/en/bend-shaping/machine/cs-440. [Accessed: 13-Nov-2018].

[35] "TJK Machinery." [Online]. Available: http://www.tjkmachinery-group.com/products/wire-cage-welding-machine/. [Accessed: 01-Dec-2018].

[36] A. M. Brandt, "Fibre reinforced cement-based (FRC) composites after over 40 years of development in building and civil engineering," *Compos. Struct.*, vol. 86, no. 1–3, pp. 3–9, 2008.

[37] "Twisted Steel Micro Rebar." [Online]. Available: http://www.helixsteel.com/. [Accessed: 13-Nov-2018].

[38] N. Hack, W. V. Lauer, F. Gramazio, and M. Kohler, "Mesh Mould: Robotically Fabricated Metal Meshes as Concrete Formwork and Reinforcement," *Proc. 11th Int. Symp. Ferrocem. 3rd ICTRC Int. Conf. Text. Reinf. Concr.*, pp. 347–359, 2015.

[39] M. Popescu, L. Reiter, A. Liew, T. Van Mele, R. J. Flatt, and P. Block, "Building in Concrete with an Ultra-lightweight Knitted Stay-in-place Formwork: Prototype of a Concrete Shell Bridge," *Structures*, vol. 14, no. February, pp. 322–332, 2018.

[40] B. Mueller, "Additive Manufacturing Technologies – Rapid Prototyping to Direct Digital Manufacturing," *Assem. Autom.*, vol. 32, no. 2, 2012.

[41] B. C. Gross, J. L. Erkal, S. Y. Lockwood, C. Chen, and D. M. Spence, "Evaluation of 3D printing and its potential impact on biotechnology and the chemical sciences," *Anal. Chem.*, vol. 86, no. 7, pp. 3240–3253, 2014.

[42] R. Jones *et al.*, "RepRap - The Replicating Rapid Prototyper," *Robotica*, 2011.

[43] "Ultimaker." [Online]. Available: https://ultimaker.com. [Accessed: 20-Nov-2018].

[44] "Makerbot." [Online]. Available: https://www.makerbot.com/. [Accessed: 20-Nov-2018].

[45] "Prusa Research." [Online]. Available: https://www.prusa3d.com/. [Accessed: 20-Nov-2018].

[46] "Alpeh Objects." [Online]. Available: https://www.alephobjects.com. [Accessed: 20-Nov-2018].

[47] A. Kealoha, "An interview with Dirk van der Kooij," 2011. [Online]. Available: https://coolhunting.com/design/dirk/. [Accessed: 20-Nov-2018].

[48] S. Mostafavi, H. Bier, S. Bodea, and A. M. Anton, "Informed Design to Robotic Production Systems: Developing Robotic 3D Printing System for Informed Material Deposition," *eCAADe 2015 Real Time - Extending Reach Comput. Vol. 2, Proc. 33rd Int.*

Conf. Educ. Res. Comput. Aided Archit. Des. Eur., vol. 2, pp. 287–296, 2015.

[49] P. Morel and T. Schwartz, "Automated Casting Systems for Spatial Concrete Lattices," *Model. Behav.*, pp. 213–223, 2015.

[50] A. Dubor, E. Cabay, and A. Chronis, "Energy Efficient Design for 3D Printed Earth Architecture," in *Humanizing Digital Reality*, K. De Rycke, C. Gengnagel, O. Baverel, J. Burry, C. Mueller, M. M. Nguyen, P. Rahm, and M. R. Thomsen, Eds. 2017, pp. 383–393.

[51] "Universal Robot UR10." [Online]. Available: https://www.universal-robots.com/products/ur10-robot/. [Accessed: 26-Oct-2018].

[52] "Spatial Extrusions." [Online]. Available: http://gramaziokohler.arch.ethz.ch/web/e/lehre/310.html. [Accessed: 20-Jan-2019].

[53] "BLB Industries The Box." [Online]. Available: http://blbindustries.se/3d-printers/the-box. [Accessed: 19-Jan-2019].

[54] "extrudr." [Online]. Available: http://www.extrudr.com. [Accessed: 20-Nov-2018].

[55] Bürkle GmbH, "Chemical resistance of plastics," Bad Bellingen, 2015.

[56] J. A. Grubb, H. S. Limaye, and A. M. Kakade, "Testing pH of Concrete," *Concr. Int.*, no. april, pp. 78–83, 2007.

[57] "What is g-code?," 2018. [Online]. Available: https://ultimaker.com/en/resources/39071-what-is-g-code. [Accessed: 01-Nov-2018].

[58] "Simplify 3D." [Online]. Available: https://www.simplify3d.com. [Accessed: 25-Nov-2018].

[59] "Ultimaker Cura." [Online]. Available: https://ultimaker.com/en/products/ultimaker-cura-software. [Accessed: 25-Nov-2018].

[60] "Slic3r." [Online]. Available: http://slic3r.org. [Accessed: 25-Nov-2018].

[61] "DROID Food4Rhino." [Online]. Available: https://www.food4rhino.com/app/droid. [Accessed: 12-Jan-2019].

[62] "Arduino." [Online]. Available: https://www.arduino.cc. [Accessed: 25-Nov-2018].

[63] E. Lloret Fritschi, L. Reiter, T. Wangler, F. Gramazio, M. Kohler, and R. J. Flatt, "Smart Dynamic Casting Slipforming with Flexible Formwork - Inline Measurement and Control," in *HPC/CIC Tromsø 2017*, 2017.

[64] P. F. G. Banfill, "Rheology of Fresh Cement and Concrete," *Rheol. Rev.*, pp. 61–130, 2006.

[65] N. Roussel and F. Cussigh, "Distinct-layer casting of SCC: The mechanical consequences of thixotropy," *Cem. Concr. Res.*, vol. 38, no. 5, pp. 624–632, 2008.

[66] I. M. Rian and M. Sassone, "Tree-inspired dendriforms and fractal-like branching structures in architecture: A brief historical overview," *Front. Archit. Res.*, vol. 3, pp. 298–323, 2014.

[67] J. T. Hewes and M. J. N. Priestly, "Seismic Design and Performance of Precast Concrete Segmental Bridge Columns," University of California, San Diego. La Jolla, California, 2002.

[68] "Raise3D N2 Plus FFF 3D Printer." [Online]. Available: https://www.raise3d.com/products/raise3d-n2-plus-fff-3d-printer. [Accessed: 02-Dec-2018].

[69] B. Wijin, P. Sanders, and J. M. Pearce, "Improved Model and Experimental Validation of Deformation in Fused Filament Fabrication of Poly Lactic Acid," *Prog. Addit. Manuf.*, vol. 3, no. 1, pp. 1–23, 2018.

[70] "Abaqus Unified FEA." [Online]. Available: https://www.3ds.com/products-services/simulia/products/abaqus/. [Accessed: 05-Jan-2019].

[71] Z. Bofang, *Thermal Stresses and Temperature Control of Mass Concrete*. Oxford: Butterworth-Heinemann, 2014.

[72] J. Gajda and M. Vangeem, "Controlling Temperatures in Mass Concrete," *Concr. Int.*, no. January, pp. 59–62, 2002.

[73] Z. Ge, "Predicting temperature and strength development of the field concrete," 2005.

[74] American Concrete Institute, *Cement and Concrete Terminology (ACI116R-00)*. Farmington Hills, Michigan, 2000, p. 73.

[75] A. A. El-kurdi, A. Abdel-hakam, and M. M. El-gohary, "Impact of Elevated Temperature on Properties of Limestone Concrete," no. 4, pp. 1–9, 2014.

[76] S. Lagundžija and M. Thiam, "Temperature reduction during concrete hydration in massive structures," 2017.

[77] "Basler & Hofmann." [Online]. Available: https://www.baslerhofmann.ch/en/home.html. [Accessed: 10-Jan-2019].

[78] "Additive Robotic Fabrication of Complex Timber Structures, Zurich, 2012-2017." [Online]. Available: http://gramaziokohler.arch.ethz.ch/web/forschung/e/0/0/0/184.html. [Accessed: 10-Jan-2019].

[79] "Spatial Timber Assemblies, Zurich, 2016-2018." [Online]. Available: http://gramaziokohler.arch.ethz.ch/web/e/forschung/311.html. [Accessed: 10-Jan-2019].

[80] A. B. Halpern, D. P. Billington, and S. Adriaenssens, "The ribbed floor slab systems of pier luigi nervi," *J. Int. Assoc. Shell Spat. Struct.*, vol. 54, no. 176–177, pp. 127–136, 2013.

[81] A. Molster, "Aanbestedingslessen uit Arnhem Centraal," *Archined*, pp. 1–9, 2012.

[82] "Debrunner Acifer Bewehrungen." [Online]. Available: https://www.bewehrungstechnik.ch. [Accessed: 14-Jan-2019].

[83] U. Hayri and B. Baradan, "The effect of curing temperature and relative humidity on the strength development of Portland cement mortar," *Sci. Res. Essays*, vol. 6, no. 12, pp. 2504–2511, 2011.

[84] R. A. Mohsini and C. H. Davidson, "Determinants of performance in the traditional building process," *Constr. Manag. Econ.*, vol. 10, no. 4, pp. 343–359, 1992.

[85] "Trace 3D Printer." [Online]. Available: https://trace3dprinter.be/en/your-professional-3d-wax-printer/. [Accessed: 09-Jan-2019].

[86] A. Morris, "Dutch designers convert algae into bioplastic for 3D printing," *Dezeen*, 2017.

[87] R. A. Buswell, W. R. L. De Silva, S. Z. Jones, and J. Dirrenberger, "Cement and Concrete Research 3D printing using concrete extrusion : A roadmap for research," *Cem. Concr. Res.*, vol. 112, no. May, pp. 37–49, 2018.

[88] P. J. M. Monteiro, S. A. Miller, and A. Horvath, "Towards sustainable concrete," *Nat. Mater.*, vol. 16, no. 7, pp. 698–699, 2017.

[89] P. J. Nedwell, "Ferrocement: Proceedings of the Fifth International Symposium on Ferrocement," in *Ferrocement: Proceedings of the Fifth International Symposium on Ferrocement*, 1994, pp. 28–30.

Appendix A

Material data sheet: extrudr PET-G

MATERIAL DATA SHEET
extrudr PETG

DESCRIPTION

Polyethylene Terephthalate Glycol (PETG) is one of the world's most common thermoplastic polymers.

APPLICATION

PETG is specifically designed to have a large and general scope of application in situations where the main requirement is the balance between mechanical and optical material properties.

STORAGE AND SHELF LIFE

Store at room temperature (18-27°C / 65-80°F), out of direct heat and sunlight, and in a dry place. When stored correctly, this material has a shelf life of 1 year

TECHNICAL SUPPORT

Contact us regarding any questions, improvement suggestions, or problems with this product.

EMAIL SUPPORT@EXTRUDR.EU

PROPERTIES

TEST	METHOD	UNIT	VALUE
Flexural modulus	ISO 527	MPa	3100
Tensile strength	ISO 527	MPa	50
Breaking stress	ISO 527-2	%	4
Breaking stress	ISO 527	Mpa	20
Elongation at break	ISO 527	%	29
E-Modulus	ISO 178	Mpa	2040
Flexural strength	ISO 178	MPa	68,3
MFR	ISO 1133	g/10 min	7
Melting temperature	ISO 3146-C	C°	180-200
VICAT A (VST)	ISO 306	C°	78
Shrinking	ISO 294-4	%	0,5
Density	ASTM D792	g/cm^3	1,3

VISUAL QUALITY 7

HIGH TEMPERATURE RESISTANCE 5

LAYER ADHESION 7

IMPACT RESISTANCE 6

ELONGATION AT BREAK 6

MAXIMUM STRESS 8

EASE OF PRINTING 7

extrudr

MATERIAL DATA SHEET
extrudr PETG

12. January 2018
Page 1/1

Appendix B

Reinforcement drawings

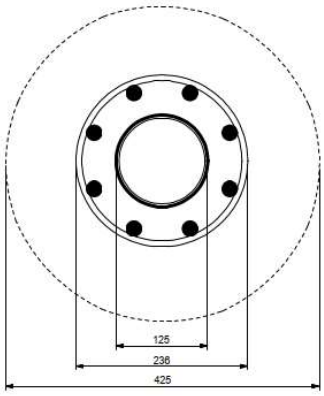

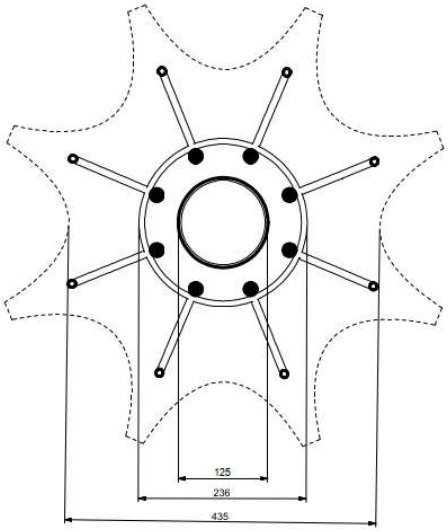

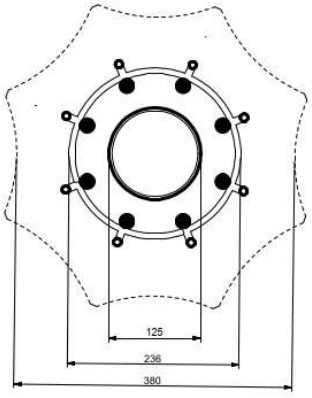

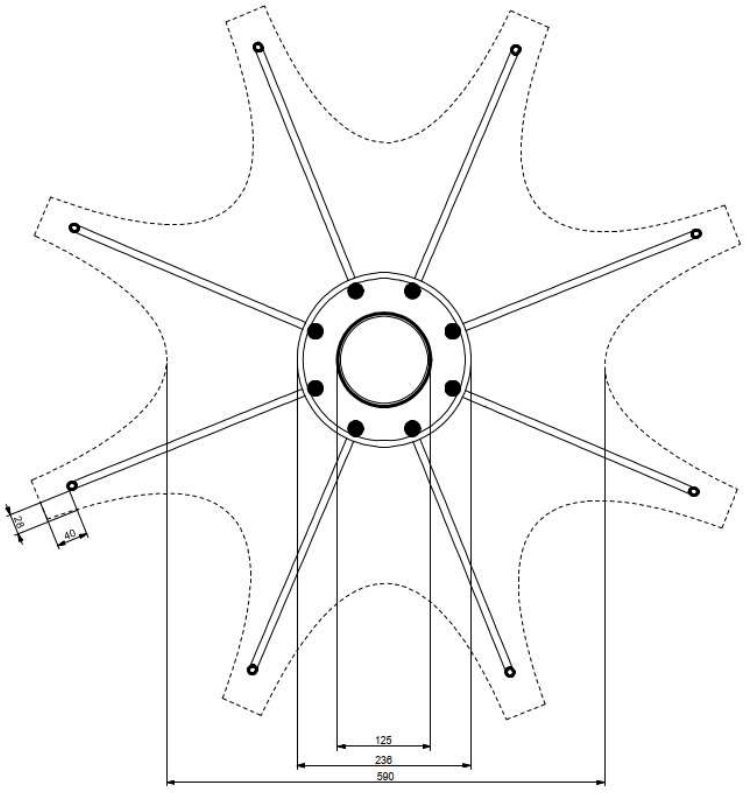

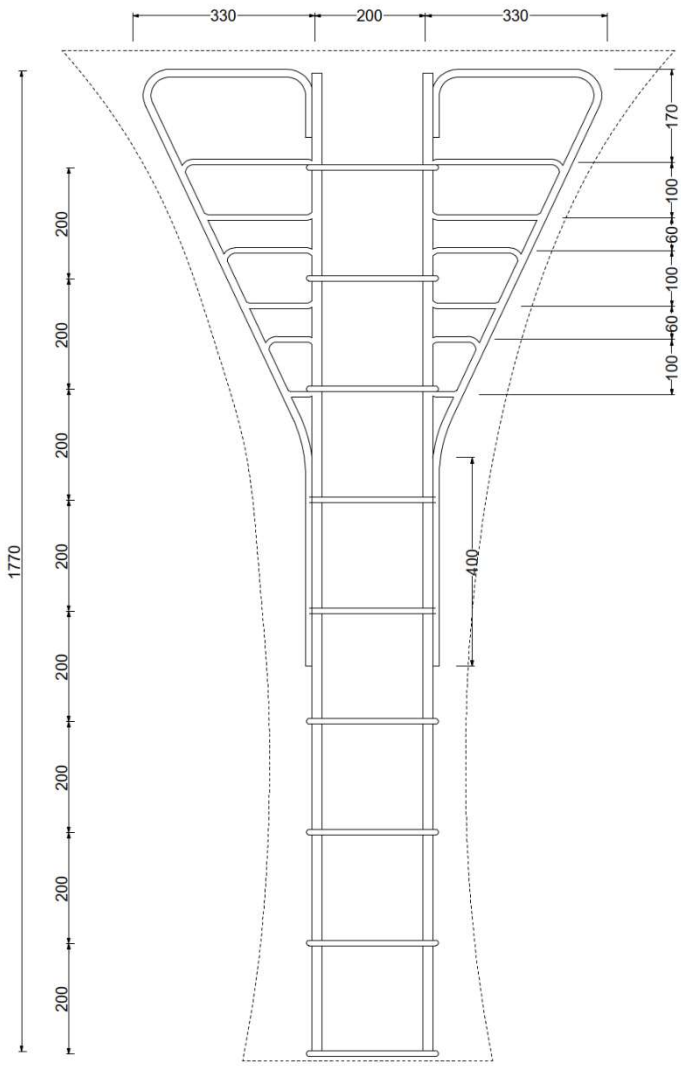
330
200
330
170
100
60
100
60
100
400
1770
200
200
200
200
200
200
200
200

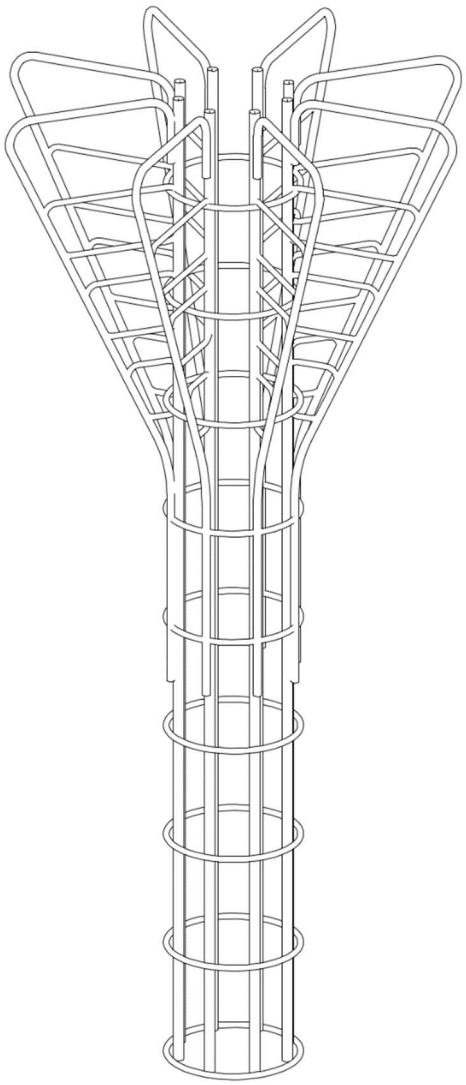

s1: ∅10 **length:** 97cm (outside) **amount:** 8

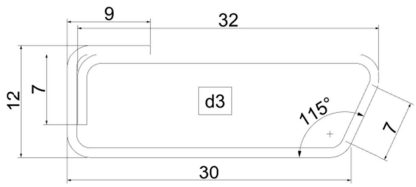

s2: ∅10 **length:** 83cm (outside) **amount:** 8

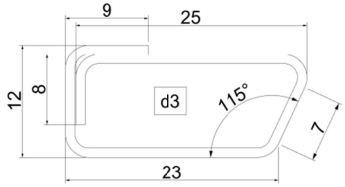

s3: ∅10 **length:** 68cm (outside) **amount:** 8

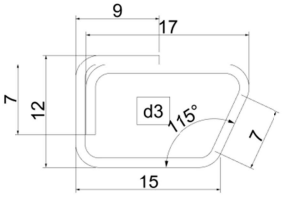

h1: ∅10 **length:** 75cm (outside) **amount:** 10

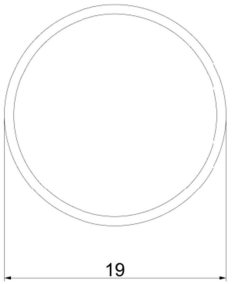

v1: ∅14 **length:** 168cm (outside) **amount:** 8

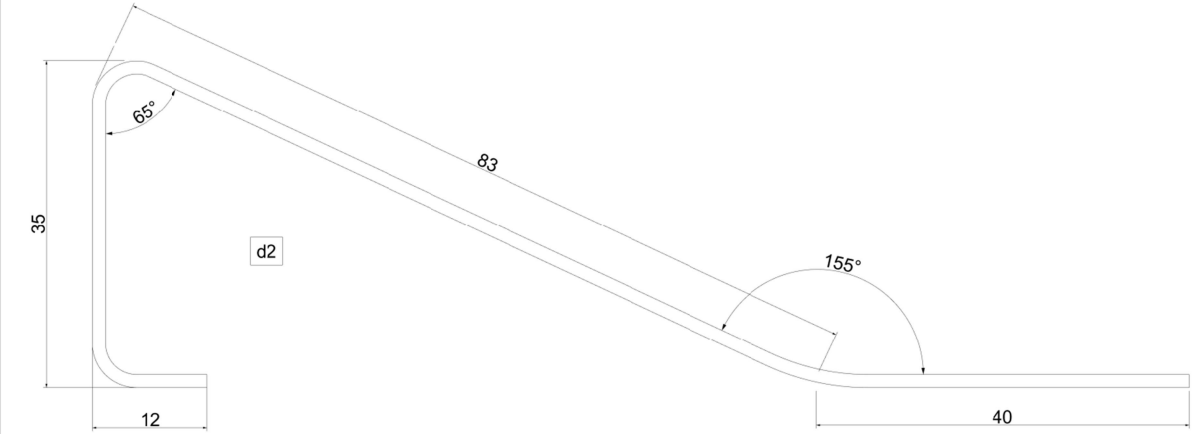

v2: ∅18 **length:** 177cm **amount:** 8